SYNTHESIS, SPECTROSCOPIC AND CRYSTALLOGRAPHIC STUDIES ON SOME TRANSITION METAL COMPLEXES

A THESIS

SUBMITTED FOR THE DEGREE OF

DOCTOR OF PHILOSOPHY

BY

VENKATA LAKSHMI NANDANAVANAM

SCHOOL OF CHEMISTRY

UNIVERSITY OF HYDERABAD

HYDERABAD - 500 134

INDIA

APRIL 1991

DEDICATED
TO
BABU MAMA

CONTENTS

CHAPTER - IV

CHAPTER - V

STATEMENT

I hereby declare that the matter embodied in this thesis is the result of investigation carried out by me in the School of Chemistry, University of Hyderabad, Hyderabad, under the supervison of **Dr. M.V. Rajasekharan**.

In keeping with the general practice of reporting scientific observations, due acknowledgement has been made wherever the work discribed is on the findings of other investigators. Any omission which might have occurred by oversight or error in judgement is regretted.

N V Lakshmi

N. VENKATA LAKSHMI

CERTIFICATE

Certified that the work contained in this thesis entitled "Synthesis, Spectroscopic and crystallographic studies on some transition metal complexes. [E.s.r., electronic, Magnetic susciptibility, Mossbauer and X-ray crystallographic studies of Ni(II), Cu(II), Co(II), Mn(III,IV), Fe(II), Ag(I) Systems" has been carried out by Venkata Lakshmi, N. under my supervision and the same has not been submitted elsewhere for a degree.

M.V. RAJASEKHARAN

(Thesis Supervisor)

DEAN

SCHOOL OF CHEMISTRY
D E A N
School of Chemistry

ii

ACKNOWLEDGEMENTS

PREFACE

The work which culminated in the present thesis was started with the aim of making mixed valence complexes with extended interactions in the lattice. At that time some partially oxidised nickel(II) stacked compounds were known with anisotropic electrical conductivity. It was thought worthwhile to prepare the Ni(III) - Ni(II) with 9,10-phenanthrenedionedioxime (pqdH$_2$), because the extended π system is likely to favour stacking interactions and therefore short Ni-Ni distance. While partially oxidised Ni(II) as well as Ni(III) compounds could be prepared with this ligand, their low solubility was not favourable for crystal growth. Since not much was known about the metal complexes of quinonedioxime bqdH$_2$, the scope of the program was enlarged to include Cu(II) and Co(II) chemistry ending up with the preparation of Co - O$_2$ adduct. Due to the difficulty in characterising the insoluble products, except by e.s.r. spectroscopy (Chapter I & II), further research was directed towards the areas like, mixed valence Mn(III,IV), complexes (Chapter III), spin crossover in Fe(II) systems (Chapter IV), and stacking interactions in Ag(I) complex (Chapter V).

These topics continued to attract considerable attention from chemists. The questions for which we sought answers were:

i. Catalytical role of Mn(III,IV) in chemical oxidation of water by reagents like Ce^{4+}. During the course of this study, we encountered the formation of MnO$_4^-$ ion in the process of water

oxidation by Ce^{4+} in the presence of Mn(III,IV) complexes. We have established its presence, conditions for the formation and stability by electronic spectral studies. However its role in oxygen evolution from water in the presence of Mn(III,IV) ions is yet to be established.

ii) Possibility of using e.s.r. of S = 1/2 impurities for characterizing $^5T_2$ - $^1A_1$ spin crossover in Fe(II) compounds. The spin crossover behaviour of the red form of $Fe(Phen)_2(NCS)_2$ was studied by carrying out the variable temperature e.s.r. measurements, using Cu^{2+} doped in to the lattice as the e.s.r. probe. We have confirmed the change in the spin state with temperature by Mössbauer measurements at 298 K and 77 K. Here we were successful in obtaining the $Fe(Phen)_3(NCS)_2 2H_2O$ and its copper doped complex in crystalline form for the first time.

iii) The reasons for the flattening distortions in Ag(I) compounds. In this part of the work a single crystal X-ray diffraction study on $(AgLNO_3)_2$ complex (where L = 6,6'-dimethyl bipyridine) was done. We noticed that the crystal consists of dimeric units of $(AgLNO_3)$ with Ag-Ag bonding. The itner and intra dimer interactions in the lattice are responsible for the flattening distortion noticed in the molecule. The molecule is found to be almost planar and on the whole the dimeric units are packed in the form of a slipped stack in the lattice, with unsymmetrically chelating bidentate NO_3 group.

Each chapter contains a brief introduction about that system, experimental section, followed by results and discussion and lastly conclusions, references and abbreviations of that chapter.

CHAPTER - I

COBALT(II) COMPLEXES OF 9,10-PHENANTHRENEDIONEDIOXIME AND BENZOQUINONEDIOXIME - E.S.R. STUDIES OF THEIR DIOXYGEN ADDUCTS IN THE SOLID STATE

1.1 INTRODUCTION:

Literature survey of planar Co(II) complexes revealed that, so far these complexes have received considerable attention mainly from two different angles. Complexes of schiff bases and related ligands have been considered as possible catalyst for the activation of molecular oxygen.[1-6] Monomeric (superoxo) as well as dimeric (μ-peroxo) dioxygen complexes are well known with this class of ligands[1,2,5]. The oxime complexes on the other hand are studied as possible models for vitamine B_{12}.[1,2,7-9]

The molecular orbital (MO) description of molecular oxygen shows a vacancy for the addition of a single electron in both the antibonding 2PΠg orbitals. The addition of one election results in the formation of superoxide (O_2^-) anion, whereas two electron addition results in the peroxide (O_2^{2-}) anion. While that being the understanding of the terms superoxo and peroxo anions, in the light of the present state of knowledge of the oxygen Co(II) adducts with complexes of schiff bases and related ligands the presence of a Lewis base is necessary to facilitate the reaction between a Co(II) square planar complexes and oxygen.[7] But for the solid state reactions in which there is no other ligand present, six co-ordinated dioxygen adducts are produced by the mutual bridging of phenolic oxygen atoms between neighbouring

1

molecules,[10] to facilitate the reaction between planar complexes and molecular oxygen. Five co-ordinated salicylaldemine Co(II) complex was found to yield a diamagnetic 1:1 $(Co-O_2)$ oxygen adduct.[11] and the Co(salen) active forms have indicated the formation of a 2:1 complex at room temperature[13] *i.e.* the peroxo type species are apparently formed even in the absence of any additional Lewis base.

Magnetic susceptibility measurement of cobalt(II) dioxygen adducts formed from these low spin d^7 cobalt(II) complexes show the presence of only one unpaired electron,[13] and the e.s.r studies of frozen solutions of these complexes revealed that the majority of the unpaired electron density resides on the dioxygen.[14,15]

However, Drago and coworkers[16] proposed that although the dioxygen cobalt complexes have an unpaired electron residing essential in a Π^* orbital and can be considered formally as Co^{III} (O_2^-), there is not necessarily a transfer of an electron from the cobalt metal centre to the dioxygen moiety upon binding. It is suggested that, for a series of cobalt(II) Schiff base compounds, there is a transfer of only 0.1 to 0.8 electron to the coordinated dioxygen fragment, depending upon the ligand environment.

The Schiff's base complexes generally have the highest occupied molecular orbital (HOMO) dominated by d_{yz} component. Axial perturbation by σ-donor ligands changes the HOMO to d_{z^2} and thereby activates the complexes towards the dioxygen binding. In

the case of triazine-1-oxide complex[17] no oxygen adducts are obtained even in donor solvents implying greater separation between d_z2 and d_{yz} orbital. Cobalt(II) dioximates are more susceptible to oxidation and dioxygen complexes which could be possible intermediates in their air oxidation have not been observed so far, except in the case of Vitamin B_{12r}.[18] itself. Most of the coboloxime studies are conducted in solution. The ready oxidation of cobalt(II) dioximates by air may mean that they have HOMO derived from d_z2 orbital even in the absence of axial ligands. However, paucity of the e.s.r. data in the diamagnetic host lattice make verification of this hypothesis difficult. In the case of coboloxime(II) appreciable interaction with oxygen occurs even in the absence of non coordinating solvents leading to departure of magnetic parameter from those of the four co-ordinate complexes.[8]

One of the most useful finger print properties of co-ordinated dioxygen is the O-O stretching frequencies (ν_{o-o}). In all most all cases reported[13,19-22] for monomeric cobalt dioxygen complexes ν_{o_2} values fall in a narrow range (~ 50 cm^{-1}) around 1145 cm^{-1}.

Analysis of the e.s.r spectra of $Co(II)(L_4)B$ and $Co(II)(L_5)$ (where $L = N_2O_2$ type ligand, B = Lewis base) complexes show that the spectrum is attributable to one unpaired electron, the presence of eight line hyperfine is due to the ^{59}Co (I = 7/2) nuclear spin. The $Co(SB_4)B$ typically have $g_\perp$ values 2.30-2.45 and $g_\parallel$ 2.01-2.02 while Co(POr)B having $g_\perp$ = ~ 2.3 an $g_\parallel$ = 2.03.

The e.s.r. spectra of the oxygenated complexes indicate that the unpaired electron has only a small spin density at the cobalt nucleus (A_{co} ~ 10-12 G) as compared with ~ 80 G for non-oxygenated parent compound.[1] The reduced anisotropy in e.s.r results from a spin polarisation mechanism with the unpaired electron residing mainly on O_2 which does not require a formal electron transfer to form O_2^-.

1.1.1 General theory of e.s.r. spectra for molecular oxygen
adducts of cobalt(II) compounds

For a spin 1/2 system, which has two energy levels in a magnetic field, resonance is observed at a fixed microwave frequency, ν, according to the relation

$$h\nu = g\beta B_0$$

where h is plancks constant, and β is the Bohr magneton. B_0 is the resonance magnetic field.[2] Fig.1.1 illustrates the resonance in a two level system, which is usually recorded as just derivative absorption with respect to the magnetic field. The presence of nuclear hyperfine coupling is due to a nucleus with nuclear spin I, leading to the occurrence of a set of $2I+1$ equally spaced nuclear levels. In this case since $I = 7/2$ eight equally spaced hyperfine lines are observed (Fig.1.2).

The spin Hamiltonian giving this spectrum including anisotropic effects in A and g is given by eq.(1)[12]
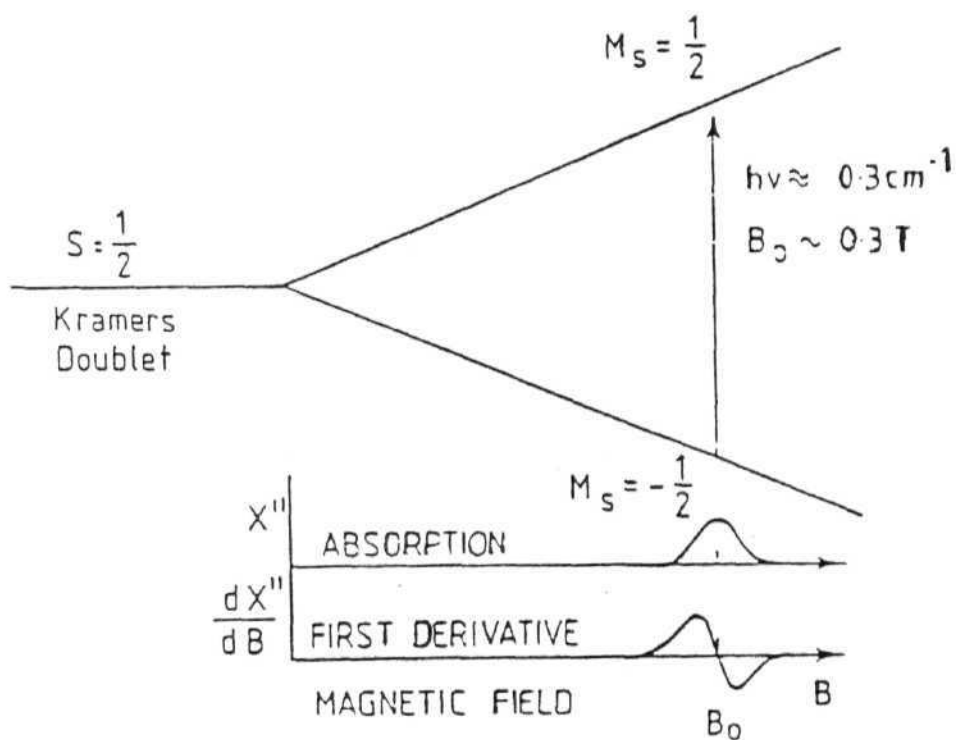
Fig.1.1 E.s.r. in an S = 1/2 doublet. Resonance absorption of energy occurs when the microwave energy(hυ) exactly equals the energy difference between the levels (Ref.2).

5
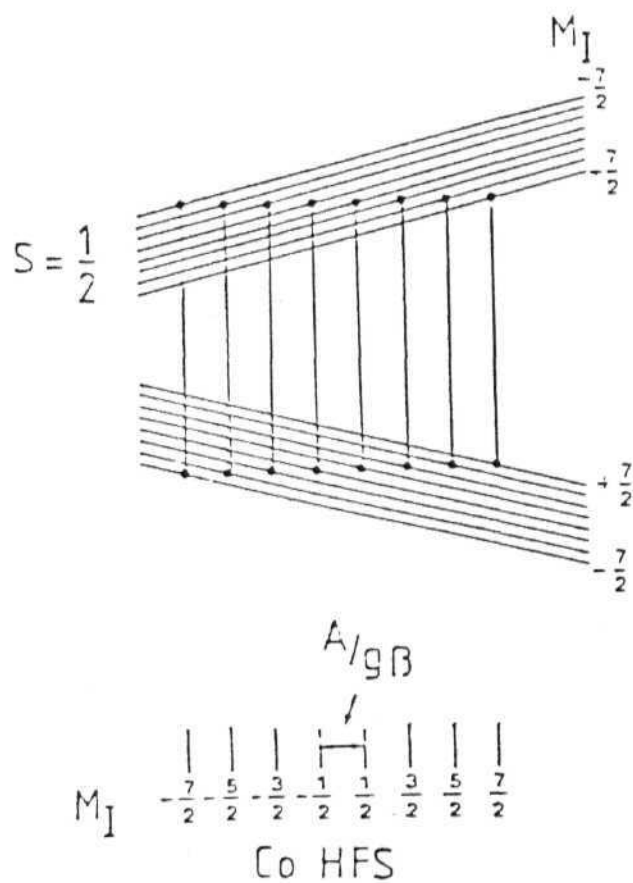
Fig.1.2 Schematic representation of energy levels for cobalt where $S = 1/2$ and $I = 7/2$. Each level of Fig. 1.1 now consists of eight nuclear sublevels. E.s.r. magnetic dipole transitions occur when $\Delta M_I = 0$ (Ref.2).

$$\mathbf{H} = \beta \, \Sigma \, g_i B_i S_i + \Sigma \, A_I S_I I_I \tag{1}$$

$$i = x_g, y_g, z_g \qquad I = x, y, z$$

Here S_i is the effective electron spin, B_i is the field, x_g, y_g, z_g are the molecular axis and x, y, z are standard co-ordinates centered on cobalt(II). Usually x_g and x do not coincide in orientation. In order to keep the analysis and necessary computer simulations manageable, the lowest symmetry 'C_s' will be considered for Co-O$_2$ complexes. When the Zeeman interaction is much larger than the hyperfine terms, which is considered as the well satisfied condition for Co-O$_2$ adducts, the g values for an angular orientation system (sing crystal) is given by eq. (2)[2]

$$g^2 = g_x^2 l_x^2 + g_y^2 l_y^2 + g_z^2 l_z^2 \quad (x = x_g, \; y = y_g, \; z = z_g) \tag{2}$$

and with in the monoclinic symmetry limit[23]

$$g^2 A^2 = A_x^2 \, [g_x l_x \cos\alpha + g_y l_y \sin\alpha]^2 + A_y^2 \, [g_x l_x \sin\alpha +$$

$$g_y l_y \cos\alpha]^2 + A_z^2 g_z^2 l_z^2 \tag{3}$$

Then at a particular orientation of the field B, (for single crystal) the resonance field is given by

$$B = B_o - A/g\beta \ M_I - a[I(I+1)-M_I^2] - bM_I^2 \qquad (4)$$

where 'a' and 'b' which are the second order corrections due to hyperfine interactions, are dependent on $\oplus$ and $\varnothing$.

Because of the anisotropy in g, the intensity of the lines also vary with orientation. In a powder this is complicated by the fact that, although the resonance field depends only on θ and $\varnothing$ values, the intensities due to given molecules with same value of θ and $\varnothing$ differ because all of them do not have same orientation relative to microwave magnetic field in cavity. Then the corrected average value when $B_\perp$ is B_{rf} (rf = resonance field) is given by eq. $(5)^{23,24}$

$$\bar{g}^2 = [g_x^2 g_y^2 \sin\theta + g_y^2 g_z^2 (\sin^2\varnothing + \cos^2\theta \cos^2\varnothing) +$$
$$g_x^2 g_z^2 \ (\cos^2\varnothing + \cos^2\theta \sin^2\varnothing)]/(2g^2) \qquad (5)$$

Line widths may also be anisotropic and for simulation purposes, these also should be considered. As the majority of the studies of $Co-O_2$ adducts are done on powders and frozen solutions, computer simulation programme must seen the spectra due to all possible orientations of the molecules with intensities weighted[2] by the solid angle element $-1/2\Delta \cos\theta \ \Delta\varnothing$ for the range of $[\theta, \theta+\Delta\theta, \varnothing, \varnothing+\Delta\varnothing]$.

8

While there are several e.s.r studies of cobalt(II) complexes of schiff bases and other N_2O_2 ligands doped in the corresponding diamagnetic complexes, with one exception,[25] the e.s.r studies of cobalt(II) dioximates are confined mainly to frozen solutions. In this chapter we present the e.s.r evidence for formation of paramagnetic dioxygen adduct in the solid complexes of cobalt(II) with 9,10-phenanthrenedionedioxime ($pqdH_2$) and benzoquinonedioxime($bqdH_2$). It has also been possible to study $Co(pqdH)_2$ doped in the corresponding nickel complex in different concentrations.

1.2 EXPERIMENTAL

1.2.1 Chemicals:

The starting materials for the preparation of ligands were either bought from Aldrich or Fluka. Other solvents and common chemicals were of reagent grade or better quality. All the organic solvents were purified by standard procedures described in Vogel.[26] Ether was stored over sodium, pyridine over potassium hydroxide pellets, dimethylformamide and diglyme were distilled in vacuum in dry nitrogen atmosphere and stored over type 4A molecular sieves.

1.2.2 Preparation of Ligands:

9,10-phenanthrenedionedioxime($pqdH_2$) is prepared according to the literature procedure.[27] Recrystallised from dry distilled

methanol. I.r and melting points are checked and the product is confirmed from the literature data.

1.2.3. Preparation of benzoquinonedioxime (bqdH$_2$):

Benzoquinonedioxime is prepared according to the literature procedure[28] with minor changes. Benzofuroxan (Aldrich) is used as the starting material. 1gm of Sodiumborohydride (fluka) is added to freshly distilled diglyme and stirred until it is completely dissolved. To this solution 3gm of benzofuroxon is added in small amounts using addition flask. Maintenance of temperature and totally dry and inert conditions are very essential during the preparation. To start with addition of benzofuroxon is done maintaining 35-40°C temperature But during the further addition the temperature of the reaction goes up, so it should be cooled externally with ice. Once addition is complete, the red coloured reaction mixture is stirred for one hour in hot water bath at around 50°C. Till the completion of the reaction, a slow current of dry N$_2$ is continuously circulated through the reaction set up. The reaction mixture is poured into 300 ml of ice-cold distilled water and quenched with 10 ml of glacial acetic acid. The solution is cooled for 5 hours at 0°C. Black crystalline solid separated out. It is recrystallised from 50% EtOH. Golden reddish crystals are obtained yield is ~ 50%, sharp m.p. at 245°c. I.r spectrum is recorded.

1.2.4. Preparation of Complexes:

a) Preparation Co(II) complex of pqdH$_2$:

To a hot solution of 60°C of 260 mg (1.05×10^{-3} mol) of (pqdH$_2$) dissolved in 60 ml methanol, a solution of 125 mg (2.12×10^{-3} mol)[28] of CoCl$_2$ 6H$_2$O in 25 ml of methanol was added drop wise with constant stirring. A reddish brown precipitate which formed immediately, was stirred in the solution for another half an hour, filtered, washed several times with hot methanol and finally with diethylether. This product was dried in vacuum at 80°C. It was sparingly soluble in chloroform and pyridine and could be recrystallisd without decomposition from chloroform. Yield : ~80%

b) Prepration of Cobalt doped Ni(pqdH)$_2$:

5% and 50% cobalt doped samples of Ni(pqdH)$_2$ are prepared using mixed metal solutions. 5% and 50% (by molar ratio) CoCl$_2$6H$_2$O is mixed with NiCl$_2$6H$_2$O in 50 ml ethanol solution. This mixed metal solution is added to the hot ligand solution following the similar procedure as described for Ni(pqdH)$_2$ in chapter II. The exact percentage of cobalt in the complexes obtained was not determined.

c) Preparation of Cobalt(II) complex of bqdH$_2$:

It is found that cobalt complex of bqdH$_2$ is more reactive

towards oxygen than the analogous pqdH$_2$ complex. So changes are made in the preparation procedure reported earlier[27] so as to avoid air completely(Fig 1.3).

To start with ethanol is distilled under nitrogen over sodiumethoxide. 402 mg of (2.91 x 10^{-3} mol) of (bqdH$_2$) is taken in a 250 ml of R.B. flask with a side arm for nitrogen inlet. This flask is connected to another 250 ml R.B. flask of similar type through a G$_4$ grade glass frit, the entire set up is placed in a mantle and flushed with a jet of dry nitrogen under warm temperatures. There the pre-distilled 50 ml ethanol is added to the ligand. The ligand in ethanol is heated gently at 60°C in methanol is totally dissolved in ethanol 200 mg (8.33 x 10^{-4} mol) of CoCl$_2$ 6H$_2$O placed in upper part of the glass frit (Fig.1.3) (before starting experiment) and 20 ml of ethanol is added on to it, flushing system with nitrogen throughout. Since at this stage nitrogen current is flowing in opposite direction, the CoCl$_2$6H$_2$O solid dissolve in 20 ml ethanol with out any further stirring in the glass frit itself and remains there only. Now the direction of nitrogen flow is reversed, then slowly the CoCl$_2$6H$_2$O ethanol solution flows in to R.B. flask containing ligand solution, mixes there and forms a black solid. Now the flask is reversed and the compound is filtered through the frit. The solid complex formed remains on the frit and is dried in a stream of dry nitrogen over night. Then transferred in to a glove-bag under nitrogen. There it is powdered well and transferred in to a dry e.s.r. tube flushed with nitrogen and sealed under nitrogen atmosphere. I.r spectrum is recorded and as it is found to be air sensitive C,H,N analysis is not

Nitrogen outlet

$CoCl_2 6H_2O$

Ligand Solution

Nitrogen inlet
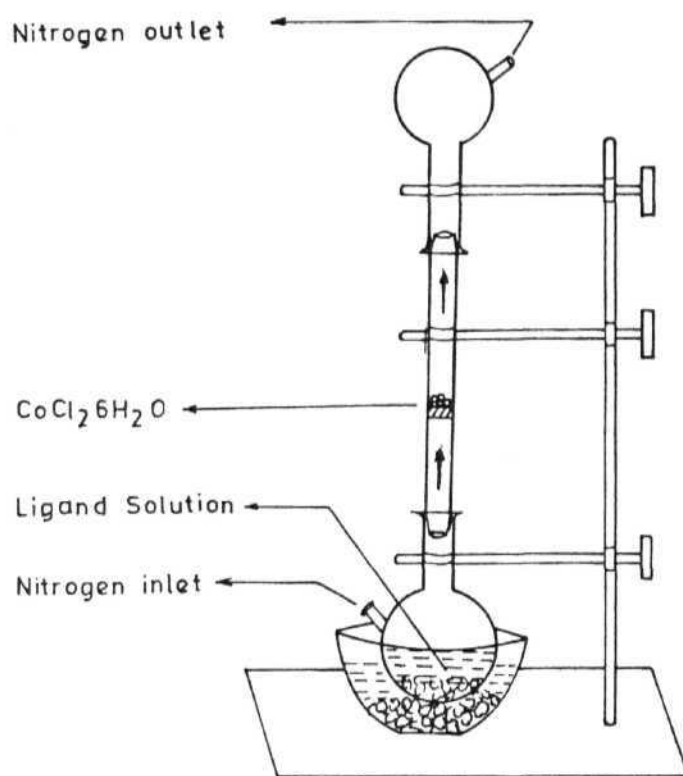
Fig.1.3 Diagram showing the experimental set-up for the
preparation of Co(II) bqdH$_2$ oxygen adduct.

performed.   Yield is around 60%

Cobalt doped $Ni(bqdH)_2$ could not be prepared as cobalt did not get doped in to the host lattice.

1.2.5. Elemental Analysis Data:

Based on the e.s.r. and magnetic susceptibility data this compound was formulated as a mixture of $Co(pqdH)_2O_2$ and a diamagnetic part.   The elemental analysis data fits better with formulation of the diamagnetic component as $Co(pqdH)_3$ rather than $(pqdH)_2$ CoO_2 $CO(pqdH)_2$.   Cobalt is estimated by gravimetry.[29]

Experimental values: C =65.1, H = 3.8, N = 10.7, Co = 8.3%

Calculated values are as follows: For $Co(pqdH)_3$

C = 65.4, H = 3 5, N = 10.9, Co = 7.7% for 78% of $Co(pqdH)_3$ + 28% $Co(pqdH)_2O_2$ C = 64.1, H = 3.5, N = 10.7, Co = 8.3%.

1.2.6. Physical Measurements:

I.r spectra were recorded on Perkin Elmer model 1310. infrared spectrophotometer.   Electronic spectra were recorded on SChimadzu.200S double beam spectrophotometer.   C,H,N analysis was done on Perkin Elmer -240C analyzer.   E.s.r. spectra at X-band were measured on JEOL FE-3X spectrometer.   Measurements below room temperature were made using controlled boil off from a liquid nitrogen cryostat.   Q-band e.s.r. spectra were measured on

varian E-112 spectrometer. To measure Q-band spectra at 77 K was used. Magnetic susceptibility in the temperature range 20-295 K was measured by the Faraday method. The sample was mounted on the cold head of a closed cycle cryostat.

1.2.7. Computer simulation of e.s.r. spectra:

Powder spectra of the magnetically dilute complexes were simulated using a previously described computer program [72] which was modified to include ligand hyperfine interaction in first order. The calculations were performed on IBM compatible P.C.L personal computer (PC XT). A typical simulation with grid spacing 3° in Θ 90° in $\emptyset$ need 25 minutes computer time.

1.3 RESULTS AND DISCUSSION:

1.3.1 I.R. spectra of Cobalt complexes of $pqdH_2$ and $bqdH_2$.

The i.r spectral frequencies of the cobalt complex of $pqdH_2$ and $bqdH_2$ are tabulated in Table 1.1. Even though ν_{o-o} stretching frequency around 1145 cm^{-1} ($\sim$ 50 cm^{-1}) are characteristic features of $Co-O_2$ adducts,[2] unfortunately no definite conclusion can be drawn from these spectra because of the interference of ligand vibrations in the 850-1150 cm^{-1} region of the i.r. spectra of cobalt $pqdH_2$ oxygen adduct and cobalt $bqdH_2$ oxygen adduct respectively.

15

Table -1.1: IR Spectra (cm^{-1}) of oxygen adducts of cobalt(II) and their corresponding ligands.

pqdH$_2$	Oxygen adduct of cobalt(II) (pqdH$_2$)	bqdH$_2$	Oxygen adduct of cobalt(II) (bqdH$_2$)
3200 (vb)	3050 (w)	3075 (b)	3000 (vb)
1600	1600 (w)	2750 (b)	1700 (w,b)
1480	1580 (sh)	1640	1680
1440	1530 (w,b)	1620	1560
1340	1480	1580 (vw)	1440
1300	1440	1500	1370 (b)
1220	1320 (w)	1440	1280 (b)
	1300		
1160 (w)	1280	1380	1200
1110	1180	1310	1180
1095	1150	1240	
1040	1120	1170	1050
1030	1100 (sh)	1080	900
1020	1080 (vw)	1030	760
910	960 (b)	900	620
880	900 (b)	840 (sh)	
840	780	820	
780	720	760	
760		720	
720		640	

b=broad, s=sharp, sh=shoulder, v=very, w=weak.

1.3.2 Electronic spectra of cobalt complex of pqdH$_2$:

The electronic spectrum of this compound in chloroform consists of a strong absorption in the visible region Fig.1.4a. In pyridine solution the band is shifted to higher energy υ = 22000 cm^{-1} (Fig.1.4b) (ε = 4.4 x 410 1 mole^{-1} cm). The high values of the extension coefficient imply that these bands correspond to charge transfer or intra-ligand excitations rather than ligand field transitions.

1.3.3 Magneticsusceptibility measurements data for cobalt complex of pqdH$_2$:

Fig.1.5 shows the variation of the gram susceptibility with temperature in the range of 20-295 K. The close fit to the curie law along with low magnetic moment (1.0 BM calculated on the basis of Co(pqdH$_2$) is consistent with the formulation of the product as a mixture of paramagnetic and diamagnetic substances. While the obvious choice for the diamagnetic component would have been the peroxo-dimer, the elemental composition favour Co(pqdH)$_3$. This is analogous to the formation of octahedral cobalt(III) complexes from cobalt(II) salts in the presence of air.[31]

1.3.4 X-band e.s.r. spectral data of the cobalt complex of pqdH$_2$ (oxygen adduct)

Fig.1.6 shows the spectrum of the cobalt complex of pdqH$_2$ recrystallised from chloroform. There is no significant change
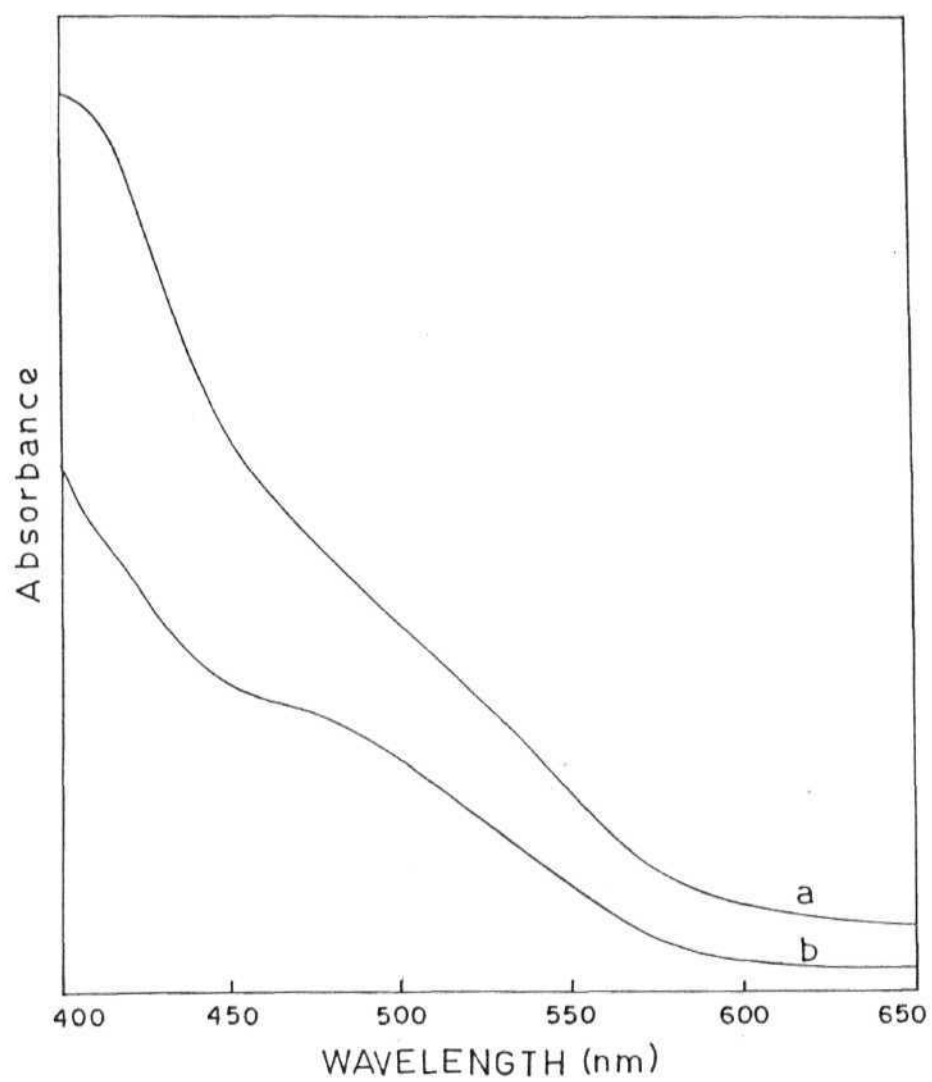
Fig.1.4 Electronic spectra of Co(II) pqdH$_2$ oxygen adduct in (a) CHCl$_3$ (b) Py.
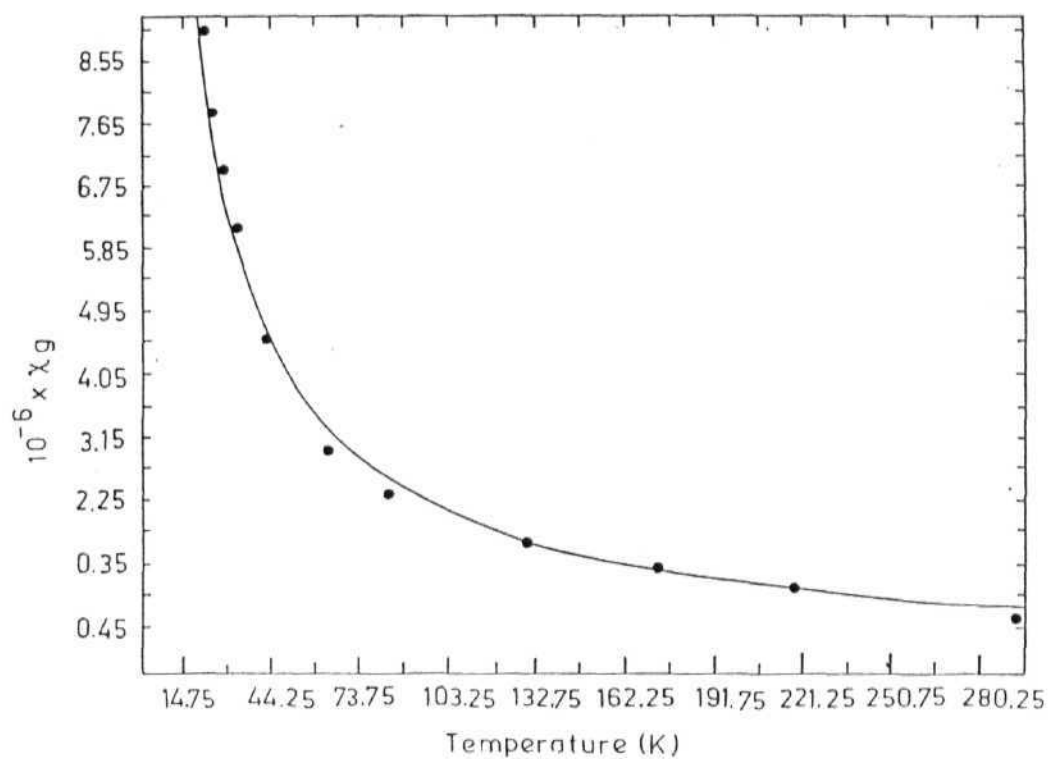
Fig.1.5 Temperature dependence of the gram susceptibility (χ_g)

of Co(II) pqdH$_2$ oxygen adduct.

. represents Experimental points.

- represents least square fitting.
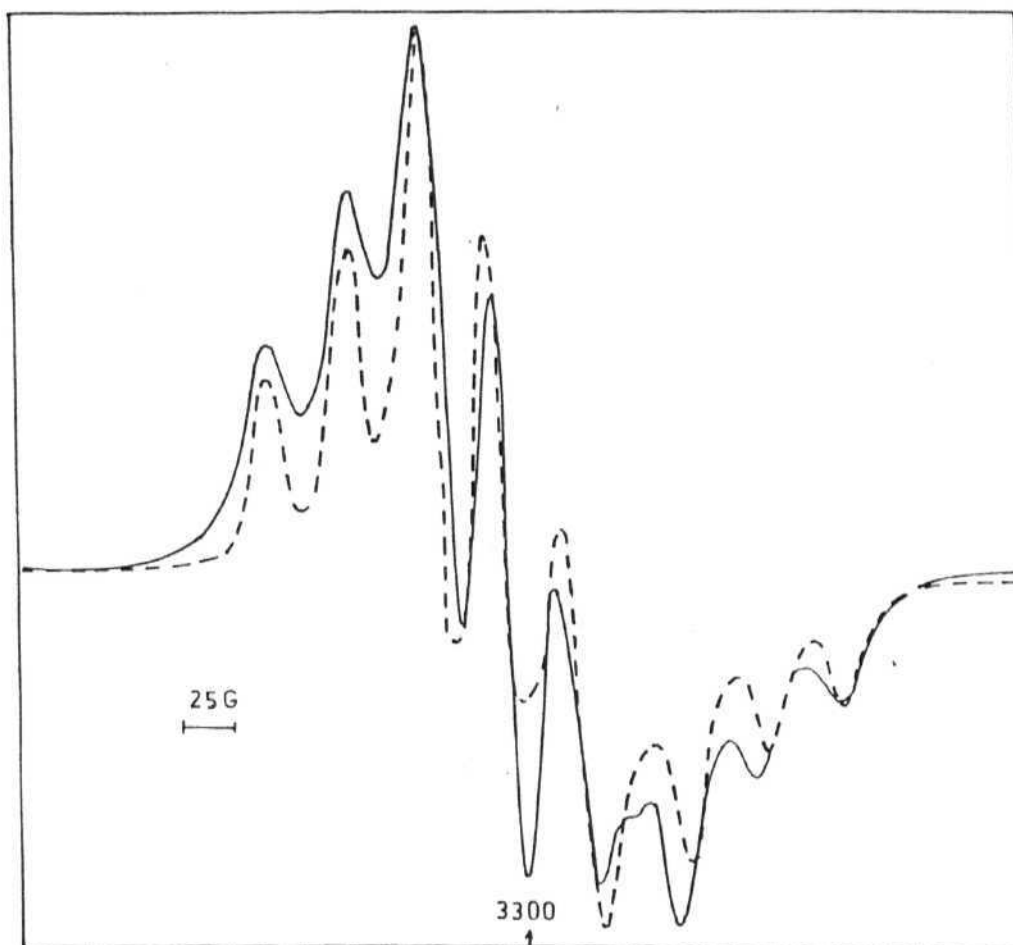
Fig.1.6   Simulated X-band e.s.r. spectrum of powder Co(II) pqdH$_2$
oxygen adduct at 298 K.

..... represents experimental spectrum.

——— represents simulated spectrum.

in the spectrum upon cooling the sample to 120 K. The resolution
of the spectrum is better in the chloroform recrystallised
sample compared to crude sample. The Q-band spectrum of the same
sample at room temperature is shown in Fig.1.7. The room
temperature X-band spectrum consists of signals from two distinct
species, one giving rise to clearly identifiable 8 lines from
^{59}Co (I = 7/2) hyperfine splitting and another which gives a
strong single line at g ~ 2. The intensity of latter varied from
sample to sample. When a freshly prepared sample is suspended in
water and oxygenated by bubbling air, the intensity of both
the signals increase initially. However, upon continued
oxygenation for a long time, the intensity of the single line
increases, while the 8-line pattern diminishes.(1.8.a,b,c) From
the e.s.r. studies on cobalt(II) four co-ordinated planar
complexes it is clear that, these complexes show a well resolved
eight line pattern with high g and A values ($g_\perp$> 2.3, and $g_\parallel$ ~
2.02, A_{Co} ~ 80G) and on co-ordination with oxygen in axial
position, a great change in the e.s.r parameters is observed.
The significant change is observed in A values which decreases to
10-12 G. This is attributed as due to d_{z^2} becoming the HOMO and
due to unpaired electron spin density polarising effects.[1]
Fig.1.9 show the M.O. diagram of Co(II) which illustrates the
electronic arrangement making dioxygen co-ordination feasible in
cobalt(II). In the present case the values obtained from the
simulated e.s.r spectra an given in Table 1.2. Very much reduced
^{59}Co hyperfine splittings clearly indicate that the spectrum can
not arise from a magnetically dilute planar four co-ordinated
cobalt(II) complex. The magnetic parameters, can be readily
understood if dioxygen on air bubbling is added on to the axial

21
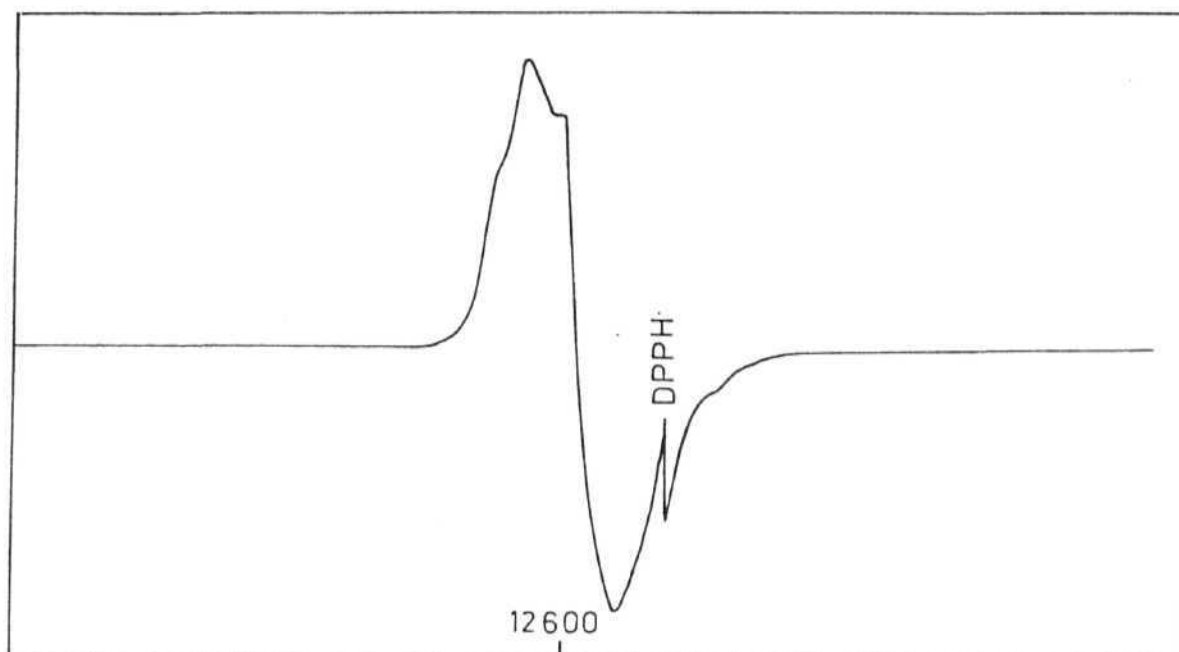
Fig.1.7 Q-band e.s.r. spectrum of powder Co(II) pqdH$_2$ oxygen
adduct at 298 K.

3475
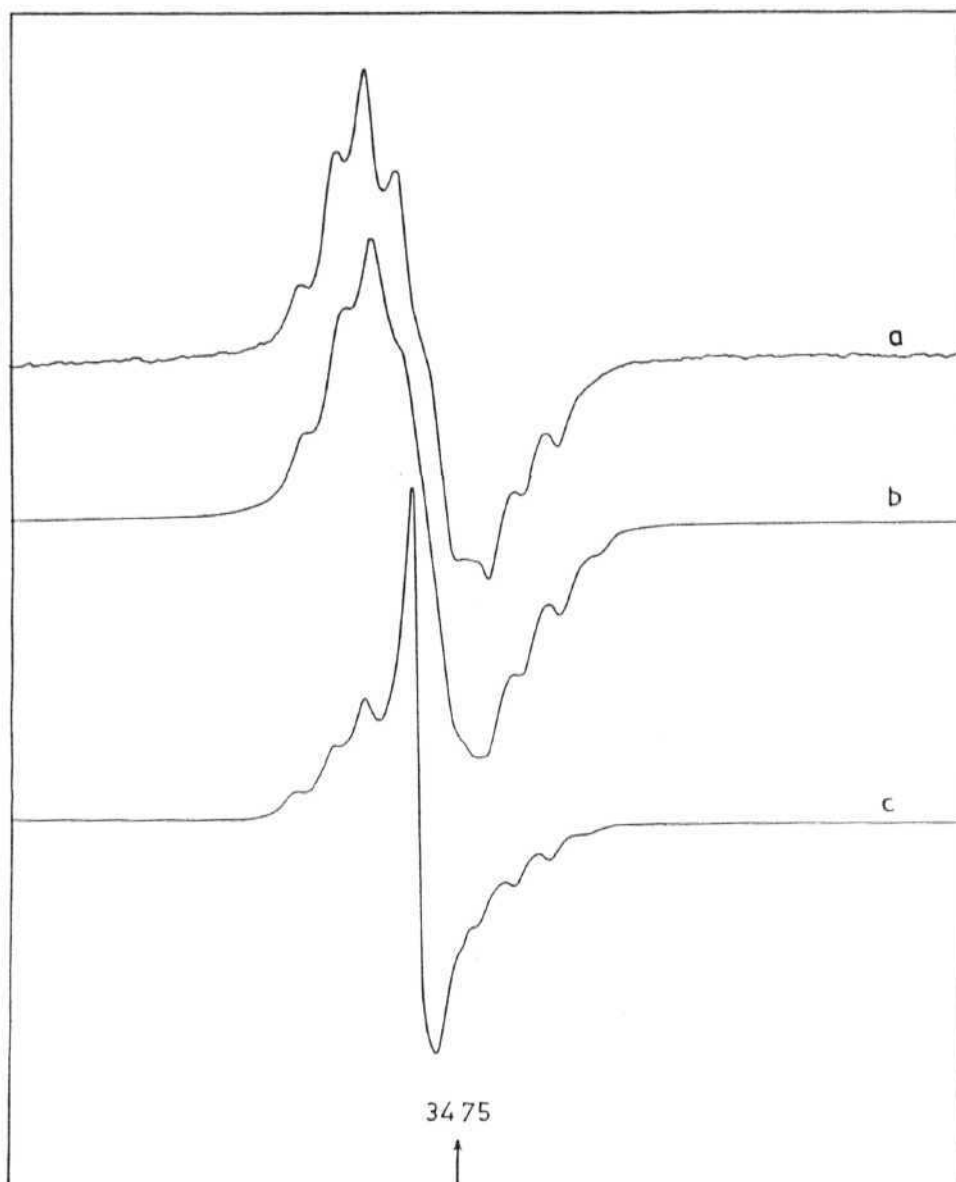
Fig.1.8 X-band e.s.r. spectrum of powder Co(II)pqdH$_2$ oxygen
adduct at 298 K.

   a) Sample prepared by usual method.

   b) Sample obtained by circulating jet of air for 24 hrs
   by suspending complex in water.

   c) Sample obtained by circulating jet of air during
   preparation process itself.

23
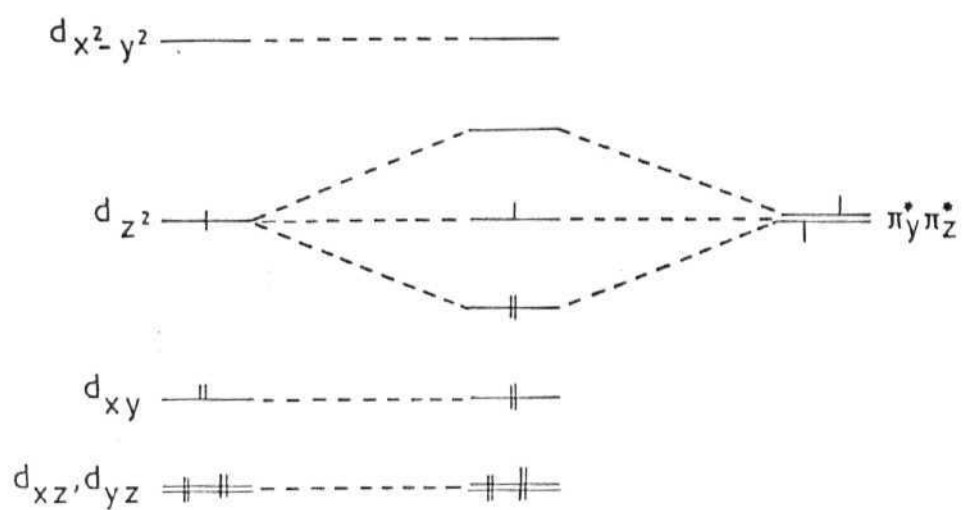
Fig.1.9 Molecular orbital interaction diagram for the coordination of dioxygen to Co(II) dioximates.

position to give $Co(pqdH)_2O_2$. Compared to the dioxygen adducts of penta coordinated Co(II) complexes ($g_{\parallel} \sim 2.08$, $g_{\perp} \sim 2.0$, $A_{\parallel} \sim 20 \times 10^{-4}$ cm^{-1}, $A_{\perp} \sim 10 \times 10^{-4} cm^{-1}$) the present complex has significantly lower g-anisotropy (Table 2) and also reduced ^{59}Co hyperfine splittings ($A_x = 2.5 \times 10^{-4}$, $A_y = 8 \times 10^{-4}$, $A_z = 19 \times 10^{-4}$ cm^{-1}). The reduced A values make it clear that the unpaired electron no longer resides on cobalt, but is shifted to oxygen confirming the formation of oxygen adduct.

The choice between superoxo and peroxo coordination in the present complex is made on following assumptions.

The e.s.r. parameters fit more to a peroxy radical ($g \sim 2.02$)[31] rather than superoxide ($g \sim 2.08$)[32] description for the coordinated molecular oxygen. While the peroxy or superoxo designation does not necessarily imply complete charge transfer, it is likely that the O-O bond is considerably weakened upon coordination with the dioximato complex. However, it could not be definitely confirmed from any other means. In a recent study Gupta et al[33] obtained a similar kind of e.s.r spectrum for $[4-NHCOCH_3C_6H_4CH_2Co^{IV} (dmgH)_2Py]^+$ in CH_2Cl_2 frozen solution and they attribute this due to the CO^{IV} by the oxidation of Co^{III} complex with Br_2. Since it is highly unlikely that aerial oxidation can lead to the formation of Co^{IV} from Co^{III}, the spectrum reported here is assigned to the O_2 adduct of the Co^{II} complex. It is worth pointing out that this spectra is very similar (with nearly same parameters) to that of the $\dot{Co}^{IV}$ species mentioned above, making it impossible to distinguish between the two, based on e.s.r. spectra alone.

1.3.5 X-band e.s.r spectral data of cobalt(II) benzoquinonedioxime (oxygen adduct):

The cobalt(II) bezoquinonedioxime also showed similar kind of behaviour in the powder e.s.r spectrum both at room temperature and low temperature. The details of the e.s.r parameters are given in the Table 1.2 (Fig.1.10) shows the simulated powder spectrum at room temperature. The g values are nearly axially symmetric and this sample is highly air sensitive. The freshly prepared samples (1) sealed under nitrogen (Fig.1.11 a) and (2) exposed to atmosphere (Fig.1.11 b) initially gave identical spectra, but on aging of the sample (2) the hyperfine disappears results in a broad signal(Fig. 1.11.c).

Whereas the sample sealed under nitrogen continued to give same spectrum even after long aging(Fig. 1.11 d). The increase in width leading to the disappearance of splitting arise from dipolar interaction. There is no evidence of any low field broad signal due to Co(II) high spin species. Fig.1.12 shows Q-band spectrum of the same sample at room temperature. Therefore the interaction showed between $Co-O_2$ centers which increase in concentration with continued exposure to air.

1.3.6 X-band e.s.r. spectral data of cobalt doped $Ni(pqdH)_2$:

Fig.1.13 shows the e.s.r spectrum of cobalt doped nickel(II)$(pqdH)_2$ complex at room temperature and Fig.1.14 shows the simulated spectrum of the same sample at low temperature.
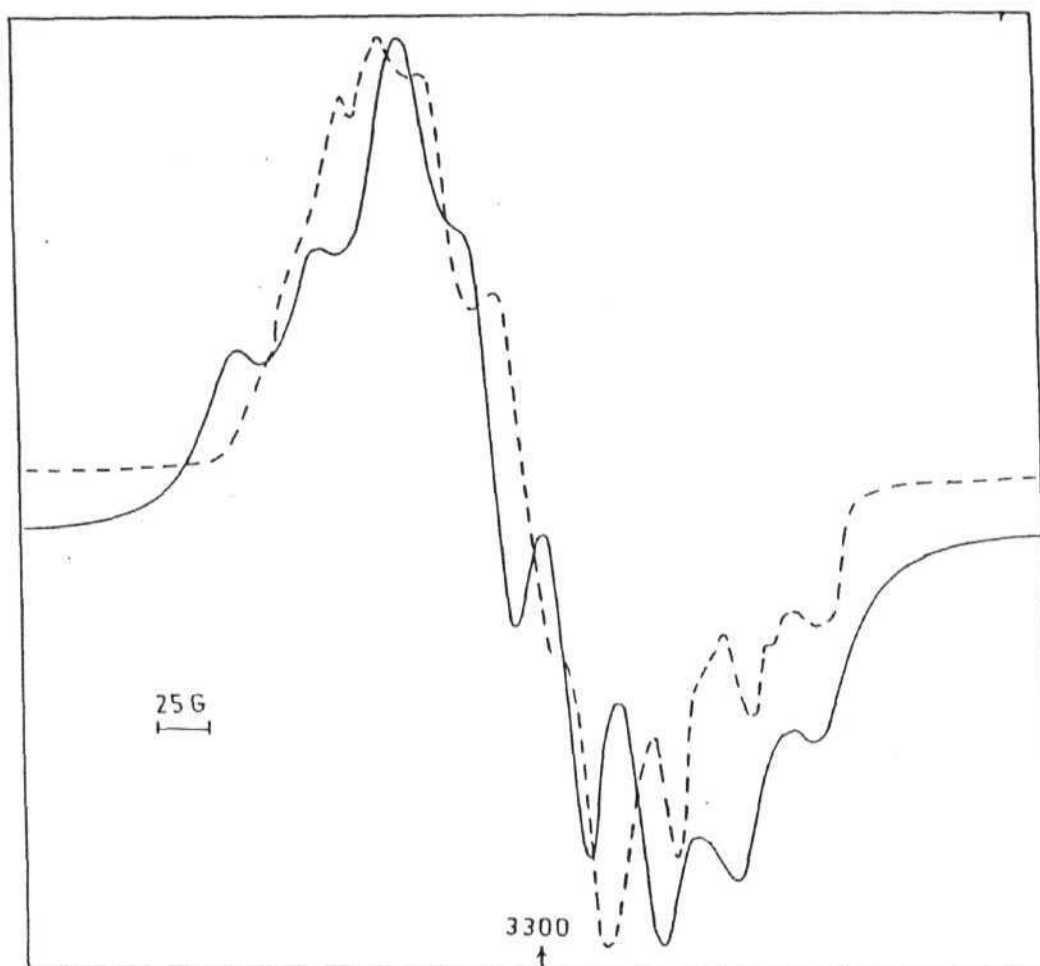
**Fig.1.10** X-band e.s.r. spectrum of powder Co(II)bqdH$_2$ oxygen
adduct at 298 K

..... represents experimental spectrum.

——— represents simulated spectrum.
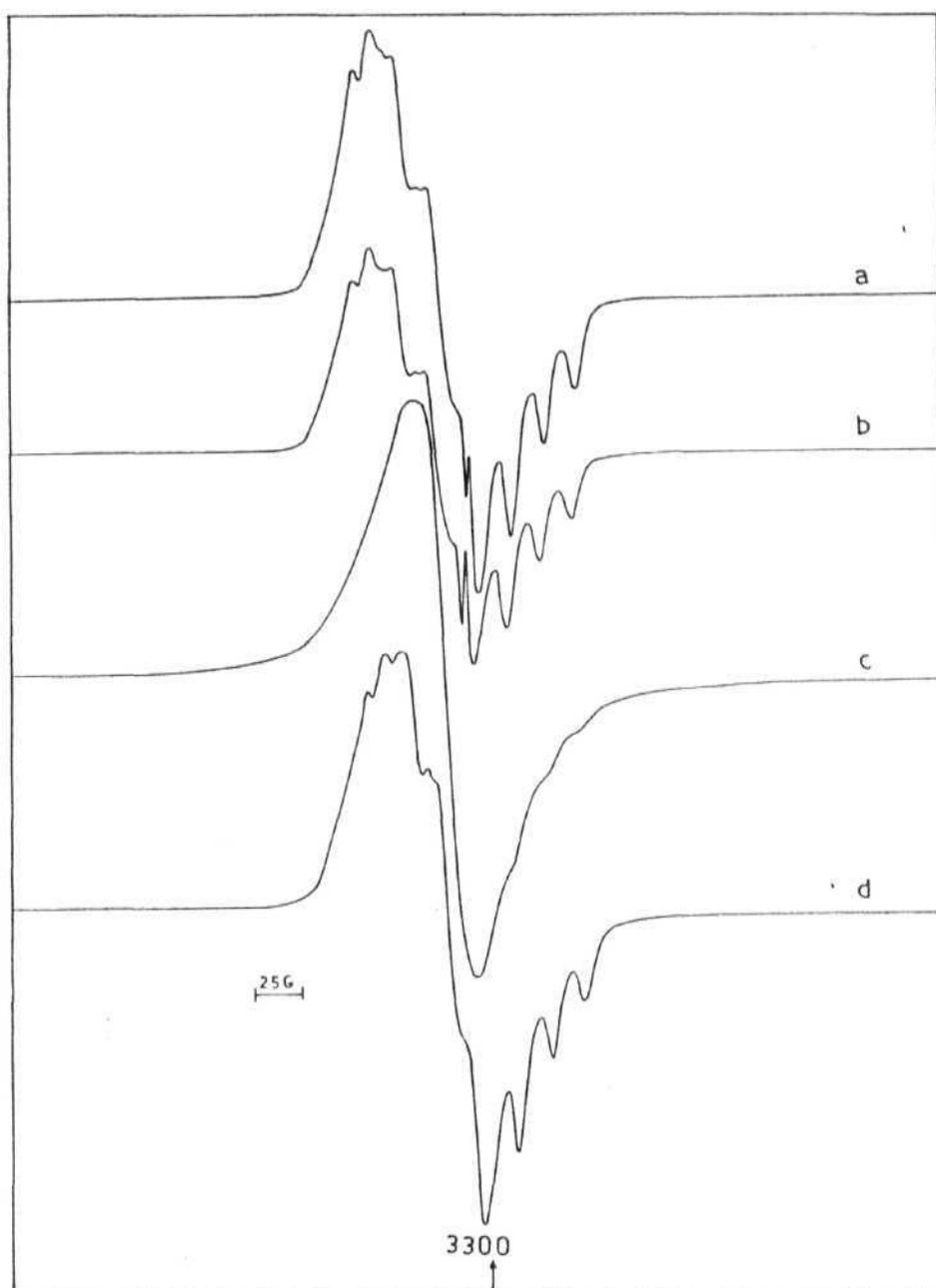
Fig.1.11 X-band e.s.r. spectrum of powder Co(II) bqdH$_2$ oxygen
adduct at 298 K

    a) Fresh sample sealed under nitrogen.

    b) Fresh sample exposed to air.

    c) Sample exposed to air for a long period.

    d) Sample sealed under nitrogen for a long period.

12400
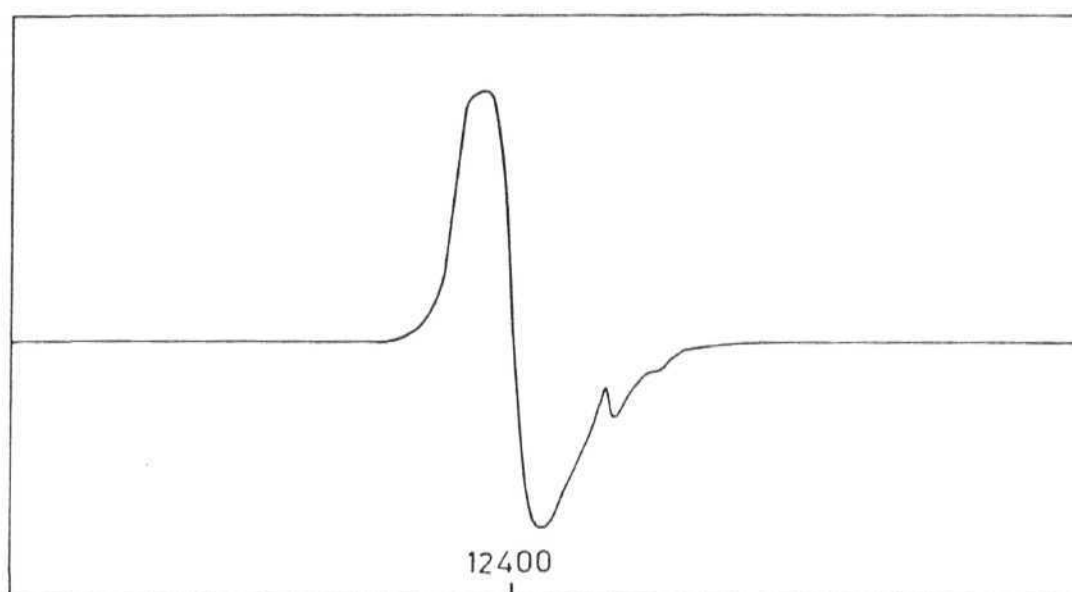
Fig.1.12 Q-band e.s.r. spectrum of powder Co(II) bqdH$_2$ oxygen
adduct at 298 K.

29

The g and A values are tabulated in (Table 1.2). The nearly axially symmetric g and A values are consistent with the square planar cobalt(II) complexes of N_2O_2 type ligands. The simulation here is hampered by the presence of an intense unidentified sharp signal in the centre of the spectrum. This signal is also seen in the host compound itself at room temperature at nearly free ectron g-value. The absence of $Co(pqdH)_2$ signals in room temperature spectrum (Fig.1.13) can be due to the fast relaxation via spin orbit coupling to low lying quartet slates, as is usual the case with planar cobalt(II) complexes. The e.s.r parameters of the low temperature spectrum clearly corresponds to a $^2A_1$ (d_z2) ground state.[3,34] Assuming that the ligand field parameters are not widely different in schiff base and oxime complexes, we find from the plots of Zelewsky et al[4] that the $^2A_1$ (d_z2) state is about 5,000 cm^{-1} below the $^2A_2(d_{yz})$ state. In the case of schiff base complexes the d_z2 ground state is observed mainly in coordinating solvents but not in nickel(II) as host compound.[3] In free co(salen), two magnetically dilute sites are observed in oxygenated samples.[5] One site belongs to d_z2 ground state, thought to arise from axial perturbation by oxygen atoms of the neighbouring molecules, while the second site which is observed only after repeated oxygenation/deoxygenation cycles belong to the d_{yz} state and is ascribed to planar four coordinate co(salen) molecules. The adoption of d_z2 ground state by the present dioximato complex in the nickel host complex implies that the separation between $^2A_1$ (d_z2) and $^2A_2$ (d_{yz}) states is small in the isolated planar complex (believed to have $^2A_2(d_{yz})$ ground state), so that weak axial perturbation by the host lattice is sufficient to cause a switch over to the $^2A_1$ (d_z2) state. This

Table -1.2: E.s.r. parameters of powder cobalt(II) complexes of pqdH$_2$ and bqdH$_2$ (Simulated values)

Compound	Temp K.	g_x	g_y	g_z	A_x	A_y	A_z
Cobalt(II) oxygen adduct of (pqdH$_2$)	298	2.018	2.011	2.009	2.5	8.0	19.0
Cobalt(II) oxygen adduct of (bqdH$_2$)	298	2.018	2.009	2.015	2.5	8.0	19.0
Cobalt(II) doped Ni(pqdH$_2$)	108	2.150	2.20	2.01	28.0	68.0	141.0
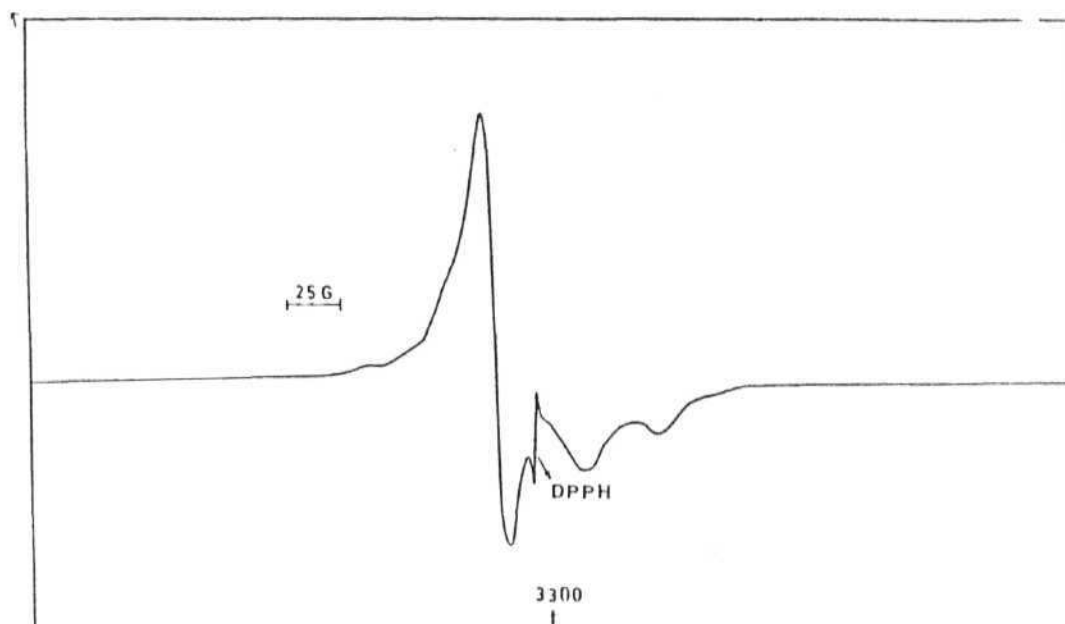
Fig.1.13 X-band e.s.r. spectrum of cobalt doped Ni(pqdH)$_2$ powder
        at 298 K.
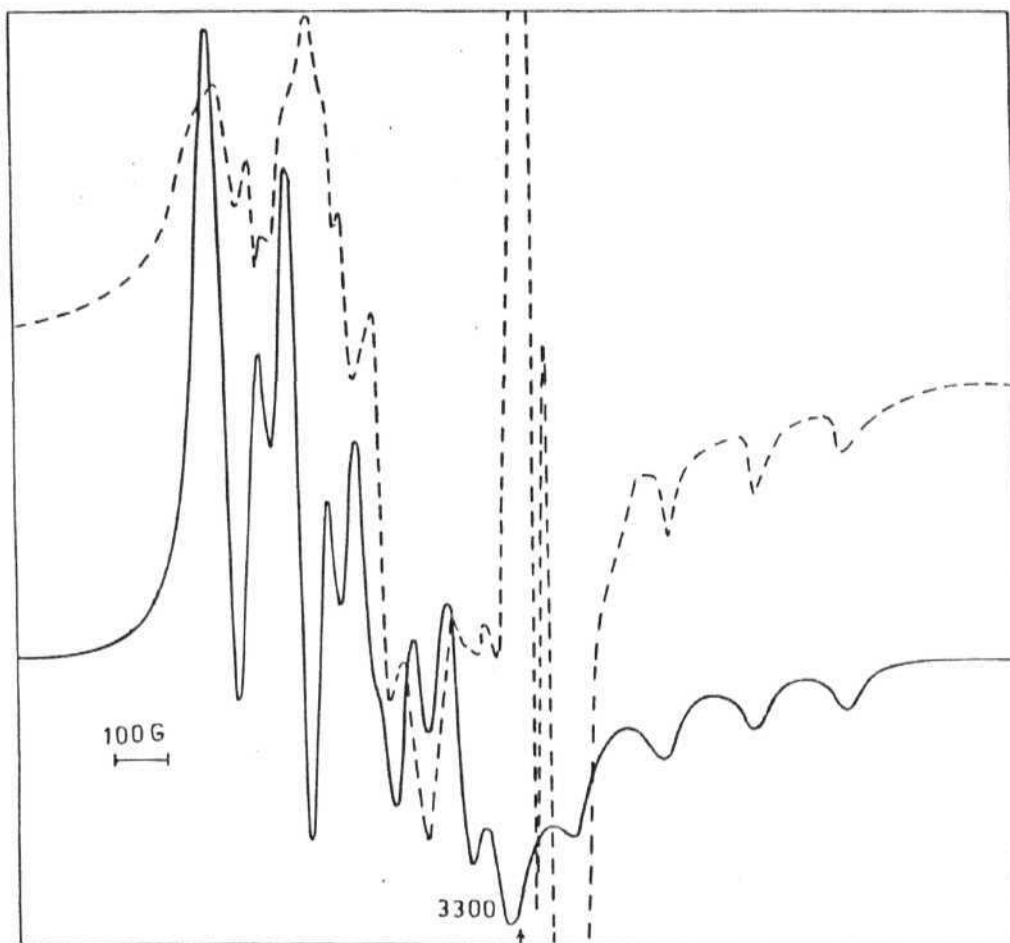
Fig.1.14 Simulated X-band e.s.r. spectrum of cobalt doped Ni(pqdH)$_2$ powder at 108 K.

.... represents experimental spectrum

———— represents simulated spectrum
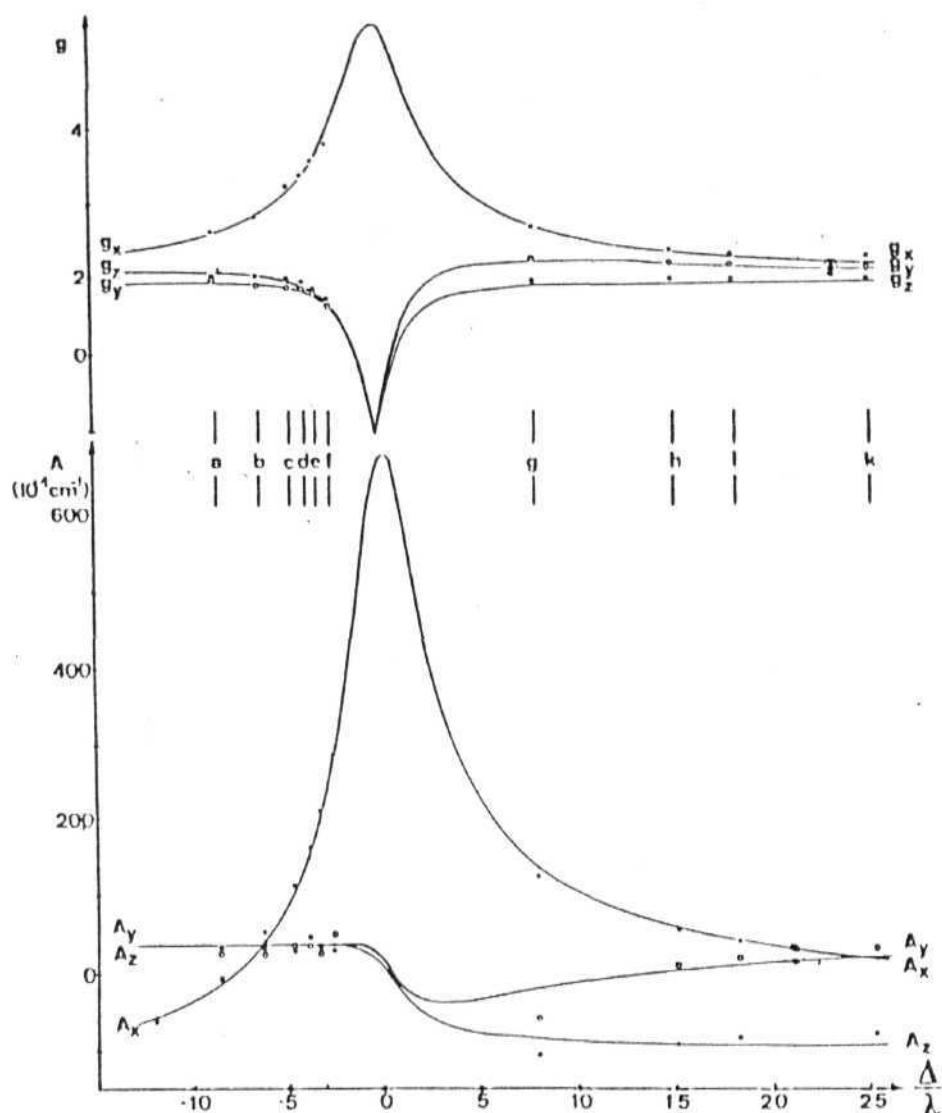
Fig.1.15 EPR parameters in the refined model including quartet states as a function of Δ/λ. The solid lines represent the functions calculated from Eq. (10).[4] The energy parameters were obtained through least square fitting of the EPR data of ten complexes: (a) Co(amben); (b) Co(tacacen); (c) Co(acacen); (d) Co(bzacacen); (e) Co(CF$_3$acacen); (f) Co(salen); (g) [Co(salen)]$_2$; (h) Co(bzacacen)py; (i) Co(salen)P(C$_6$H$_5$)$_3$; (k) Co(saphen)py$_2$.P = 220.8.10^{-4} cm^{-1}; k = 0.2 (scaled with a^2); Δ_{xz} = 9.4 λ, Q = 2.5 λ; R = 2.2 λ. (Ref.4).

is consistent with greater reactivity towards oxygen leading to eventual oxidation of the metal.

1.3.7 Q-band e.s.r. spectral details of cobalt complexes of $pqdH_2$ and $bqdH_2$

The Q-band spectra of oxygen adducts of both the complexes did not give any hyperfine both at room temperature and low temperature. Instead they showed only a broad single signal. Fig.1.7 and 1.12 shows the details of the spectra.

1.4 CONCLUSIONS:

1. Co(II) dioximate systems studied in this chapter have affinity towards oxygen in the solid state even in the absence of axially perturbing bases unlike schiff base complexes.

2. From the e.s.r. parameters of pure cobalt(II) complexes, it is likely that the paramagnetism is due to oxygen centered peroxy radical.

3. The e.s.r. parameters of the cobalt doped nickel complex show that it is a typical system of four coordinated planar $cobalt^{2+}$ with $(^2A_1)$ (d^2_z) ground state.

1.5   Abbreviations:

pqdH$_2$: 9,10-Phenanthrenedionedioxime

bqdH$_2$: benzoquinonedioxime

dmgH$_2$: dimethylglyoxime

SB   : Schiff base

pOr   : porphyrin

1.6   REFERENCES:

1.   Jones, R.D.; Summerville, D.A.; Basolo, F. *Chem. Rev.*, 1979, **79**, 139.

2.   Smith, T.D.; Pilbrow, J.R. *Coord. Chem. Rev.*, 1981, **39**, 296.

3.   Daul, C.; SChlapfer, C.W.; Zelewsky, A.V. Structure and Bonding 1979, **36**, 129.

4.   Hitchman, M.A. *Inorg. Chem.*, 1977, **16**, 1985.

5.   Murray, K.S.; Bergin, A.V.; Kennedy, B.J..; West.B.O. *Austl. J. Chem.*, 1986, **39**, 1479.

6.   Herron, N. *Inorg. Chem.*, 1986, **25**, 4714.

7.   Rockenbauer, A.; Zahonyi, E.B.; Simandi, L.I.J. *Chem. Soc. Dalton Trans.*, 1975, 1729.

8.   Baumgarten, M.; Lubitz, W.; Winscom, C.J. *Chem. Phys. Letters*, 1987, **133**, 102.

9.   Lopaez, C.; Alvarez, S.; Solans, X; Font-Altaba, M. *Inorg. Chem. Acta,* 1986, **L 19**, 111.

10. Niswander, R.H.; Taylor, L.T. *J. Am. Chem. Soc.*, 1977, **99**, 5935.

11. Bailer, R.H.; Calvin, M. *J. Am. Chem. Soc.*, 1947, **69**, 1717.

12. Calligaris, M.; Narden, G.; Randaccio, C.D.; Ripemonti, A. *J. Chem. Soc.* A, 1970, 1069.

13. Floriani, C.F.; Calderazzo, F. *J. Chem. Soc.* A, 1969, 946.

14. Hoffman, B.M.; Dieminte, D.L.; Basolo, F. *J. Am. Chem. Soc.*, 1970, **61**, 92.

15. Getz, D.; Melemud, E.; Silver, B.C.; Dori, Z. *J. Am. Chem. Soc.*, 1975, **97**, 3846.

16. Tovrog, B.S.; Kitko, D.J.; Drago, *J. Am. Chem. Soc.,* 1975, **97**, 3846.

17. Chako, V.P.; Manoharan, P.T. *J. Magn. Res.*, 1974, **16**, 75.

18. Jorin, E.; SChweiger, A.; Gcuthard, H. *Chem. Phys. Letters*, 1979, **61**, 228.

19. Crumbliss, A.L.; Basolo, F. *Science* 1969, **164**, 1168.

20. Crumbliss, A.L.; Basolo, F. *J. Am. Chem. Soc.* 1970, **92**, 55.

21. Collman, J.P.; Brauman, J.I. Halbert, T.R.; Suslick, K.S. *Proc. Natl. Acad. Sci.*, U.S.A. 1976, **73**, 3333.

22. Cape, T.W.; Szymanski, T.; Duyne, R.V. Basolo, F. *J. Chem. Soc. Chem. Commun.*, 1979, 5.

23. Pilbrow, J.R.; Winfiled, M.E. *Mol. Phys.*, 1973, **25**, 1073.

24. Pilbrow, J.R. *Mol. Phys.*, 1969, **16**, 307.

25. Lubitz, W.; Winscom, C.J.; Dregruber, H.; Mosilu, R. unpublished results quoted in reference.[6]

26. Furniss, B.S.; Hanaford, A.J.; Rogers, V.; Smith, P.W.G.; Tatchell, A.R. Ed. ELBS (1978), Vogels Text-book of practical oranic chemistry.

27. Schmidt, J.; Soll, *J. Ber.* 1907, **40**, 2456.

28. Boyear, J.H.; Ellzcue, Jr. S.E. *J. Am. Chem. Soc.*, 1960, **82**, 2526.

29. Basset, R.C.J.; Denney, R.C.; Jeffery, G.H.; Ed. Meudham, J. Vogels Text-book of Quantitative Inorganic Analsysis. P.461, ELBS and Longman, London, 1982.

30. Graeenwood, N.N.; Earnshaw, A. Chemistry of The Elements, 1984, P.1302, Pergman Press, Oxford.

31. Biskupic, S.; Valko, J. *Mol. Struct.* 1975, **27**, 97.

32. Kanzing, W.; Cohen, M.H. *Phys. Rev. Lett.*, 1959, **3**, 509.

33. Gupta, B.D.; Kumari, M.; Roy, S. *Inorg. Chem.* 1989, **28**, 11.

34. McGarvey, B.R. *Can. J. Chem.* 1975, **53**, 2498.

CHAPTER - II

LINEAR CHAIN MIXEDVALENT NICKEL(II) AND COPPER(II) COMPLEXES OF BIS(9,10-PHENANTHRENEDIONEDIOXIME) AND BIS(BENZOQUINONEDIOXIME). ELECTRICAL CONDUCTIVITY AND E.S.R. STUDIES OF THE COMPLEXES IN SOLID STATE.

2.1 INTRODUCTION:

2.1.1 General View of the Properties of Linear Chain Mixed Valence Transition Metal Complexes.

Solids with strongly uni-dimensional structural and electronic interactions have attracted much attention from chemists and physicists in recent times. The crucial features resulting from the co-operative phenomenon of these molecular solids are unusually quasi-metals, electrical conductors and interesting optical and magnetic behaviour. Coordination complexes containing direct metal-metal (M-M) interactions forming chains fall into this category of solid compounds. These can be classified into mainly two types.[1]

1.   Complexes containing discrete units like dimeric complexes and metal clusters. This class of complexes contain a discrete number of directly interacting metal atoms.

2.   Linear chain complexes which contain an infinite array of directly interacting metal atoms arranged in linear chain throughout the crystal lattice.

In general the planar or nearly planar units can stack one above the other resulting in columnar stacked compounds (Fig.2.1)[1] As d^8 metal complexes are known to adopt stable square planar structure with D_{4h} symmetry, this group of complexes are widely studied under this title. The interactions in these complexes are interpreted by many different theories. But mainly they are found to have either purely electrostatic interactions or Metal-metal (M-M) overlap. P. Day[2] discussed the electrostatic approach of intramolecular interactions as being due to crystal field effects of neighbour molecules in the stacks, where as Rundle[3], Miller[4] and Ingraham[5] discussed the orbital overlap model on the grounds of band formation (Fig.2.2)[1]. Krogman[6,7] suggested that bonding within the metal atoms of chain could be strengthened if electrons were removed from the upper part of the band between metal atoms in the stack by partial oxidation of the metal ions. This partial oxidation can be a chained by treating the compounds with anions. This kind of partial oxidation results in the mixedvalent systems of the type class III B of Robin-Day scheme.[8]

The existence of M-M interactions can be mainly judged from X-ray crystal structure determination and also from spectroscopic measurements, magnetic behaviour, electrical conductivity and solubility data of these complexes. Yamada[9] in single crystal electronic spectrum of these complexes observed a strong perpendicularly polarised band in the low energy region. It is attributed due to the presence M-M bond $\perp^{lr}$ to the plane of the molecule. Later it is showed that the presence of low energy band
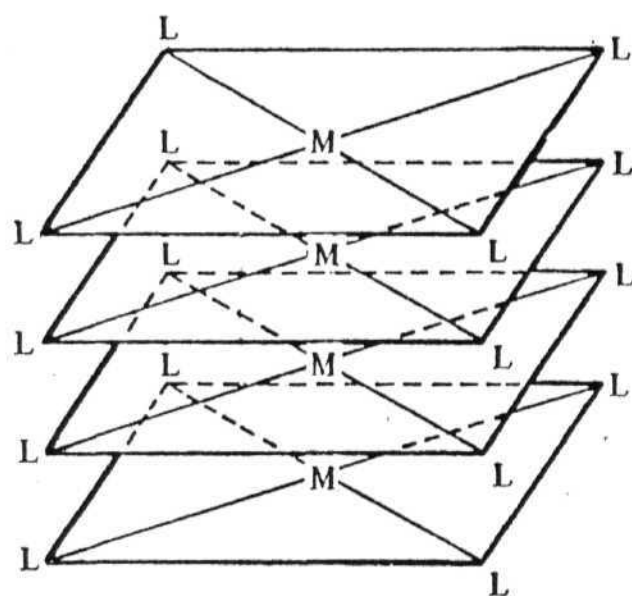
Fig.2.1   Planar units stacking into   columnar stacks. (Ref.1).
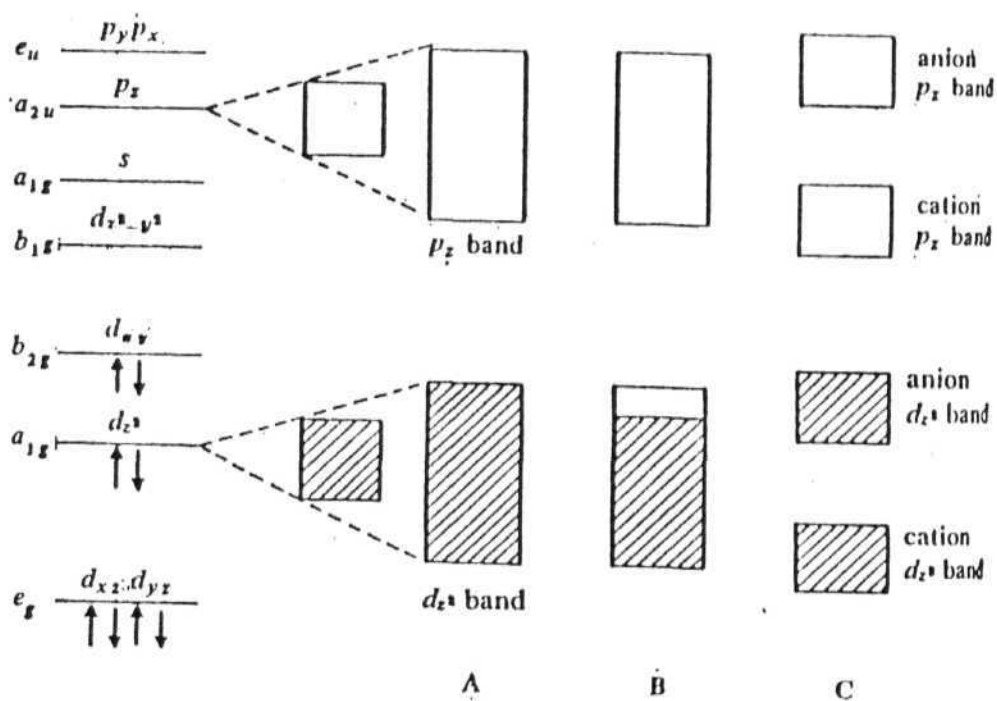
Fig.2.2   Diagrammatic representation of the band structure in d^8
metal-atom chain compounds.   Effect of (A) decreasing
inter-metallic distance, (B) partial oxidation, and (c)
alternating   anion-cation   chain.   Shaded   portion
indicates filled band. (Ref.1)

is a conclusive evidence for M-M interactions along the stack.[10-12]

As d^8 square planar complexes are diamagnetic the magnetic behaviour of these complexes are much less informative. Where as the conductivity studies in solid state revealed that these complexes usually fall into the semiconductors range, with electron delocalisation along M-M chain. Partial oxidation of these complexes increased the conductivity. These solids show extremely low solubility due to the presence of M-M bond in the solid state.[13-16]

Keller[40] in his article discussed in detail about the preparation and structural chemistry of these mixedvalent systems Containing infinite linear arrays of non bridged transition metals. The earliest recognised stacked square planar complexes are bis glyoxemates of nickel(II), palladium(II) and platinum. $Ni(dpg)_2I$ and $Pd(dpg)_2I$ are golden Olive needle type crystals. Their electrical conductivity and other spectroscopic characterisation have been done by Cowie et al[18]. It is found the crystals show at least 10^5 times greater conductivities than the pressed pellets along M-M stack. Using Resonance Raman spectroscopy it is found that in these complexes iodine is present as I_5^- and metal is assigned 2.33 integral oxidation state. The polyiodide salts of the complex formed by partial oxidation showed good increase in the conductivity.[18] The effect of inter planar spacing on the charge transfer characteristics of partially oxidised samples is discussed in M bis(benzoquinone dioxime).[20]

In the case of metallo-phthalocyanin complexes it is found that upon oxidation the electron is removed from ligand Π-orbital.[19]

In such cases assignment of integral oxidation state (IOS) to the metal atom is questionable. Substitution on the macrocyclic rings resulted in increased conductivity due to increased intermetallic spacing in M-porphyrins (M = Ni, Pt).

Detailed literature survey revealed that even though the synthesis of the nickel complexes 9,10-phenanthrenedionedioxime has been reported long time back[25], there was no further work reported on these complexes. It is to be noted that $pqdH_2$ has more provision for Π-delocalisation compared to dpg and $bqdH_2$ due to the absence of bulky substituents and also with a large ring system, it should have more electrical conductivity.

2.1.2 E.S.R. STUDY OF THE STACKED COMPOUNDS

E.s.r. studies are most widely used alternative to draw some conclusions about the structure in the absence of X-ray diffraction data in the transition metal complexes. Since these stacked systems are mostly of (d^8) configuration they are all e.s.r. inactive and much information is not obtained. But upon oxidation of these complexes, a single sharp line is observed, which may be due to the free delocalisation of electron, as in the case of organic radicals. Hence usually a paramagnetic guest species is introduced into these systems and structural information is deduced by studying the e.s.r. spectra of the

paramagnetic probe in the host lattice.[22] Since copper(II) can take square planar geometry easily upon coordination with the N-donor ligands like phthalocyanine and bis(α,β-dionedioximes), it can be used as a paramagnetic probe. The spin Hamiltonian parameters obtained can be used to establish the metal ligand bond nature. The copper(II) ion with a $[CuN_4]$ chromophore in e.s.r. shows a four line pattern.[21] Each line is again split into 9 lines. All four sets of 9 lines will be of same intensity indicating the four equal or nearly equal nitrogen donor atoms surrounding the copper(II) ion.

In explaining the complex hyperfine structure observed in the e.s.r. spectra, it is assumed that each of the four ligand atoms has availed 2s, $2p_x$, $2p_y$ and $2p_z$ orbitals for the formation of molecular orbitals (MO) with the $3d_z^2$ orbitals of the copper atom. Since the square planar complexes have D_{4h} symmetry, the following are the anti-bonding wave functions[22] (Fig.2.3).

$$\psi_{B1g} = \alpha\, d_{x^2-y^2} - \alpha'\, (-\sigma_x^{(1)} + \sigma_y^{(2)} + \sigma_x^{(3)} - \sigma_y^{(4)})/2 = \beta_1$$

$$\psi_{B2g} = \beta_1 d_{xy} - \beta'_1\, (p_y^{(1)} - p_x^{(2)} - p_y^{(3)} + p_x^{(4)})/2 = \beta_2$$

$$\psi_{A1g} = \alpha_1 d_{z^2} - \alpha'\, (\sigma_x^{(1)} + \sigma_y^{(2)} - \sigma_x^{(3)} - \sigma_y^{(4)})/2$$

$$\psi_{E1g} \quad
\begin{aligned}
&= \beta d_{xz} - \beta'\, (p_z^{(1)} - p_z^{(3)})/2^{1/2} \\
&= \beta d_{yz} - \beta'\, (p_z^{(2)} - p_z^{(4)})/2^{1/2}
\end{aligned}$$
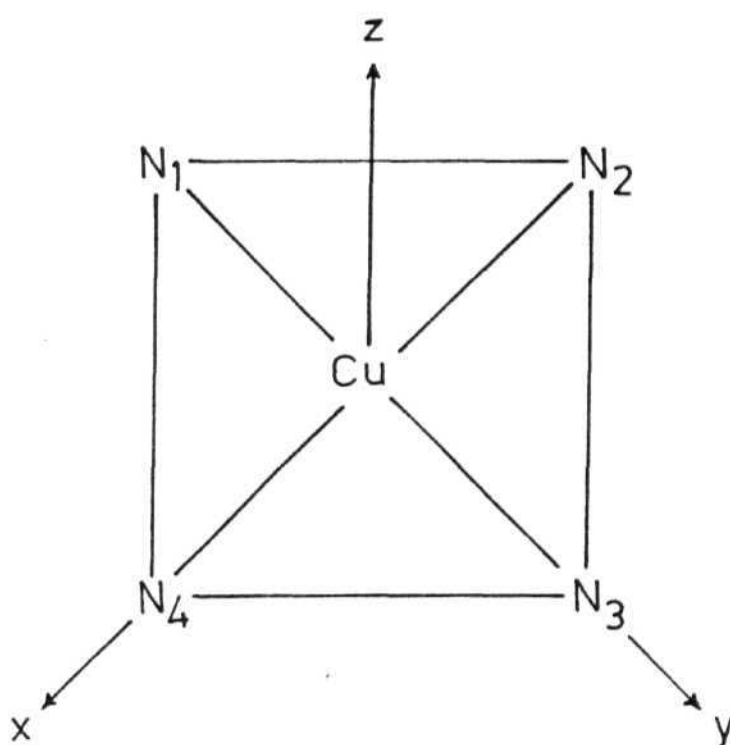
Fig.2.3 Diagram showing coordinate axis and numbering scheme of the ligands.

where $\alpha_1 \beta_1$ and β_2 are the coefficients which express the covalent character of the σ-bonding, in plane and out of plane Π-bonding respectively. The other symbols have their usual significance.

A spin Hamiltonian reflecting the four fold axial symmetry is given by[23]

$$H = \beta_o [g_\parallel H_z S_z + g_\perp (H_x S_x + H_y S_y) + A_{cu} S_z I_z + B_{cu} (S_x I_x +$$

$$S_y I_y) + A_N S_z I_z^N + B_N (S_x I_x^N + S_y I_y^N)] + Q' [I_z^2 - 1/3(I+1)]$$

β_o is the Bohr magneton, A_{cu}, B_{cu} are copper hyperfine interaction constants, Q' is the copper quadruple interaction constant, A_N and B_N are nitrogen hyperfine constants.

By applying these antibonding wave functions to the Hamiltonian mentioned above from the e.s.r. parameters obtained $\alpha, \alpha', \beta, \beta'$ coefficients can be calculated.

With these ideas we have synthesised the $Ni(pqdH)_2$ and $Ni(pqdH)_2I$, and investigated the complexes in detail. In addition prepared $Cu(pqdH)_2$, $Cu(bqdH)_2$ and copper doped $Ni(pqdH)_2$, $Ni(bqdH)_2$ in different concentrations. A detailed e.s.r. studies done on these compounds is also discussed in this chapter.

2.2 EXPERIMENTAL

2.2.1 Chemicals:

The starting materials for the preparation of ligands are bought from *Aldrich or Fluka*. Other solvents and common chemicals were of reagent grade or better quality. All the organic solvents are purified by standard procedures described in *Vogel*[24]. Ether is stored over sodium, pyridine over potassium hydroxide pellets dimethyl formamide is vacuum distilled in dry nitrogen atmosphere and stored over 4A molecular sieves.

2.2.2 Preparation of Ligands:

$pqdH_2$ and $bqdH_2$ are prepared according to the procedures described in the previous chapter experimental sections[1.2.1-2.2]

2.2.3 Preparation of bis(9,10-Phenanthrenedionedioximato)Ni(II): $Ni(pqdH)_2$
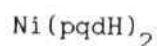
$Ni(pqdH)_2$ is prepared according to the literature procedure[25]. It is obtained as brown flaky material, which is insoluble in all most all non co-ordinating solvents. Sparingly soluble in pyridine. Hence recrystallisation of the complex is not possible.

Yield = 80%

2.2.4 Preparation of partially Oxidised Ni(pqdH)$_2$ and Ni(III) Complex of pqdH$_2$:

860 mg (0.026 mol) of Ni(pqdH)$_2$is oxidised with 6 gm (0.47 moles) of triply sublimed molecular iodine, by refluxing it in o-dichloro benzene for 12 hours.

During the first attempt a large amount of (more than 3/4 of starting material) black, crystalline residue is left out. Only a small amount of partially oxidised Ni(pqdH)$_2$I$_x$ is obtained upon cooling from the mother liquor.

The residue was found to be a Ni(III) complex based on e.s.r. data. However the preparation was not reproducible, further attempts to prepare this complex resulted in mostly unreacted material.

2.2.5 Preparation of bis(9,10-phenanthrendionedioximato)Cu(II): Cu(pqdH)$_2$):

500 mg(2.9×10^{-3} mol) of CuCl$_2$.2H$_2$O dissolved in 100 ml of dry distilled methanol and this is added to 1 gm (4.2×10^{-3}moles) of hot(60°c) ligand solution in methanol drop wise and the brown flaky precipitate obtained is washed with hot methanol and dry ether. Dried over vacuum at 80°c.

Yield : ca.80%.

2.2.6 Preparation of Copper doped Ni(pqdH)$_2$:

1%, 5%, 10%, 25%, 50% by molar ratio (Table 2.1) copper doped Ni(pqdH)$_2$ complexes are prepared by mixing mixed metal solution Cu/Niwith ligand solution. The preparation procedure is exactly same as in the case of Ni(pqdH)$_2$ preparation. The brown flaxy material obtained is dried in vacuum at 80°C and used for further investigation.

2.2.7 Preparation of bis(benzoquinonedioximato)Ni(II):Ni(bqdH)$_2$

125 mg of (5.26 x 10^{-4} mol) of NiCl$_2$6H$_2$O dissolved in 25 ml of ethanol. This is added drop wise to the hot solution of 250 mg (1.8 x 10^{-3} mol) of bqdH$_2$ dissolved in 50 ml of ethanol. The black micro crystalline product obtained is not soluble in non coordinating solvents hence the recrystallisation is not attempted.

Yield   ~ 50%

2.2.8 Preparation of Bis(benzoquinonedioximato)Cu(II): Cu(bqdH)$_2$:

When Cu(bqdH)$_2$ is prepared similar to Ni(bqdH)$_2$, the solid is not precipitated out. Hence 125 mg (7.3 x 10^{-4} mol) of CuCl$_2$2H$_2$O is dissolved in 25 ml of distilled water and this solution is added to 250 mg (1.8 x 10^{-3} mol) of ligand solution in methanol solution hot condition. The black crystalline product obtained is used without further recrystallisation.

2.2.9 Preparation of Copper dopped Ni(bqdH)$_2$:

1%, 10%, 25%, 50% (by molar ratio) copper doped Ni(bqdH)$_2$ are prepared by mixing the mixed metal solution of Cu/Ni to hot ligand (bqdH$_2$)solution in methanol.(table 2.1)   The brown poly crystalline material obtained is washed several times with hot methanol and then with ether.   Dried in vacuum.   Yield was only 45%.

2.2.10 Preparation of Pellets for Electrical Conductivity

Measurements:

Pressed pellets of approximately 10 mm thickness are prepared with dry powder complex. These pellets are coated with silver metal for contact and electrical conductivities are measured using four probe method in d.c. voltage.

2.2.11 Physical Measurements:

E.s.r. measurements are carried with variable temperature on JEOL FE 3X spectrometer equipped with variable temperature cryostat.DPPH is used as a standard for calibration (g = 2.0035). I.R. spectra for solid complexes are by KBr pellets using Perkin Elmer-I.R.1310 spectrophotometer.   Electronic spectra are measured using Schimadzu 200S UV-Visible spectrophotometer.

Table 2.1 : Details of the composition of the metals mixed in different copper doped complexes

Complex	CuCl$_2$ 2H$_2$O mg	NiCl$_2$ 6H$_2$O mg	Ligand (pqdH$_2$/bqdH$_2$)mg
1% Cu/Ni	1.8	247.1	500
5% Cu/Ni	8.95	237.1	500
10% Cu/Ni	17.9	224.7	500
25% Cu/Ni	51.2	204.0	500
50% Cu/Ni	89.5	124.8	500

Photo acoustic spectra (P.a.s) are recorded on PARC photo acoustic spectrometer using $Mg\ CO_3$ as a standard diluent.

2.2.12 Computer Simulations:

The previously described computer program (Chapter 1.2.5) is used, for e.s.r. simulation which includes the ligand hyperfine interactions in first order. The simulation of copper doped Ni(II) complexes of $pqdH_2$ and $bqdH_2$, including ligand hyperfine interactions needed 4 hr of computer time on IBM PC (XT)

2.3   RESULTS AND DISCUSSION:

2.3.1 Electronic Spectra of $Ni(pqdH)_2$:

The solid P.a.s spectrum of $Ni(pqdH)_2$ (fig.2.4) showed 3 bands in the visible region (350 - 800 nm), at 22.2 kK, 19.6 kK and 16.0 kK. In the literature most of the electronic spectral discussion of stacked compounds is centered on the presence of a low energy band at 18-20 kK. The presence of this band in $Ni(dmg)_2$ solid spectrum and disappearence in solution is attributed by some authors[1] to $3d_{z^2} - 4p_z$ transition with some $3d_{z^2} - \overset{\bullet}{\pi}\ b_{1u}$ mixing, due to M-M interactions in the solid. But Day[2] argued that this band is a result of electrostatic crystal field interaction between neighbouring intramolecular transition dipoles. It is emphasised that the presence of M-M interaction is not essential for this band to be observed. According to Anex and

53
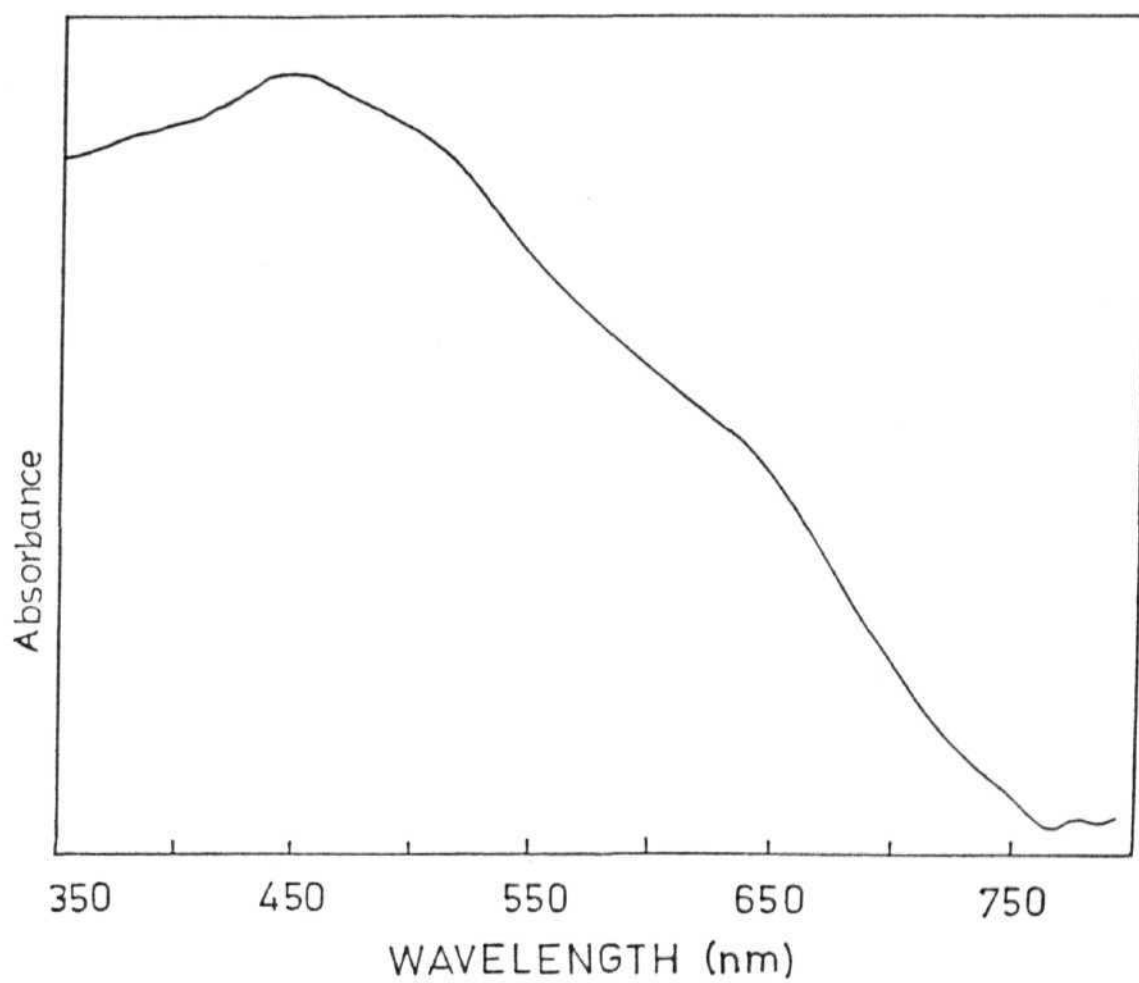
Fig.2.4   P.a.s. spectrum of Ni(pqdH)$_2$

54

Krist[10] the presence of this low energy band is due to a side effect of stacking but not essentially due to M-M interaction. In addition to the band at ~ 20 kK an intense band at ~ 50 kK is proposed by Ohashi *et al*[26] in single crystal $Ni(dmg)_2$ as due to intermetallic charge transfer transition. As $Ni(pqdH)_2$ is insoluble in non coordinating solvents, the solution spectrum could not be studied, hence the band seen in solid p.a.s. spectrum of this compound at ~ 20 kK (19.6 kK) can not be unambiguously assigned M-M interactions in the solid.

2.3.2 Electrical Conductivity Studies of Partially Oxidised $Ni(pqdH)_2$

The electrical conductivity data of the partially oxidised samples of $Ni(pqdH)_2$ are given in the Table 2.2. the data reveal that all these compounds are in semi-conductor ranged 303 K. The partial oxidation with molecular iodine did not improve conductivity like in $Ni(dpg)_2I_x$ and $Pd(dmg)_2I_x$[21]. In light of the dependency of the conductivity on M-M interactions, the excess conductivity showed by $Ni(dpg)_2Ix$ over $Pd(dpg)_2Ix$ (Table 2.3)[20] is surprised as the M-M distances in both complexes are exactly same and the metallic reading only differ by 0.16 A. Where as the difference in conductivity between $Ni(dpg)_2I_x$ and $Ni(bqd)_2I_x$[18,20] stress upon the fact, that ligand orbitals play an important role in the conductivity behaviour. Increased Π delocalisation and absence of bulky substituents on the ligands should increase conductivity allowing more electron delocalisation as seen in the case of $Ni(TMBP)I_{0.33}$ over $Ni(OMTBPH_2)I_{0.33}$.[21] In such cases 9,10-phenanthrenedionedioxime should be a better ligand over dpg.

Table 2.2 : Conductivity at temperature 303 K and 10 V in pressed pellets of ~ 1 mm thickness

Compounds	Current in amperes	Conductivity Ω^{-1}
Ni(pqdH)$_2$	11.9 x 10^{-9}	1.45 x 10^{-9}
Ni(pqdH)$_2$	25.5 x 10^{-1}	2.8 x 10^{-8}
Ni(III)residue	85.2 x 10^{-7}	8.5 x 10^{-7}

Table 2 3: Single Crystal D.C. Conductivities at 300 K

Compound	Conductivity Ω^{-1}
$Ni(dpg)_2$	$< 8 \times 10^{-9}$
$Ni(dpg)_2I$	$2.3\text{-}11 \times 10^{-3}$
$Pd(dpg)_2I$	$7.7\text{-}4.7 \times 10^{-4}$
$Ni(bqd)_2$	$<9 \times 10^{-9}$
$Ni(bqd)_2I_{0.018}$	$<9 \times 10^{-9}$
$Ni(bqd)_2I_{0.52}S$	$1.8\text{-}11 \times 10^{-6}$
$Pd(bdq)_2I_{0.5}S$	$7.8\text{-}8.1 \times 10^{-5}$

S=solvent

But that is not the case observed in electrical conductivity of $Ni(pqdH)_2I_x$ compound $Ni(dmg)_2I_x$. The possible explanation can be obtained from the fact that the conduction in the pressed pellets depends more on contact between particles of the powder along with intra particle conduction.[21] In the absence of X-ray diffraction data, we could not confirm the amount of iodide and also there by the extent of oxidation. In the case of $Ni(bqd)_2I_{0.018}$ show very less conductivity, than in $Ni(bqd)_2I_{0.52}$.[20] Thus the poor conductivity observed in partially oxidised $Ni(pqdH)_2I_x$ may be due to the powder nature and insufficient oxidation.

2.3.3 E.s.r. Studies of $Ni(pqdH)_2I_x$:

Partially oxidised $Ni(pqdH)_2I_x$ shows a sharp signal (Fig.2.8) at g = 2.011, like in other reported partially oxidised complexes.[28] This can be due to the lattice defects. The sharp signal is the characteristic property of high spin exchange interaction energy.[27]

2.3.4 E.s.r. Studies of Ni(III) complex of $pqdH_2$:

The crystalline black residue left in the reaction mixture, in e.s.r. study revealed the presence of Nickel(III) species (Fig.2.9). The three different g values, (Table 2.4) shows that the spectrum is rhombic in nature. The spectrum looks similar to that reported by Kruger and Holms[29]

This product is readily soluble in pyridine. The frozen

Table 2.4 X-band e.s.r parameters

Compound	Temp. K	g	A
Partially oxidised $Ni(pqdH)_2$	298	2.011	
Residue	298	$g_1 = 2.071$	
		$g_2 = 2.035$	
		$g_3 = 1.994$	
Residue in pyridine	128	$g_\parallel = 1.915$	$A_\parallel(N) = 20.0 \times 10^{-4}\ cm^{-1}$
		$g_\perp = 2.026$	
$Cu(PqdH)_2$	298	$g = 2.054$	
$Cu(bqdH)_2$	298	$g_\parallel = 2.167$	$A_\parallel = 173.1 \times 10^{-4}\ cm^{-1}$
		$g_\perp = 2.054$	$A_\perp = 28.77 \times 10^{-4}\ cm^{-1}$

solution (128 K) pyridine adduct of this compound gives an axially symmetric e.s.r. spectrum (Fig.2.10). The quintet super hyperfine on parallel line is similar to that observed in spectrum of dipyridine adducts reported for other Ni(III) complexes[29]. The analysis of g values ($g_\perp > g_{||}$) of this complexes shows that a d^2_z ground slate is required for these conditions of the spectrum. The A_N values ($\sim$ 20 G) are close to earlier reported Nickel(III) complexes.[30-37]

2.3.5 Electronic Spectra of Cu(pqdH)$_2$ and Cu(bqdH)$_2$

The electronic spectra of Cu(pqdH)$_2$ recorded (400-850 nm) in Nujolmull shows a broad band at around 22.2 kK (Fig.2.5). In the p.a.s. spectrum (Fig2.6) this compound is showing another band at 20.6 kK in addition to 22.2 kK peak. Cu(bqdH)$_2$ Nujolmull spectrum (400-850 nm) showing (Fig.2.7) a weak shoulder at $\sim$ 22 kK and another at 20.0 kK. These two transition energies are similar to the earlier reported values for many compounds of this type.[22] These transition energies ($\sim$ 20 kk) and ($\sim$ 22 kK)$_3$ are attributed due to $^2B_{2g} \longleftarrow ^2B_{1g}$ and $^2E_g \longleftarrow ^2B_{1g}$ electronic transitions.

2.3.6 E.s.r. Studies of Cu(pqdH)$_2$ and Cu(bqdH)$_2$

The room temperature X-band e.s.r. spectrum of solid Cu(pqdH)$_2$ shows a broad isotropic signal (Fig.2.11) at g = 2.054. This is a typical spectrum of magnetically concentrated copper(II) complexes.
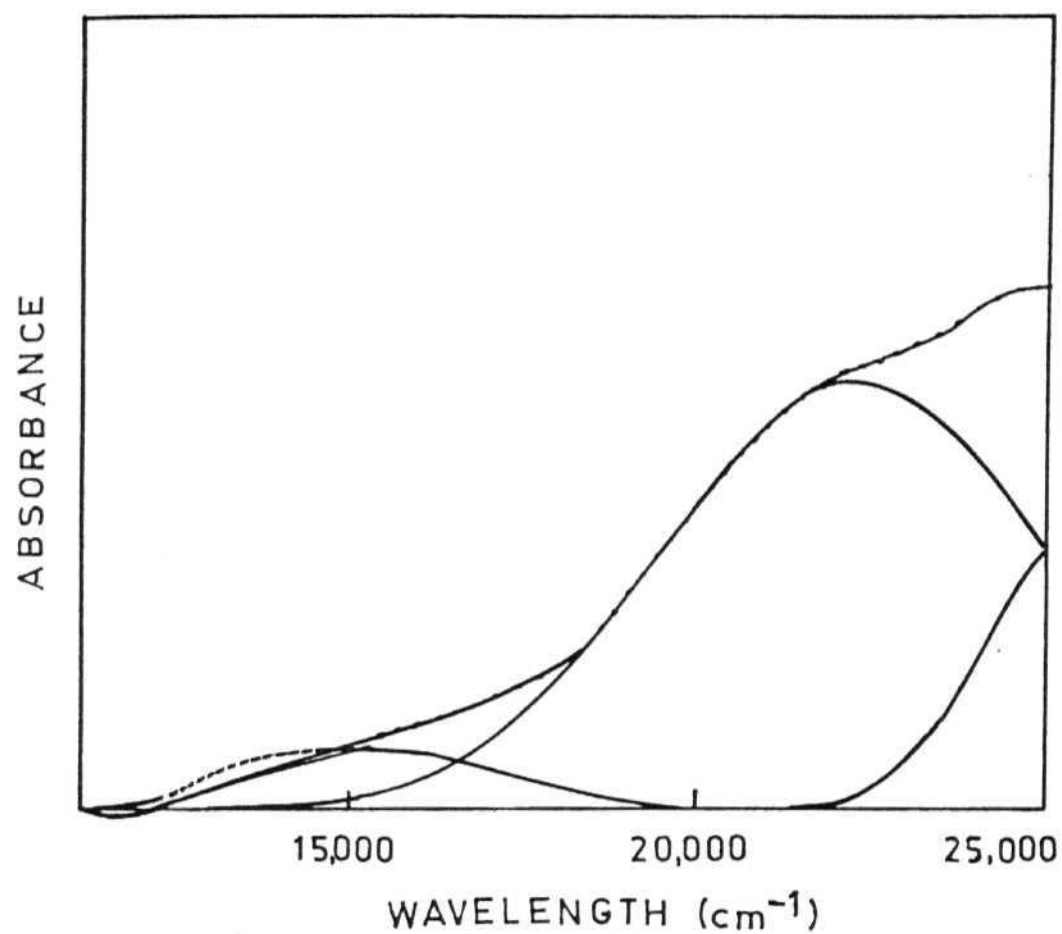
Fig.2.5   Deconvoluted electronic spectrum of Cu(pqdH)$_2$ in Nujol mull, showing component bands; ..... experimental spectrum; ———calculated spectrum.
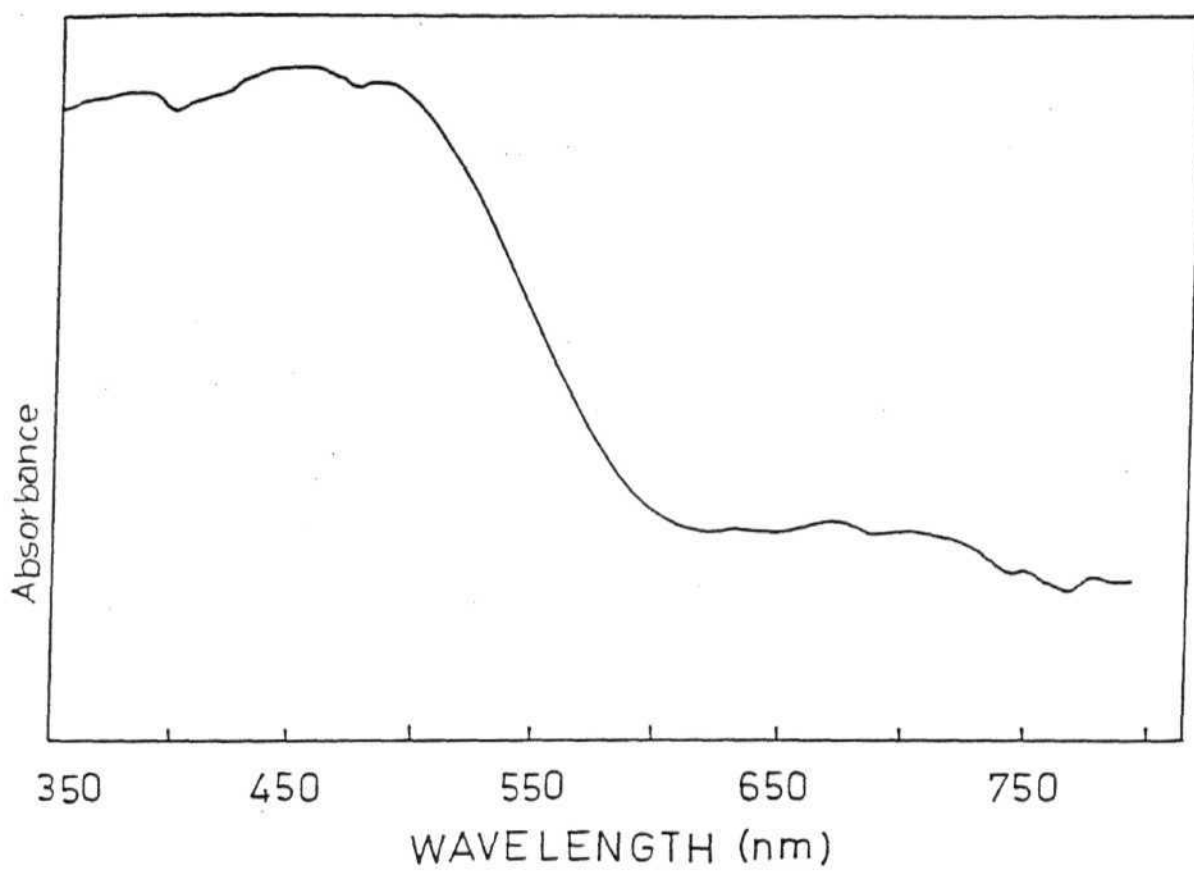
Fig.2.6   P.a.s. spectrum of Cu(pqdH)$_2$
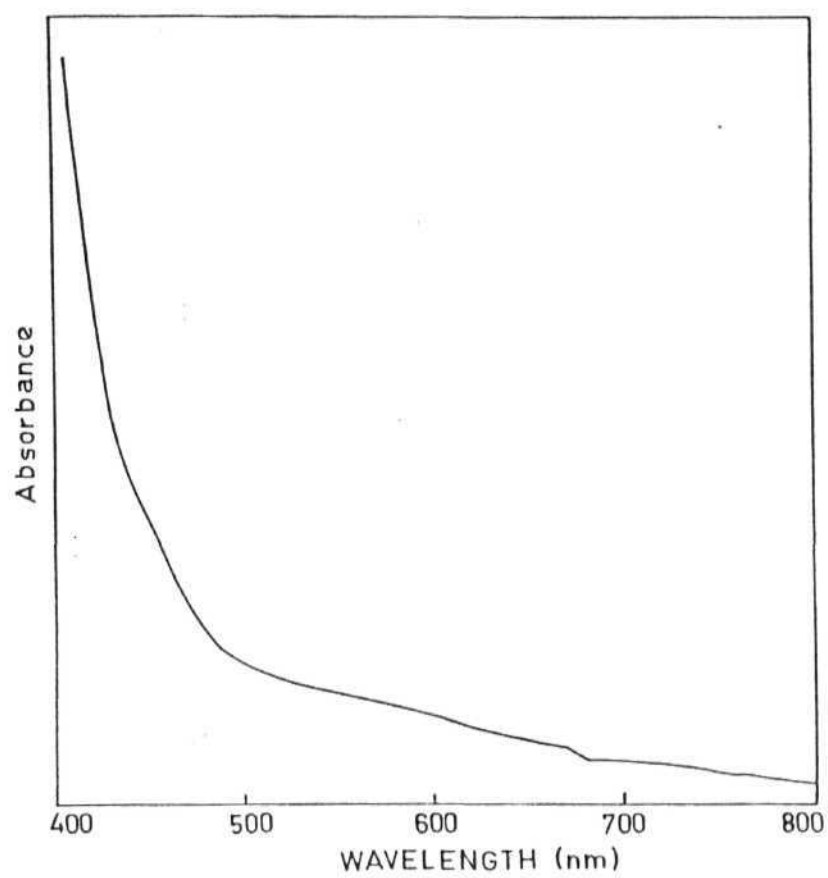
Fig.2.7   Electronic spectrum of Cu(pqdH)$_2$ in Nujol mull.

Microcystalline $cu(pqdH)_2$ unlike its analogous $pqdH_2$ complex showed a resolved hyperfine with 2 parallel lines (Fig 2.12.a) and other two merged in perpendicular portion. The larger $g_{\parallel}$ value and larger difference in $A_{\parallel}$ and $A_{\perp}$ values (Table 2.4) confirms the $d_{x^2-y^2}$ ground state. There is no nitrogen super hyperfine observed in the spectrum. This resolution of the spectrum disappears upon grinding resulting in a broad line spectrum. (Fig 2.12.b) This well powdered sample upon storage form fine needle shaped, golden coloured crystals Under going solid state crystalline. These crystals do not show any e.s.r. signal in X-band at room temperature. However, the behaviour of the complex has to be established in detail.

2.3.7 E.s.r. Studies of Copper doped $Ni(pqdH)_2$ and $(bqdH)_2$ at different Concentrations

Copper could be doped in various concentrations into the nickel host lattice, in the $Ni(pqdH)_2$ and $(bqdH)_2$ complexes. Both the complexes exhibit similar e.s.r. behaviour at X-band at room temperature, showing that they are analogous compounds.

10% copper doped samples of Cu $Ni(pqdH)_2$ and 25% Cu $Ni(bqdH)_2$ showed a well resolved 4 line pattern with nitrogen super hyperfine splitting at X-band (Fig.2.13,14). There is no change in e.s.r. parameters upon cooling to low temperatures. The simulated values of the e.s.r. parameters are given in Table 2.4. The analysis of e.s.r. parameters $g_{\parallel} > g_{\perp}$, $A_{\parallel} \gg A_{\perp}$ (Table 2.5) show that the spectrum is arising due to axially symmetric square

3300
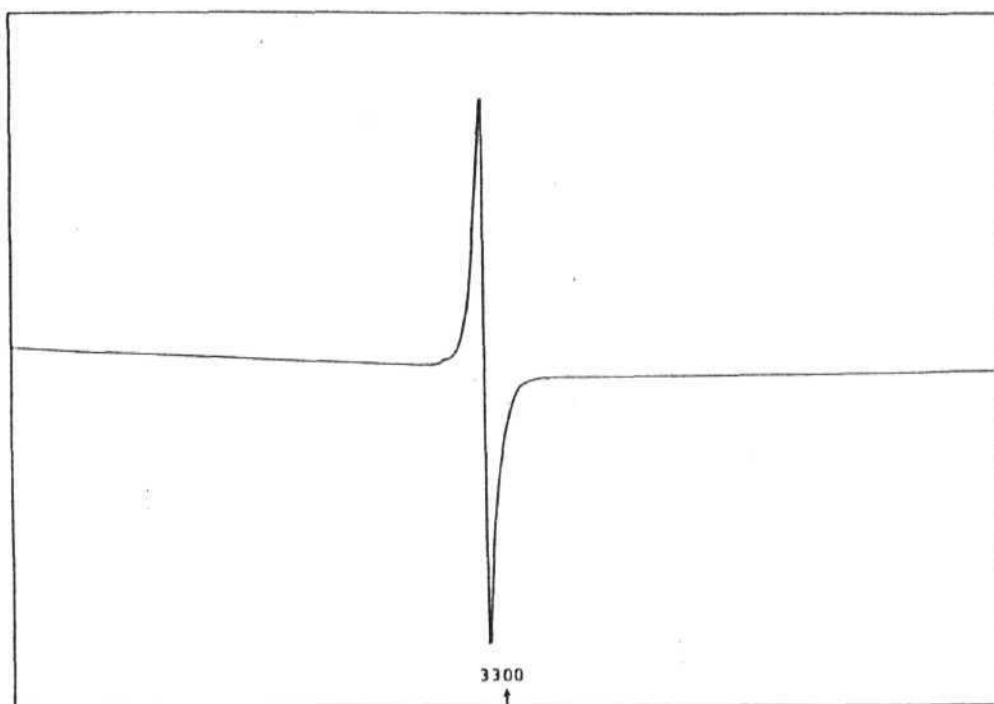
Fig.2.8   X-band   e.s.r.   spectrum   of   partially   oxidised
Ni(pqdH)$_2$I$_x$ at 298 K.
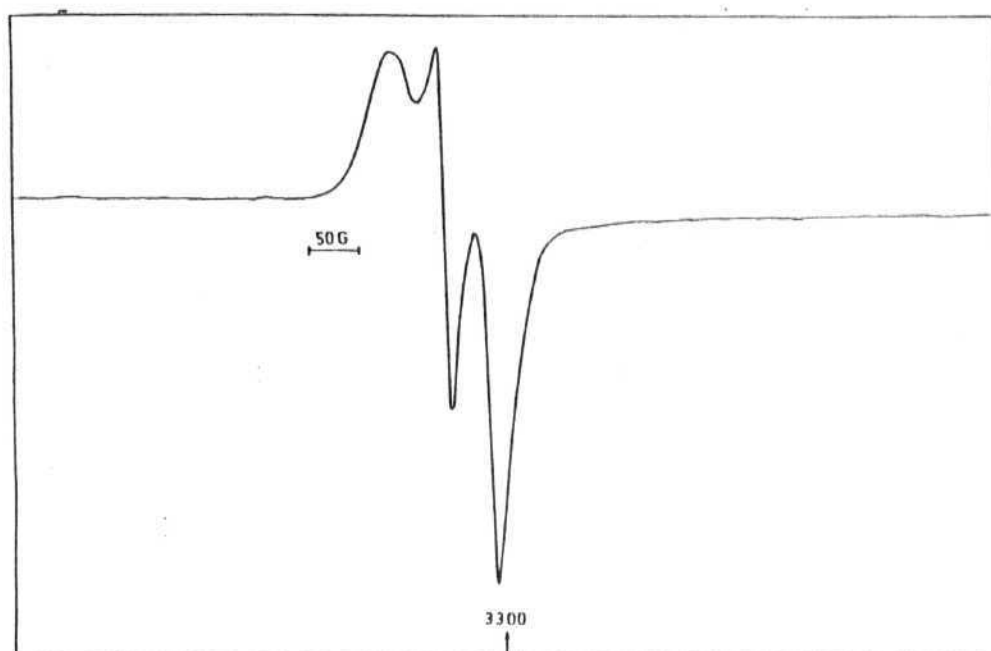
Fig.2.9   X-band e.s.r. spectrum of residue showing Ni(III)
          species at 129 K.

Table - 2.5 : E.s.r. parameters of copper doped Nickel complexes.

Complex	$g_{\parallel}$	$g_{\perp}$	cm^{-1}			
			$A_{\parallel}Cu$	$A_{\perp}Cu$	$A_{\parallel}N$	$A_{\perp}N$
Cu Ni(pqdH)$_2$	2.128	2.033	0.0193	0.0027	0.0014	0.0017
Cu Ni(bqdH)$_2$	2.129	2.033	0.0196	0.0027	0.0014	0.0017
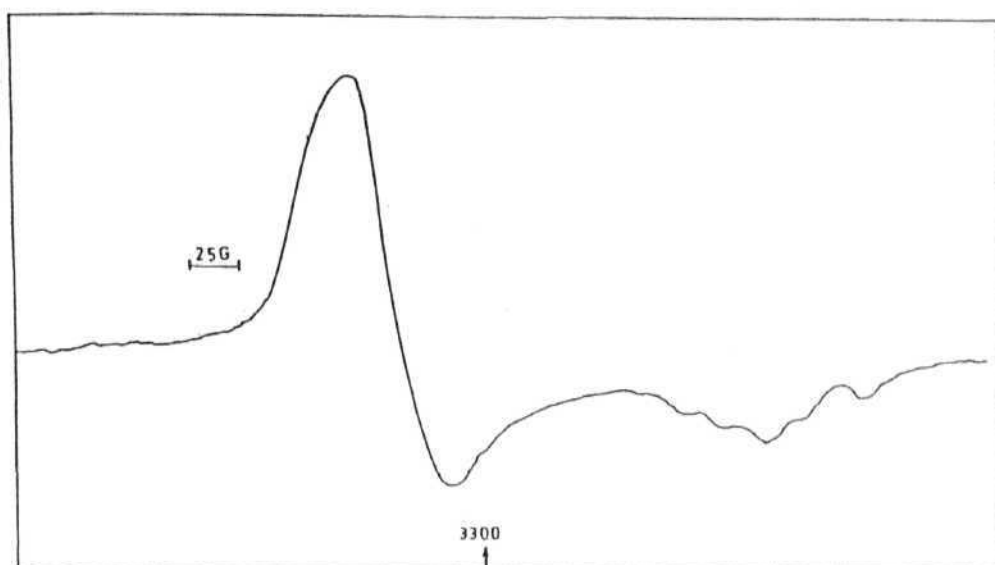
Fig.2.10 Frozen solution X-band e.s.r. spectrum of residue in pyridine at 128 K.

100 G

3300
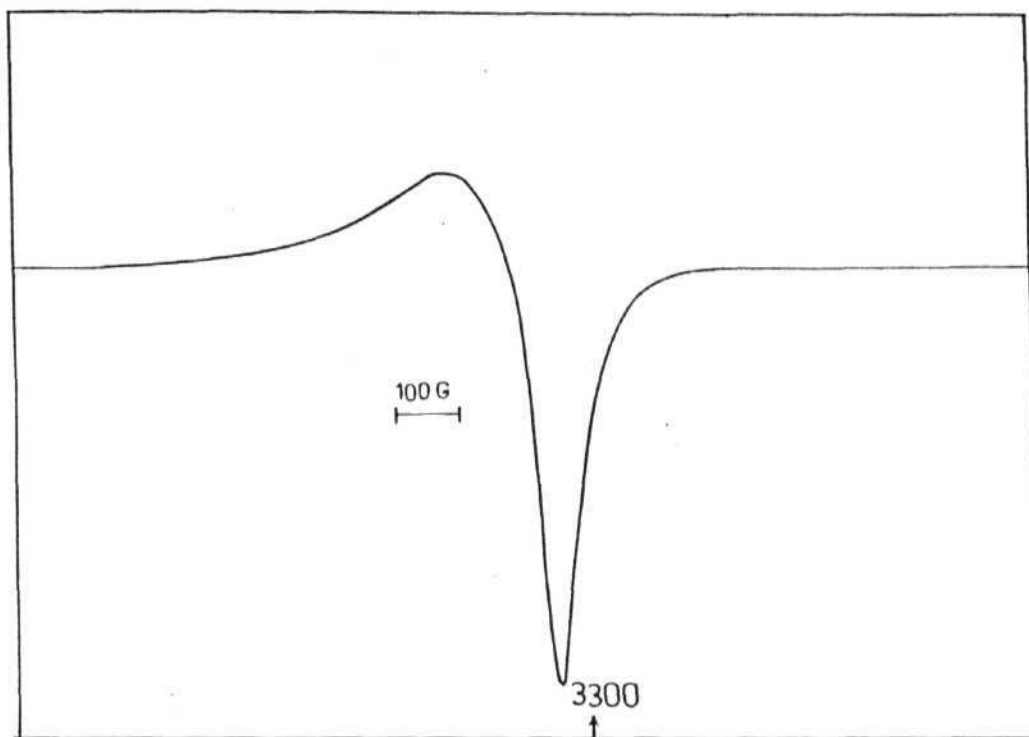
Fig.2.11 X-band e.s.r. spectrum of Cu(pqdH)$_2$ at 298 K.
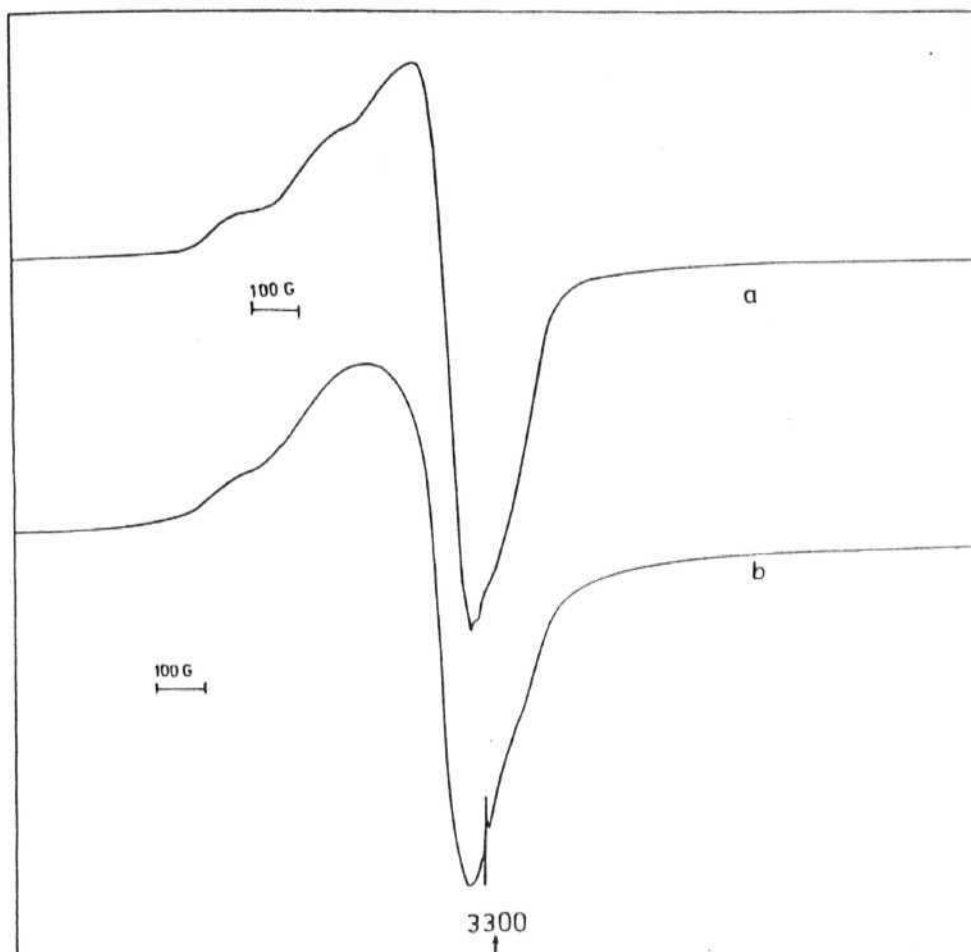
Fig.2.12 X-band e.s.r. spectrum of Cu(bqdH)$_2$ at 298 K (a)
microcrystalline sample (b) powdered sample.
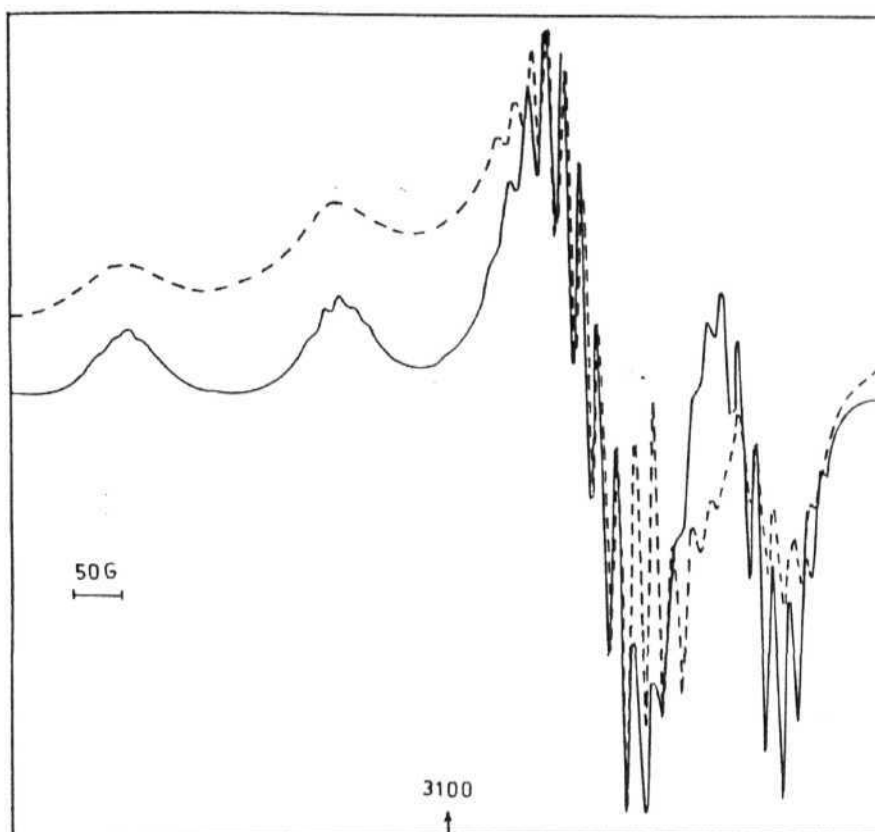
Fig.2.13 X-band e.s.r. spectrum of 10% Cu doped Ni(pqdH)$_2$ at
298 K.

..... experimental spectrum

——— simulated spectrum
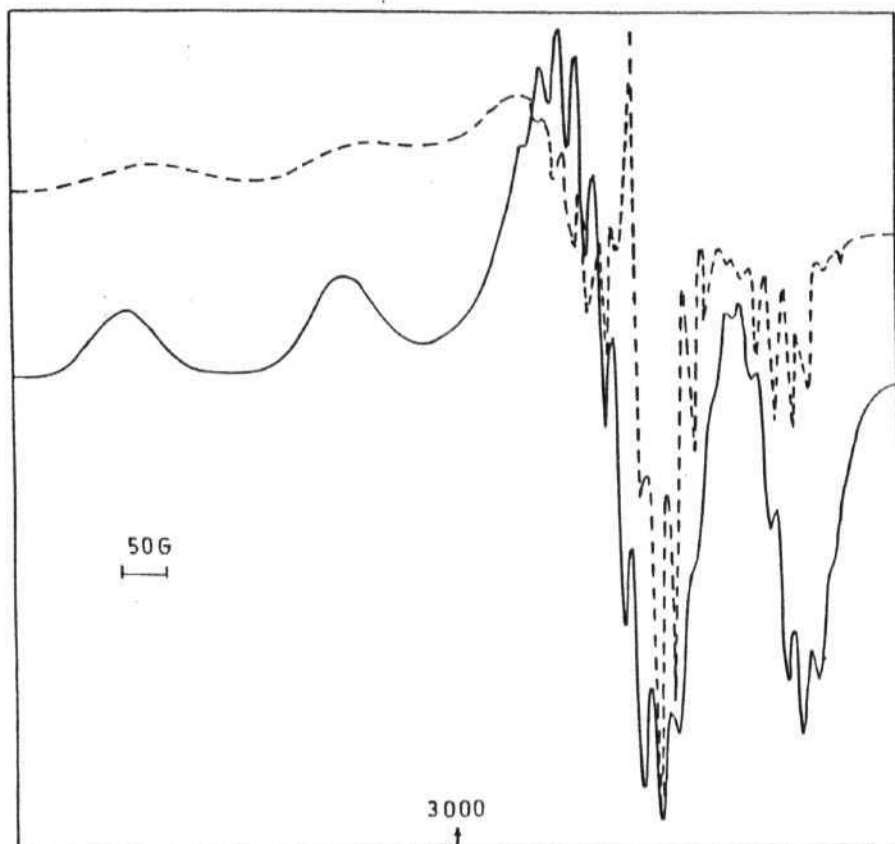
Fig.2.14 X-band e.s.r. spectrum of 25% Cu doped Ni(bqdH)$_2$ at
298 K.

.... experimental spectrum

——— simulated spectrum

planar copper(II) species with $d_{x^2-y^2}$ ground state. The nine line hyperfine showed on each signal are of similar nature and the A_N ‖, A_N ⊥ values clearly state that, in the [CuN$_4$] chromophore all four nitrogens are equally coordinated in square planar D_{4h} symmetry. The values obtained from Q-band spectrum of this sample are in support of the axial symmetry (Fig.2.15).

The increased concentration of Copper (5%, 25%, 30%) showed continuous broadening of the signal (Fig.2.16) at X-band. This indicates the dipolar broadenig, due to the interaction between more and more copper sites available

2.3.8 THEORETICAL ANALYSIS OF E.S.R. SPECTRA

As discussed in the introduction of the Chapter (2.1) copper(II) with [CuN$_4$] chromophore forms a square planar complex with D_{4h} symmetry. The wave functions of the anti-bonding orbital for a d^9 system with D_{4h} symmetry and the related spin Hamiltonian. (eq.2) are discussed there in. The experimental spin-Hamiltonian parameters can be related to the characteristics of the electronic state of the system, by deducing the following equations from the above mentioned Hamiltonian, taking second order perturbations in to consideration.

$$g_\| - g_e = \Delta g_\|$$

$$g_\perp - g_e = \Delta g_\perp \qquad\qquad (3)$$

73

100G

12000

0
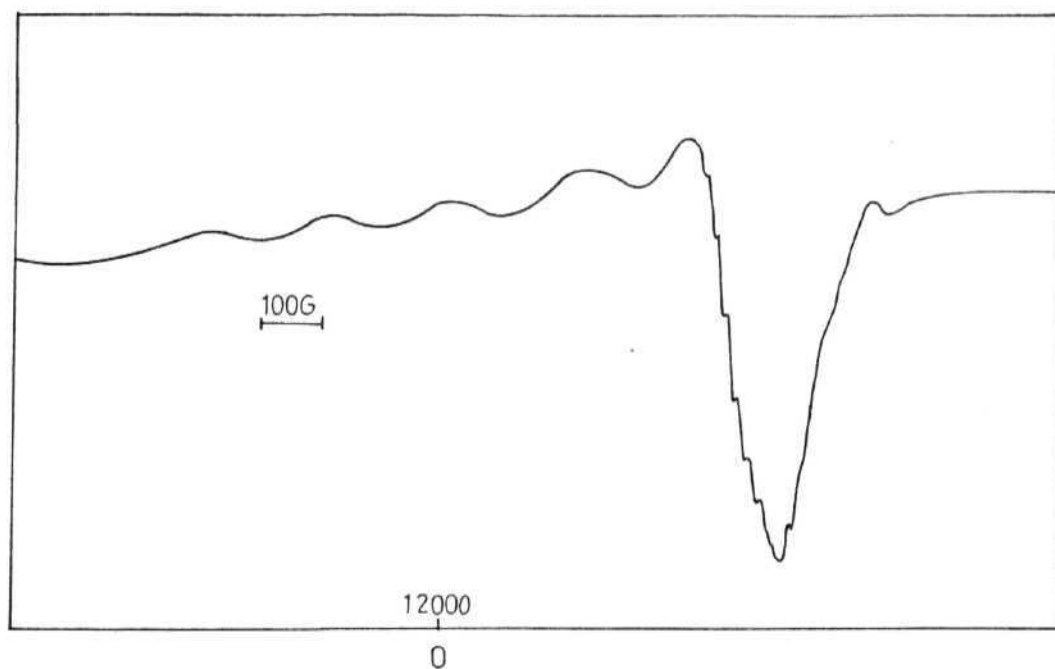
Fig.2.15   Q-band e.s.r. spectrum of 10% Cu doped Ni(pqdH)$_2$ at
298 K.
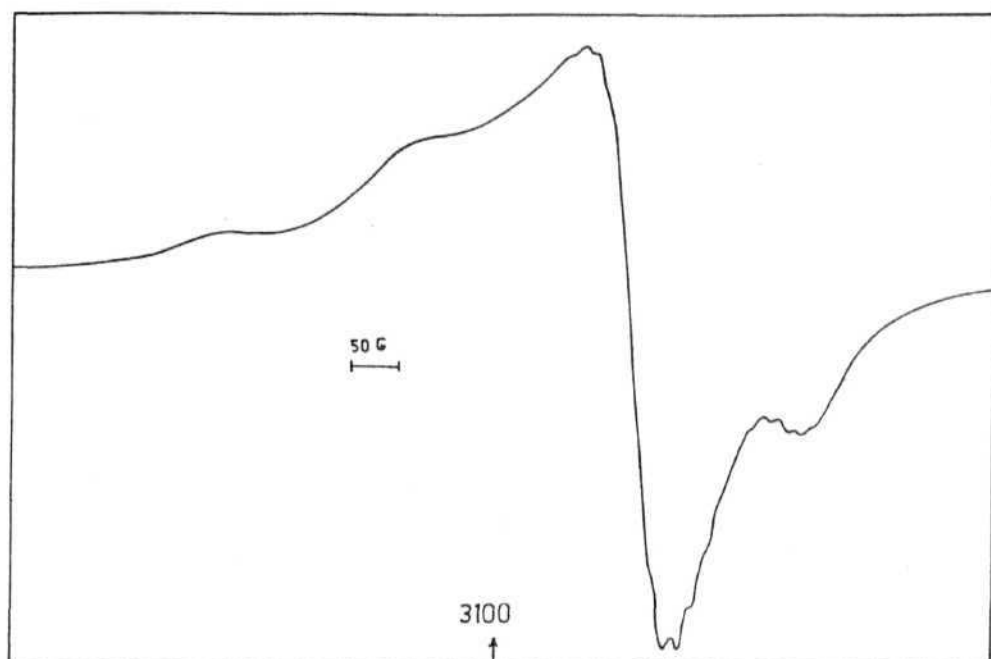
Fig.2.16 X-band e.s.r. spectrum of 50% Cu doped Ni(pqdH)$_2$ at 298 K.

$$A_{\parallel} = A_F + 2A_D + A_{\parallel} \quad (1)$$

$$A_{\perp} = A_F + A_D + A_{\perp} \quad (1)$$

where $g_e = 2.0023$ is the free electron g-value. The significance of the various terms in the above equations are briefly discussed below.

(1) $\Delta g_{\parallel}$ and $\Delta g_{\perp}$:

These quantities measure the deviation of the proposed g-values from the free electron value. In an electronically non-degenerate state (L = 0) the g-anisotropy arises due to mixing of the excited state in to the ground state by spin-orbit interaction. Using perturbation theory, and retaining only terms in the first power of the interaction, these equations are given by

$$\Delta g_{\parallel} = - 8E_{\parallel} K_{\parallel}$$

$$\Delta g_{\perp} = -2E_{\perp} K_{\perp} \quad (4)$$

where

$$E_{\parallel} = \lambda / (E_1 - E_2)$$

$$E_{\perp} = \lambda / (E_1 - E_{3,4}) \quad (5)$$

E_1, E_2, E_3 and E_4 are the energies of the appropriate molecular

orbitals and λ is the spin-orbit coupling constant. (-828 cm for copperII). $K_\parallel$ and $K_\perp$ are the covalency reduction factors which are functions of the overlap integral, S and a quantity T, which is related to the orbital angular momentum matrix elements of the ligand part of the molecular orbitals

$$K_\parallel = \beta_1^{\,2}\,\beta_2^{\,2}\,\{1 - (\beta_1'/\beta_1)S_1 - (\beta'_1\beta'_2/2\beta_1\beta_2)T\}$$

$$K_\perp - \beta_1^{\,2}\,\varepsilon^2\{1 - (\beta_1'/\beta_1)S_1 - (\beta_1'\varepsilon'/2\beta_1\varepsilon)T\} \qquad (6)$$

since λ is negative for d^9 system, equations (4) and (5) imply that $g_\parallel$ and $g_\perp$ will be greater than ge. $g_\parallel$ deviates from g_e due to mixing of the $|\,d_{x^2-y^2}>$ state and $g_\perp$ deviates from g_e due to mixing of $|\,d_{xz}>$ and $|\,d_{yz}>$ states into the ground state derived from $|\,d_{xy}>$. The deviation is proportional to the spin-orbit coupling constant and is inversely proportional to the energy separation between the ground state and the respective excited states connected by the spin-orbit interactions. Equation (6) implies that the anisotropy is reduced by covalent delocalisation. It may be noted that spin-orbit coupling due to ligand atoms is negligible due to the much smaller values of λ (N or O).

(ii) A_F is the Fermi contact interaction constant and it is an isotropic term contributing equally to $A_\parallel$ and $A_\perp$. This interaction arises due to the presence of unpaired electron (spin) density, $\phi^2_{spin}(0)$, at the nuclei. $\phi^2_{spin}(0)$ can be either due

77

to S contribution (4 S in the case of Cu) to the HOMO via configuration interaction or, more importantly, due to core polarisation. In simple terms polarisation of the inner S-shells takes place because the unpaired electron in 3d orbital ($\wedge$ spin) repels one of the two electrons (the $\wedge$ spin electron) in the S-shell *less* than the other. In other words the exchange interaction between the electrons having identical spin ($\wedge$ or α) leaves a net β spin density at the nucleus. The contact contribution is given as

$$A_F = 8\Pi/3 \ g_e \ \beta_e g_n \beta_n \ \{ |\phi_\wedge \ (o) \ |^2 - |\phi_v \ (o)^2 | \} \qquad (7)$$

where g_e and g_r are electronic and nuclear Lande factors and β_e and β_r are electronic and nuclear Bohr magnetons respectively. For convenience, we define

$$\beta_1^{\ 2} K = 8\pi/3 \ \{ |\phi_\wedge \ (0)|^2 - |\phi_v \ (0)|^2 \} / \ <r^{-3}>_{d_{x^2-y^2}} \qquad (8)$$

and

$$P = g_e \beta_e g_n \beta_n \ <r^{-3}> \ d_{x^2-y^2} \qquad (9)$$

so that

$$A_F = -\beta^2 \ P \ k \qquad (10)$$

It is clear that in the free atom or ion (i.e, in the absence of covalency) accurate calculation for $A_F = -Pk$. Both 'P' and 'K' can be obtained for atoms by unrestricted Hartree-Fock[38]. Accurate calculations for molecules are more involved and approximation methods like X-α have been used for the purpose with some

success.[39]

iii) A_D is the dipolar contribution to hyperfine splitting and is primarily responsible for the anisotropy in the observed splittings. Its value depends on the d-orbital containing the unpaired electron (For the present case/$d_{x^2-y^2}$ ground slate) we have

$$A_D = (-2/7)\beta_1^2 P. \tag{11}$$

Here again, covalency reduces the anisotropy due to the factor β_1^2 (<1) in equation (11), and also due to the reduction in the value of P. P is reduced by covalency because the d-orbital becomes more diffuse due to reduction in effective nuclear charge of the metal.

iv) $A_\parallel^{(1)}$ and $A_\perp^{(1)}$ are the first order corrections to the hyperfine splitting due to spin-orbit interaction. These correlations are related to the g- anisotropy by the following equation.

$$A_\parallel^{(1)} = (\Delta g_\parallel + 3/7\ \Delta g_\perp)\ P = 8E_\parallel P\beta_1^2\beta_2^2 - (6/7)E_\perp P\beta_1^2\varepsilon^2$$

$$A_\perp^{(1)} = 11/14\ \Delta g_\perp P = (-22/14)E_\perp\ P\beta_1^2\varepsilon^2 \tag{13}$$

2.3.9 Interpretation of e.s.r. parameters:

Using equation (3) the bonding parameters for the Cu Ni(pqdH)$_2$ complex listed in Table 2.5 have ben calculated and are tabulated in the Table 2.6. As mentioned in the earlier part of

79

Complex	$\Delta g_{\parallel}$	$\Delta g_{\perp}$	$10^{-3}E_{xy}$ cm^{-1}	$10^{-3}E_{xz,yz}$ cm^{-1}	$10^{4}A_{F}$ cm^{-1}	$10^{4}A_{D}$ cm^{-1}	$10^{-4}A_{\parallel}$ Cu cm^{-1}	$10^{-4}A_{\perp}$ Cu cm^{-1}	β_1^2	β_2^2	ℓ^2	K
Copper doped in Ni(pqpH)$_2$	0.126	0.031	20.62	22.62	46.4	73.4	0.0193	-0.0027	1.0	1.0	0.86	0.38
Copper doped in Ni(bqpH)$_2$	0.127	0.031	20.62	22.22	47.3	74.3	0.0196	-0.027	1.0	1.0		0.39

[a] Calculated with (λ = -828 cm, S_1 = 0.093, t = 0.333), P = 39.8 x 10^{-3}, S_2, S_3, S_4 = 0,0; (r^{-3})Cu = 8.258, g_n = 1.513 A$_{\perp}$ is taken to be - ve and A$_{\parallel}$ to be +ve.

the discussion $\beta_1\beta_2$ and ϵ represents the σ-bondings in plane and out of plane parameters respectively. If $\beta_1{}^2 = 1.0$, the corresponds to total plane π bonding if $\beta_1{}^2 = 0.5$, it is totally covalent in nature. The values obtained in the present system, $\beta_2{}^1 = 1.0$ shows more ionic nature σ bonding. From the total ionic character in in plane π bond is clear that there is electron delocalisation in out of plane π bonding in the present case. The large value of A_D (0.007 cm^{-1}), than A_F (0.004 cm^{-1}) shows that the anisotropic contribution in the hyperfine interaction is more than the isotropic part (A_F).

The difference in $A_\parallel$ (193 G) and $A_\perp$ (27 G) is in accordance with the above discussion. The K value (0.38) is also similar to that observed in the usual copper(I) square planar complexes.

2.4   CONCLUSIONS:

1.   The pratially oxidised $Ni(pqdH)_2I_x$ complexes are falling in to the semi conductors range.

2.   E.s.r. studies of copper doped $Ni(pqdH)_2$ and $(bqdH)_2$ complexes confirms the square planar geometry of these complexes.

81

2.5 Abbreviations:

dpg	:	diphenylglyoxime
dmg	:	dimethylglyoxime
$pdqH_2$	:	9,10-Phenanthrenedionedioxime
$bqdH_2$	:	benzoquinonedioxime
TMBP	:	tetramethylbenzoporphyrin
OMTBP	:	1,4,5,8,9,12,13,16-octamethyltetrabenzoporphyrin

2.6 REFERENCES:

1.   Thomas, T.W.; Underhill, A.E. *Chem. Soc. Rev.*, 1972, **1**, 99.

2.   Day, P. *Inorg. Chem. Acta. Rev.*, 1969, **3**, 81.

3.   Rundle, R.E. *J. Phys. Chem.*, 1957, **61**, 45.

4.   Miller, *J. Chem. Soc.*, 1965, 713.

5.   Ingraham, L.L. *Acta. Chem. Scan.* 1966, **20**, 283.

6.   Krogman, K. *Angew. Chem.* Internat. *edn.* 1969, **8**, 35.

7.   Krogman, K.; Dodel, P.;Hansen, H.D. *prog. VIII Internat. conf. coord. chem.ed. Gutman, V.* p.157.

8.   Robin, M.B.; Day, P. *Adv. Inorg. Chem. Radio. Chem.*, 1967, **10**, 247.

9.   Yamada, S. *J. Am. Chem. Soc.*, 1951, **73**, 1579.

10. Anex, B.G.; Krist, F.K. *J. Am. Chem. Soc.*, 1967, **89**, 6114.

11. Day, P.; Orchand, F.F.; Thomson, J.; Williams, P. *J. Chem. Phys.* 1965, **43**, 3763.

12. Ferguson, J. *Chem. Phys.* 1961, **34**, 611.

13. Sharpe, A.G.; Wakefield, D.B. *J. Chem. Soc.*, 1957, 281.

14. Banks, C.V.; Barnum, D.W. *J. Am. Chem. Soc.*, 1958, **30**, 3579.

15. Rundle, R.E.; Banks, C.V. *J. Phys. Chem.* 1963, **67**, 508.

16. Banks, C.V.; Anderson, S. *J. Am. Chem. Soc.*,1962, **84**, 1486.

17. Rundle, R.E.; William, D.E.; Whoelaner, G. 1959, **81**, 755.

18. Cowie, M.; Gleizes, A. *J. Am. Chem. Soc.*, 1979, **101**, 2921.

19. Schram, C.J.; Staja Kovic, D.R.; Hoffman, B.M.; Marks, T.J. Science 1978, 200, 47.

20. Brown, L.D.; Kalina, D.W.; Mcclure, M.S. *J. Am. Chem. Soc.*, 1979, **101**, 2937.

21. Phillips, T.E.; Hoffman, B.M. *J. Am. Chem. Soc.*, 1977, **99**, 7704.

22. Ray, R.K. *Polyhedron*, 1989, 8, 7, and references therein.

23. Bleany, B.; Stevens, K.W.H. Rept. Progr. Phys. 1953, **16**, 108.

24. Vogels "Text book of Practical Organic Chemistry", Furniss, B.S.; Hannaford, A.J.; Rogers, V.; Smith, P.W.G. Tatchell, A.R. ed. ELBS. 1978.

25. Walter, C. *Gazz. Chem. Ital.*, 1936, **66**, 5911.

26. Ohashi, Y.; Hanazaki, K.; Nagkurt, S. *Inorg. Chem.*, 1970, **9**, 2551.

27. Inoue, M.; Inoue, M.B. *Inorg. Chem.*, 1986, **23**, 37.

28. Zhukhoovistski, V.B.; Kidekel, M.L.; Dyumael, K.M. *Russ. Chem. Rev.*, 1985, **54**, 144.

29. Kruger,H.J.; Holms,R.H. *Inorg. Chem.* 1987,**24**,3645.

30. Lappin, A.G.; Murray, C.K.; Margerun, D.W. *Inorg. Chem.*, 1978, **17**, 1630.

31. Kirvan, G.E.; Margerum, D.W. *Inorg. Chem.*, 1985, **24**, 3245.

32. Subak, E.J.; Loyolan, Jr. V.M.; Magerum, D.W. *Inorg. Chem.*, 1985, **24**, 4350.

33. Pappenhagen, T.L; Kemady, W.R.; Bowers, C.P.; Margerum, D.W. *Inorg. Chem.*, 1985, **24**, 4356.

34. Kimura, E.; Sakonaka, A.; Machide, R.; Kodama, M. *J. Am. Chem. Soc.*, 1982, **1041**, 4251.

35. Yamashita, M.; Nonaka, Y.; Kidai, S.; Hamane, Y.; Aoki, R. *Inorg. Chem. Acta*, 1981, **52**, 43.

36. Cooper, D.A.; Higgins, S.J.; Levason, W. *J. Chem. Soc. Dalton Trans.* 1983, 2131.

37. Evans, J.; Lavason, W.; Peroy, R.J. *J. Chem. Soc. Dalton Trans.* 1990, 3691.

38. Goodman, B.A.; Raynor, J.B. *Adv. Inorg. Chem. Radio Chem.*, 1970, **13**, 134.

39. Rajasekharan, M.V.; Bucher, R.; Deiss, E.; Zoller, L.; Salzer, A.K.; Moser, E.; Weberk, J.; Ammeter, J.H. *J. Chem. Soc.*, 1983, **105**, 7516.

40. Keller, H.J. 'Mixed Valence Compounds', Ed. Brown, D.B. NATO Advanced Study Institutes series, D. Reidel Publishing Company, USA, 1979, **58**, 387.

CHAPTER - III

OXIDATION OF WATER BY Ce^{4+} IN PRESENCE OF MN(III,IV) COMPLEXES – FORMATION OF MnO$_4^-$ AND INFLUENCE OF COUNTER IONS

3.1 INTRODUCTION:

Oxygen evolution by di-μ-oxo bridged binuclear manganese complexes during water oxidation is a current research topic gaining much attention. The understanding of this mechanism might play a key role in the synthesis of synthetic leaf. It also helps to the technological development in the field of solar energy conversion to chemical energy. Oxygen evolution in the presence of excess cerium(IV) ions when di-μ-oxo bridged binuclear manganese complexes suspended as heterogeneous system, was reported by Ram Raj et al.[1] Many reports are there in literature about the oxidation of manganese(II) by cerium(IV) and the kinetic studies of this process was done in detail.[2-5] There are reports about evolution of oxygen from water on oxidation by permanganate. But so far to the best of our knowledge there is no report about the stabilisation of higher oxidation state of manganese (> MnIV) by cerium(IV) and the formation of any permanganate ion during the process of water oxidation. During our attempt to develop a mechanism for oxygen evolution, and quantitative measure of oxygen evolved during oxidation of water by cerium(IV) in the presence of binuclear manganese complexes as heterogeneous system, it is noticed that MnO$_4^-$ is formed in varying amounts depending on the concentration of the solution and the counter ions present. Some results on these aspects are presented in this chapter.

3.2   EXPERIMENTAL:

3.2.1 Chemicals:

The starting materials used for the preparation of ligands are either bought from Aldrich or Fluka. Other solvents and common chemicals are of reagent grade or better quality. All the organic solvents are purified by standard procedures described in Vogel.[6] Ether is stored over and sodium, pyridine over potassium hydroxide pellets. DMF is distilled under vacuum in dry nitrogen atmosphere and stored over type 4A molecular sieves.

3.2.2 Preparation of the Manganese complexes with 2,2'-bipyridine and 1,10-phenanthroline

All the di-μ-oxo complexes of manganese complexes with phen and bipy ligands are prepared according to the earlier reported procedures.[7,8] In the place of perchlorate salt, ammonium hexaflurophosphate (Fluka) is used in PF_6 complexes to salt out the complex.

3.2.3 Preparation of Substituted Complexes:

Py and DMF substituted complexes are prepared by dissolving complexes to make a saturated solution in these solvents. The filtrate is allowed to stand for seven days in a desiccator free from moisture. Then the solution changed to red colour. This red coloured solution was precipitated by the addition of ether

87

in the case of L = phen complexes and ethylacetate in L = bipy complexes. The brown solid separated from the mother liquor is filtered off, washed with small amounts of ethanol and dry ether and dried in vacuum. The i.r of the complex is recorded and checked with the earlier reports.[8]

3.2.4 Experimental conditions maintained for oxygen evolution studies:

For oxygen evolution measurements, 200 mg of complex is suspended in 10 ml of $(9.12 \times 10^{-1}$ M) 50% cericammoniumnitrate solution. The experimental set-up used for the quantitative measure of oxygen evolved is shown in Fig.3.1. A simultaneous blank experiment is carried out under similar conditions and the volume of oxygen evolved is corrected. By connecting another chamber having alkaline pyrogallol to reaction chamber, the evolving gas is confirmed as oxygen, which turned colourless pyrogallol to black. Water level in the set-up remained unchanged, as long as pyrogallol chamber is intact.

3.2.5 Experimental conditions for kinetic studies and optical spectral studies:

The solutions used for kinetic studies and optical spectral experiments are prepared by standard flask and burettes of grade A quality. A standard solution of manganese perchlorate of 1.5×10^{-2} M concentration is made and kept as a stock solution. The same solution is used in all experiments and diluted accordingly as per required concentration. While doing time drive (TDRV)
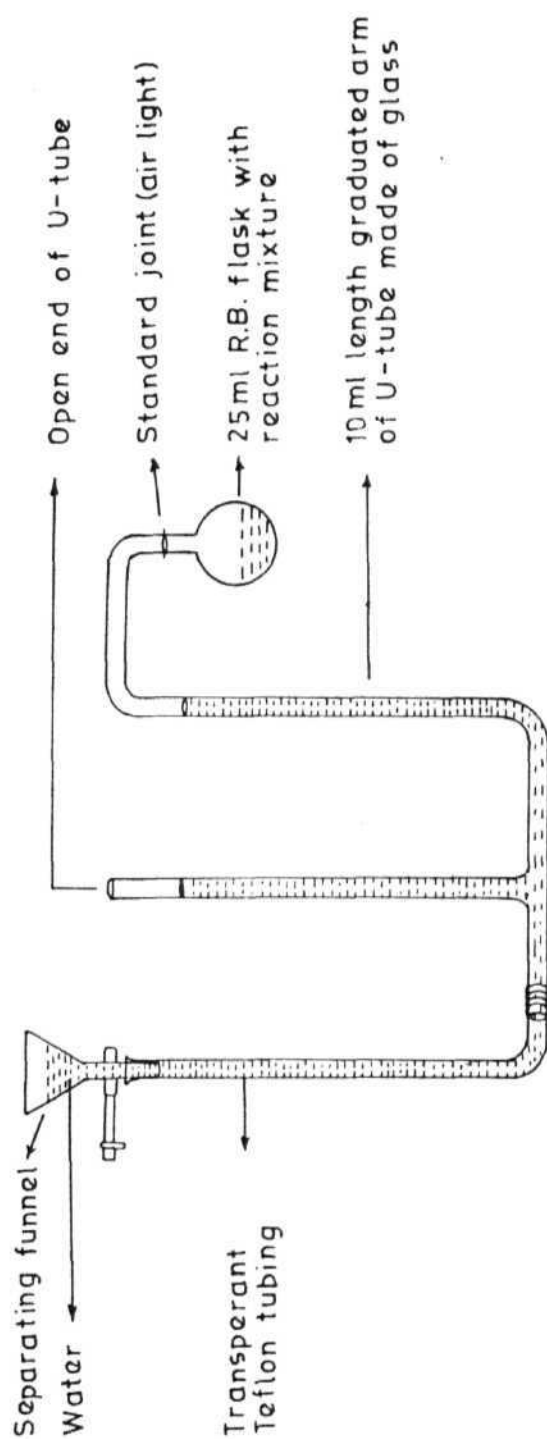
Fig.3.1   Diagram showing the experimental set-up used for the quantitative study of oxygen evolution.

Open end of U-tube

Standard joint (air light)

25 ml R.B. flask with reaction mixture

10 ml length graduated arm of U-tube made of glass

Separating funnel

Water

Transperant Teflon tubing

89

scans in the kinetic studies, stop clock is used to note the exact lag time between actual starting of reaction and the starting of TDRV scan. Glass distilled water is used for making standard solutions. P^H of the solutions are maintained with pH meter.

3.2.6 Physical measurements:

Infra-red spectra are recorded on Perkin Elmer (Model 1310) IR spectrophotometer. Kinetic studies are carried out in Perkin Elmer Spectrometer (LAMBDA-3A). Some of the optical spectra are recorded on Schimadzu-200S double beam spectrophotometer. All weighings are done on a single pan Metler-balance.

3.3 RESULTS AND DISCUSSION

3.3.1 Oxygen evolution studies on di-μ-oxo bridged Manganese Complexes:

When Mn^{III} - Mn^{IV} complexes are subjected to oxygen evolution studied, it is found that in the presence of excess cerium(IV) ions, all parent complexes of bipy and phen μ-oxo dimers, the DMF and Py substituted complexes give oxygen. The amount of oxygen evolved is found to be different for different complexes. Thus when these manganese complexes suspended in cericammoniumnitrate solution of concentration $(9.12 \times 10^{-1}$ M), oxygen gas starts bubbling out of the surface of the solid suspended. These solutions are not subjected for any agitation. The reaction mixture turns reddish as soon as the complex is

90

added. The optical spectrum recorded for this solution after aging for 24 hr showed the presence of permanganate (MnO_4^-) bands (Fig.3.2a; 3.2b; 3.2c). When cericammoniumsulphate is used in the place of cericammoniumnitrate and the oxygen evolution studies are carried out, there is no gas evolution and the solution did not show any evidence of permanganate band in optical spectrum. Cerium(IV) concentration in the two solutions made by cericammoniumnitrate and cericammoniumsulphate salts are maintained 0.2 M and 200 mg of the same manganese complex is used for the comparative oxygen evolution studies. The solution containing cericammoniumnitrate gave 6.5 ml of oxygen, the other solution did not give any oxygen. The rate of which oxygen is evolved from different complexes is tabulated in Table 3.1. It is found that the rate of oxygen evolved depends on the concentration of Ce^{IV} ions, (9.1×10^{-1} M solution is found to be ideal concentration.). It is also observed that the Py and DMF substituted complexes gave oxygen rapidly in the beginning and the process is slowed down over a period of time ($\sim$ 10 hr). The DMF substituted complex evolve oxygen more rapidly than pyridine substituted complexes but for a short time ($\sim$ 5 hr). It is also observed that when the Ce(IV)solution is replaced with a fresh solution, the gas bubbles out again at the same rate, but after two to three replacements the compound becomes inactive.[9] The PF_6^- anion complexes give less oxygen than ClO_4^- anionic complexes. These experimental results reveal that there is formation of MnO_4^- species in the due course of the reaction. Which is possible only at certain potentials. The potentials are maintained by certain anions like NO_3^-, ClO_4^- where as sulphate is not providing the required potential. But the role of MnO_4^-

91
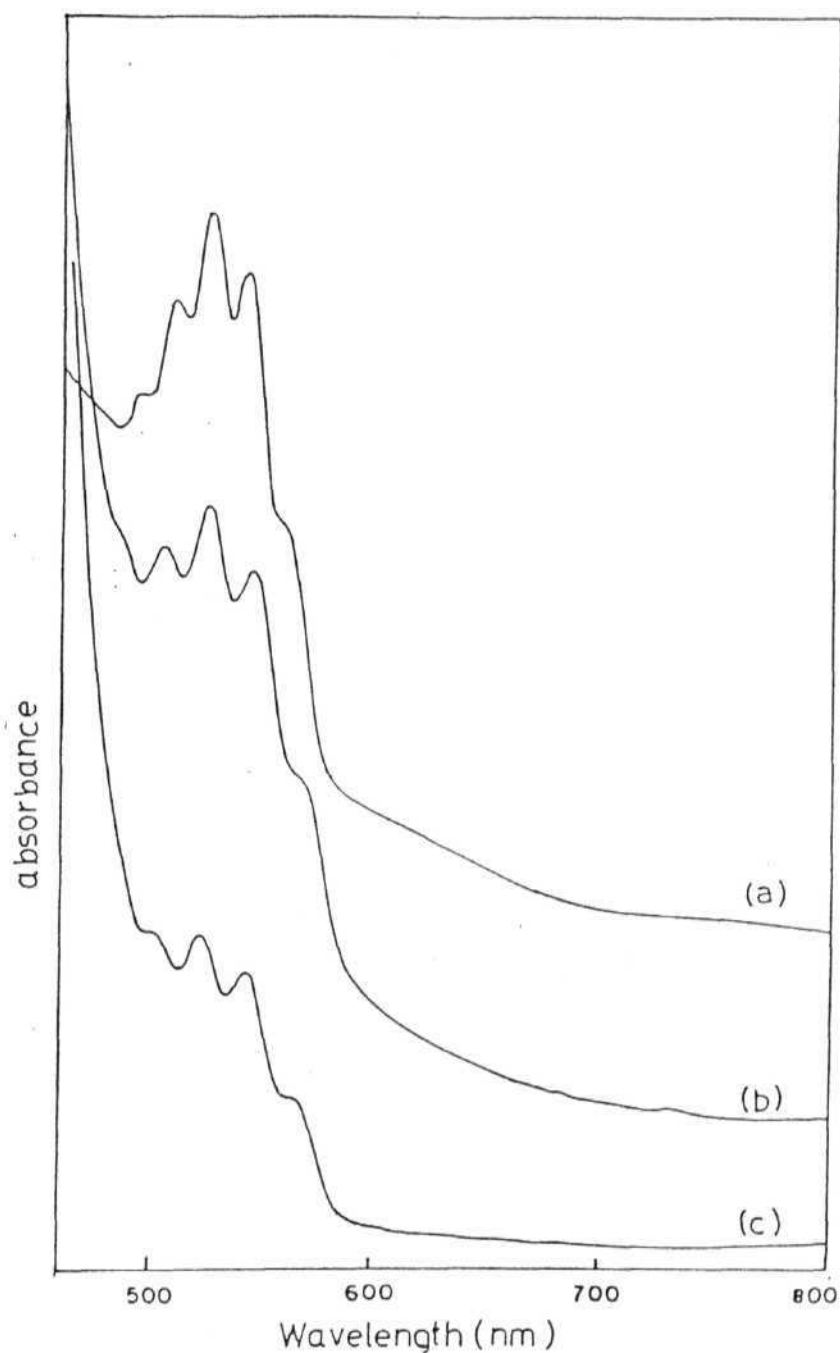
Fig.3.2.   a)   Electronic   spectrum   of $[Mn_2O_2bpy_4](ClO_4)_3$ and

$[Ce(NO_3)_6$ $(NH_4)_2$ medium after aging for 24 hrs.

b) Electronic spectrum of $Mn(ClO_4)_2$ in $[Ce(NO_3)_6](NH_4)_2$

and water medium after aging for 24 hrs.

c) Electronic spectrum of $KMnO_4$ in $[Ce(NO_3)_6](NH_4)_2$ and

water medium (Ce^{4+} = 9.1 x 10^{-2}M, Mn^{2+} = 3.14 x 10^{-4}M;

MnO_4^- = 5.7 x 10^{-5} M).

92

Table 3.1 Volume of oxygen evolved from different Mn^{III} - Mn^{IV} complexes in the presence of cerium(IV) salts.

Name of the Compound	Weight of sample used Mg	Anion in the complex	Substitution	Type of CeIV salt	CeIV con. Mol/lit	O$_2$ evolved ml	Total Time hours	Rate of O$_2$ evolved ml/hour
[MnO(Phen)$_2$]$_2$(ClO$_4$)$_3$	200	ClO$_4$	---	Ce(NO$_3$)$_6$(NH$_4$)$_2$	0.912	38	149	0.26
[Mn$_2$O$_2$(bipy)$_3$Py$_2$](ClO$_4$)$_3$	200	ClO$_4$	Py	Ce(NO$_3$)$_6$(NH$_4$)$_2$	0.912	13.4	200	0.07
[MnO(Phen)$_2$)]$_2$(PF$_6$)$_3$	200	PF$_6^-$	--	Ce(NO$_3$)$_6$(NH$_4$)$_2$	0.912	26.5	170	0.16
[Mn$_2$O$_2$(Phen)$_3$(DMF)$_2$](PF$_6$)$_3$	200	PF$_6^-$	DMF	Ce(NO$_3$)$_6$(NH$_4$)$_2$	0.912	25.8	204	0.13
[Mn$_2$O$_2$(bipy)$_3$Py$_2$](PF$_6$)$_3$	200	PF$_6^-$	Py	Ce(NO$_3$)$_6$(NH$_4$)$_2$	0.912	12.1	100	0.12
[Mn$_2$O(bipy)$_2$Py$_2$](ClO$_4$)$_3$	200	ClO$_4$	---	Ce(NO$_3$)$_6$(NH$_4$)$_2$	0.912	25	100	0.25
[Mn$_2$O(Phen)$_2$)]$_2$(PF$_6$)$_3$	200	PF$_6^-$	---	Ce(NO$_3$)$_6$(NH$_4$)$_2$	0.912	11.8	100	0.12
[MnO(Phen)$_2$]$_2$(PF$_6$)$_3$	200	PF$_6^-$	DMF	Ce(NO$_3$)$_6$(NH$_4$)$_2$	0.912	25.8	204	0.13
[Mn$_2$O$_2$(Phen)$_3$(DMF$_2$)](PF$_6$)$_3$	200	PF$_6^-$	β-Picol	Ce(NO$_3$)$_6$(NH$_4$)$_2$	0.912	10.7	100	0.11
[Mn$_2$O$_2$(bipy)$_3$(-Pi)$_2$(PF$_6$)$_3$	200	BF$_4^-$	---	Ce(NO$_3$)$_6$(NH$_4$)$_2$	0.912	23.5	100	0.24
[MnO(bipy)$_2$(bipy)$_2$]$_2$(BF$_4$)$_3$	200	BF$_4^-$	---	Ce(NO$_3$)$_6$(NH$_4$)$_2$	0.912	23.5	100	0.24
[MnO(Pha)$_2$(BF$_4$)$_3$	200	BF$_4^-$	---	Ce(NO$_3$)$_6$(NH$_4$)$_2$	0.912			
[MnO(Phen$_2$)$_2$(ClO$_4$)$_3$	200	ClO$_4^-$	---	Ce(NO$_3$)$_6$(NH$_4$)$_2$	0.2	6.5	22	0.3
[MnO(Phen)$_2$]$_2$(ClO$_3$	200	ClO$_4^-$	---	2(NH$_4$)$_2$SO$_4$ Ce(SO$_4$)$_2$.2H$_2$O	0.2			

in the oxygen evolution is ambiguous. The results are also suggesting that the oxygen evolution is depending on several factors like symmetry around the metal centre, grain size, temperature, Ce(IV) concentration etc. But all these factors are yet to be established in detail. During this course of studies the notice of MnO_4^-, demanded our attention towards that. Hence we analysed the causes and conditions for the formation of MnO_4^- ions.

3.3.2 Optical spectral and kinetic studies of the permanganate ion (MnO_4^-) formation in the reaction between ceric salts and Manganese(II) salts:

When the manganese perchlorate is added in small amount to the solution of cericammoniumnitrate, it turns to purple red. This solution showed the bands of MnO_4^- in ligands like bpy and phen to this solution did not affected the spectrum.

When cerium(IV) salt is added to water the solution gave pH of ~ 1. Under these pH conditions the rate of formation of MnO_4^- was slow (Fig3.3a), it took around 12 hr for the total amount of manganese(II) to get converted to MnO_4^-. Hence we observed slow increase in the intensity of the bands with time (Fig3.3b). The well resolved spectrum of MnO_4^- is observed only after 24 hr (Fig3.3c). When the same solution is allowed to age, slow decrease in MnO_4^- band intensity (3.3d) is observed and finally the spectrum becomes flat totally (3.3e). This might be due to the total conversion of cerium(IV) to cerium(III) which can not stabilise MnO_4^- species. Therefore in order to stabilise MnO_4^-,

94
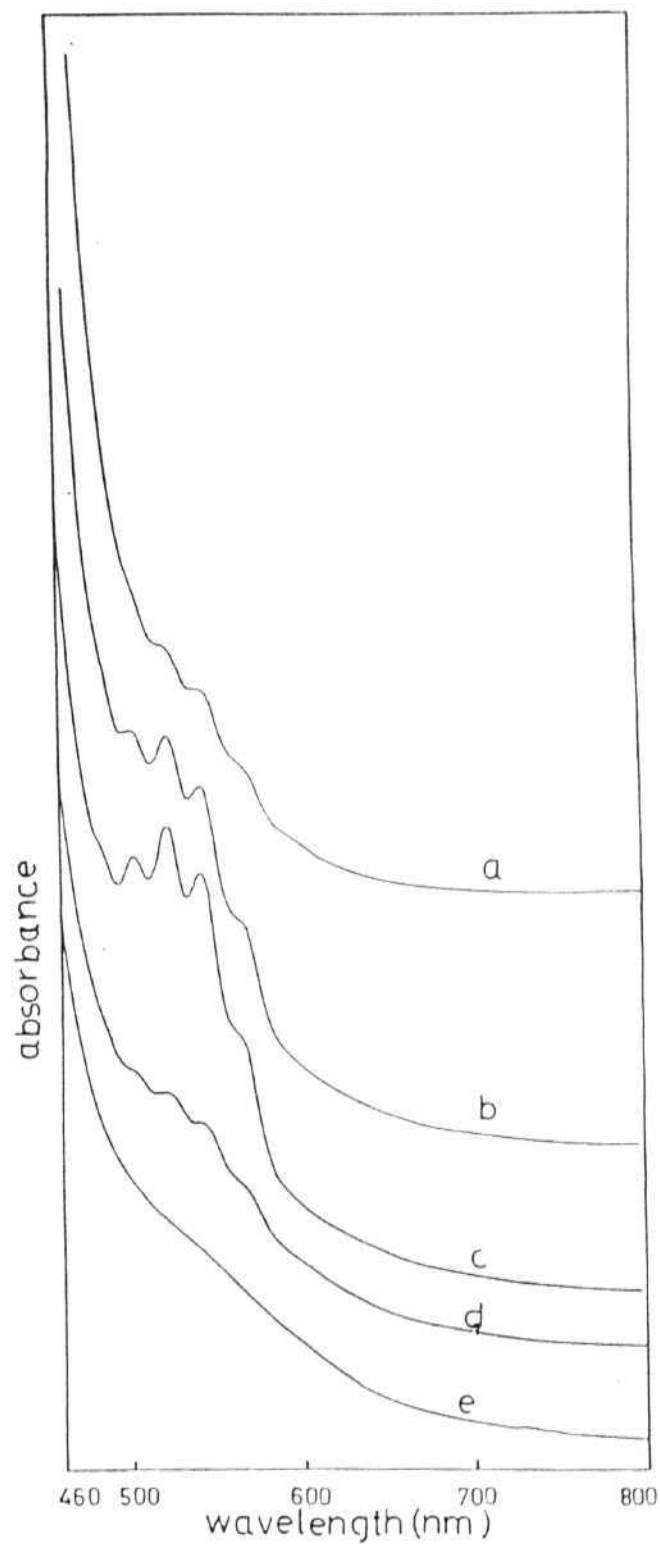
Fig.3.3 Electronic spectra showing the formation of MnO_4^- band in water medium from $[Ce(NO_3)_6](NH_4)_2$ and $Mn(ClO_4)_2$. Changes in the band intensity with aging are shown (a) initial (b) after 11 hrs (c) after 17 hrs (d) after 49 hrs (e) after 96 hrs.

excess cerium(IV) should be present in solution. This problem can be solved by making cericammoniumnitrate solution in acid medium using 1N nitric acid (HNO_3). This solution showed a pH of 0.3. Solution remained stable for long time and did not precipitated cerium(III) by hydroxide or polymer. The presence of acid is also found to help in the complete conversion of Mn^{2+} ---> MnO_4^- in a short time compared to acid free solution (Fig.3.4). The MnO_4^- formed this way are stable even after 8 months. The presence of excess NO_3^- ions raises Ce^{4+}/Ce^{3+} potential In the presence of nitrate medium Ce^{4+}/Ce^{3+} potential $E^0=1.61V$, whereas in sulphate medium is found to be 1.44 V.[10] The potential required for Mn^{2+} ----- MnO_4^- equilibrium to exist is reported as 1.52 V.[10] This shows that the presence of SO_4^- ions in the medium reduce the potential and thus may not lead to the formation of MnO_4^- formation. Further the low pH also prevents the hydrolysis of Ce^{4+}.(Table 3.2)

The kinetic study of these reactions revealed that the rate of the reaction is too fast for our method - the system reaches a steady state with in 2 minutes (Fig.3.5 and 3.6). Since it is a 5 electron oxidation the reaction must be following a step wise electron transfer but the other oxidation states are so short lived that we could not trace their presence in the optical spectrum. Where the same reaction is carried out with ceric ammoniumsulphate in sulphuric acid maintains same pH 0.3, there is no sign of MnO_4^- formation, but the brown turbidity is noticed in the solution. However, when the SO_4^{2-} is replaced $NO_3^{\cdot -}$ by the addition of bariumnitrate the solution changed to MnO_4^- colour and gave identical MnO_4^- spectrum.
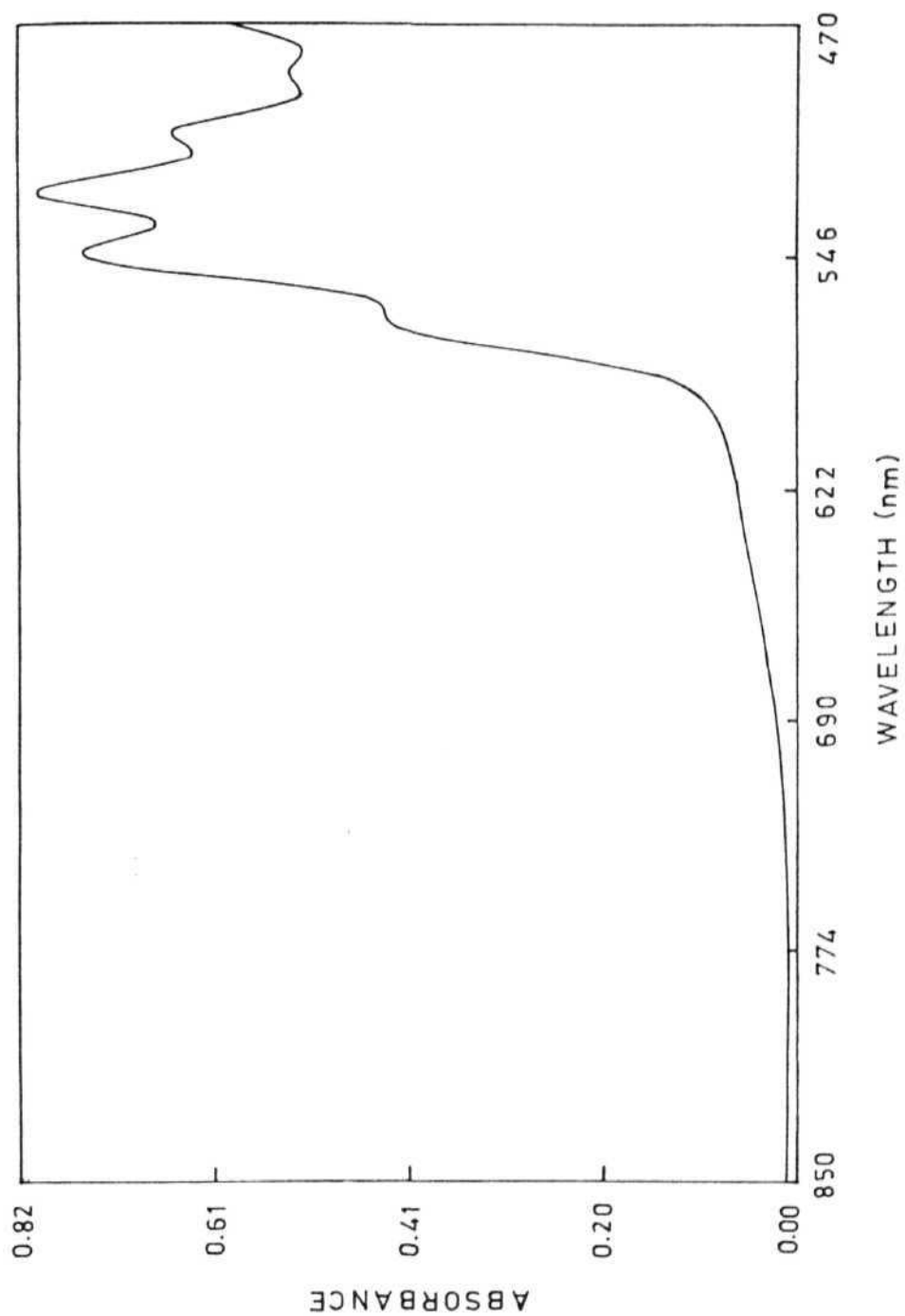
Fig.3.4 Electronic spectrum showing the well formed MnO_4^- band from $Mn(ClO_4)_2$ and $[Ce(NO_3)_6](NH_4)_2$ in 1M HNO_3 medium only after 2 1/2 hrs.
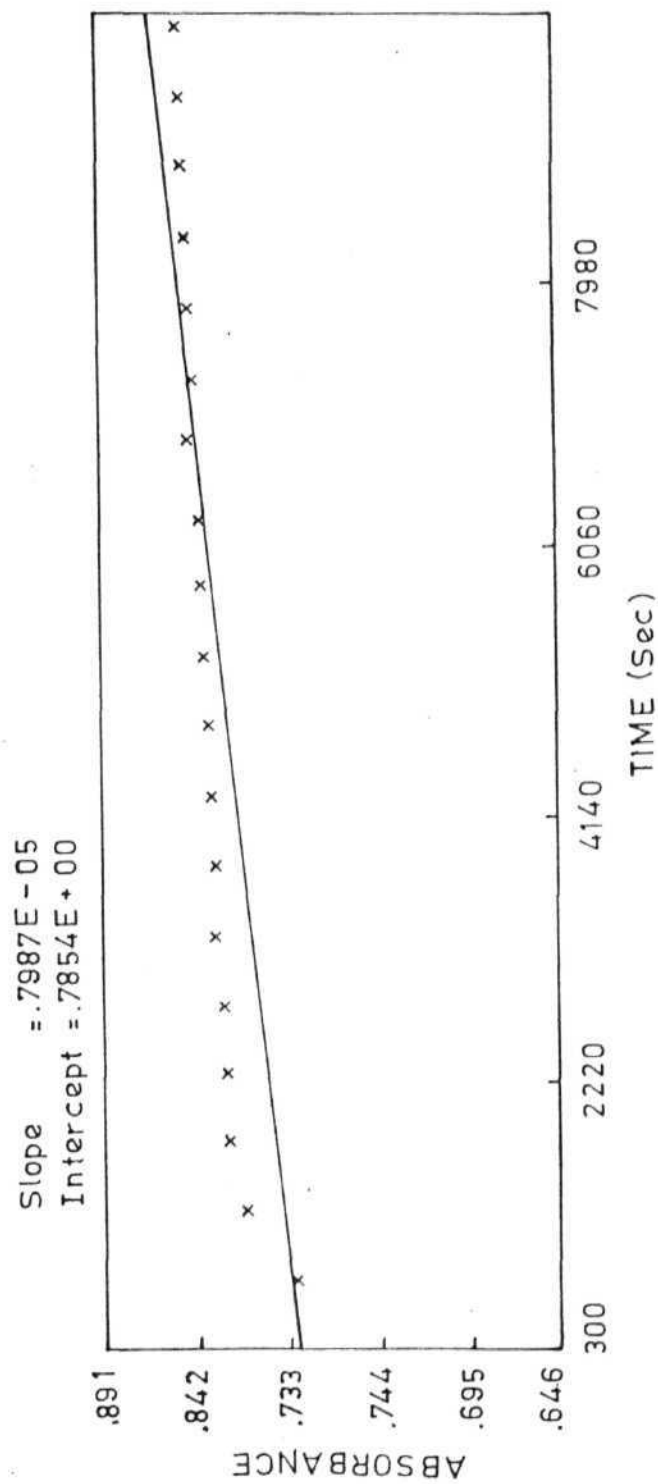
Fig.3.5 Spectrum showing the TDRV scan of the MnO_4^- formation from $Mn(ClO_4)_2$ in the presence of $[Ce(NO_3)_6](NH_4)_2$ in 1M HNO_3 medium. ($Ce^{4+} = 9.1 \times 10^{-2}$ M, $Mn^{2+} = 3.14 \times 10^{-4}$ M).

Slope = 2056-04
Intercept = 4651E+00
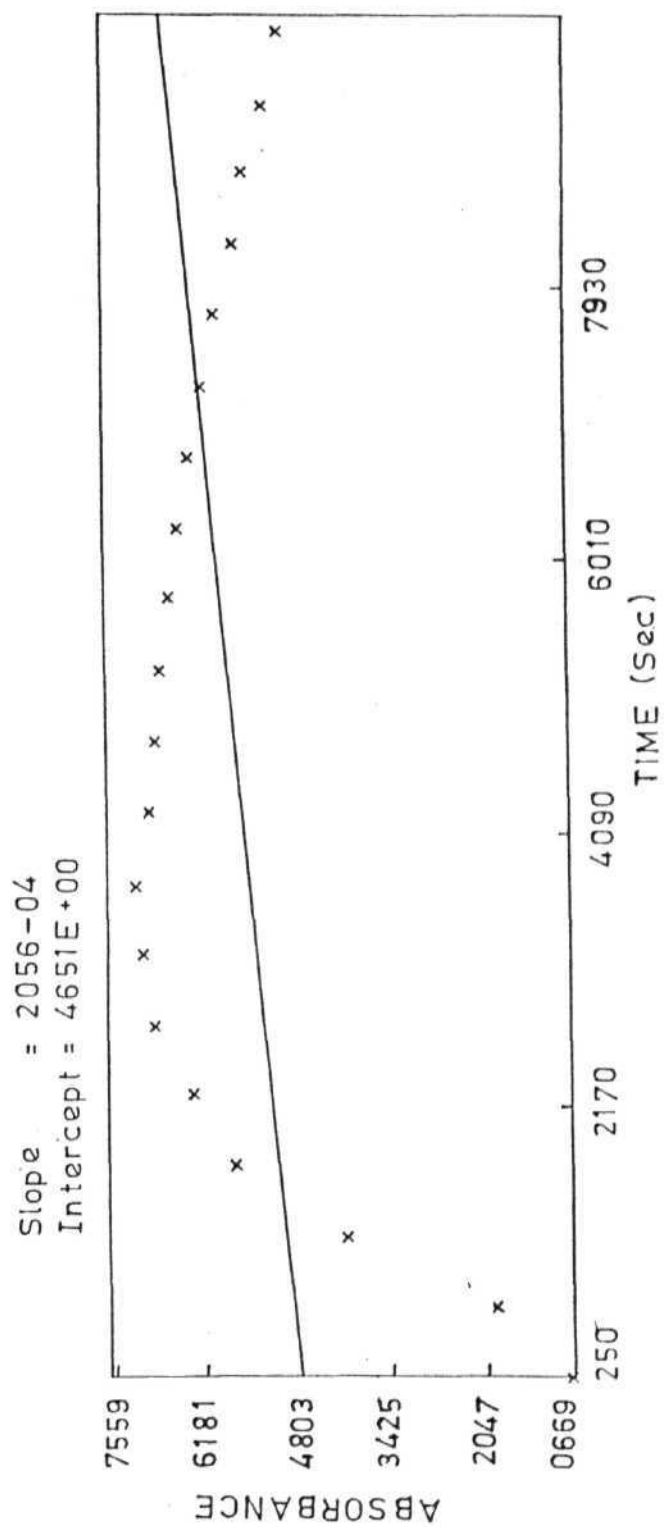
Fig.3.6 Spectrum showing the TDRV scan of the turbid solution due to less $[Ce(NO_3)_6](NH_4)_2$ concentration. $(Ce^{4+} = 9.1 \times 10^{-4}$ M, $Mn^{2+} = 3.14 \times 10^{-4}$ M].

66

Table 3.2. Effect of cerium (IV) concentration on the rate of formation of MnO_4^- species

Solution	Con. of Ce(IV) ion M	Conc Mn^{2+} ions M	Behaviur of solutions during kinetic run	Absorbance at 524 mm after[b] 1×10^4 sec
Solution 1	9.12×10^{-2}	3.15×10^{-4}	Initially very fast. After 5 minutes reached steady state.	0.852 (99%)
Solution 1/20	4.57×10^{-3}	3.13×10^{-4}	Initially very fast. After 5 minutes reached steady state.	0.664 (85%)
Soltion 1/100	9.23×10^{-4}	3.03×10^{-4}	The solution becomes turbit and gives a precipitate in 10 minutes	....

[a] $(NH_4)_2$ $[Ce(NO_3)_6$ and $Mn(ClO_4)_2$ are used to make solutions in 1N HNO_3.

[b] % conversion of Mn^{2+} to MnO_4 based on ε is given in brackets.)
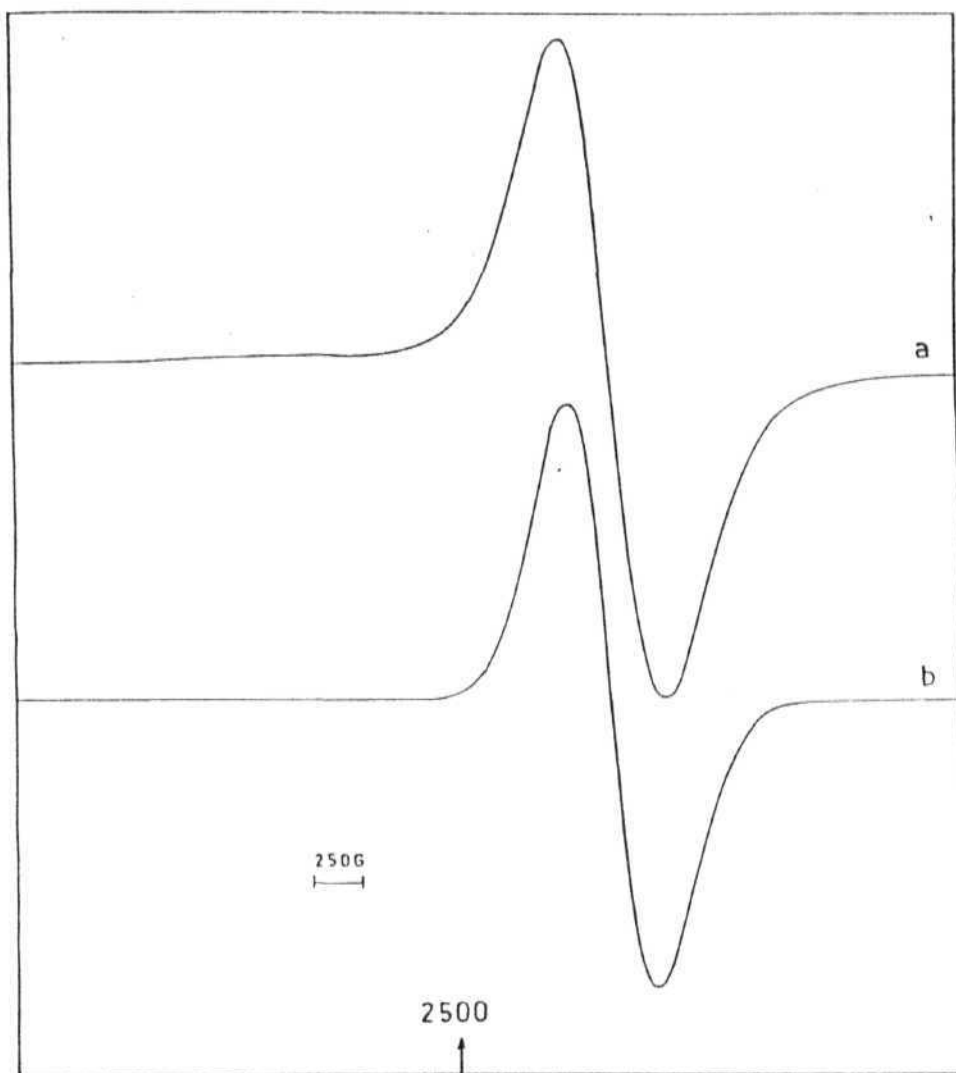
Fig.3.7 X-band e.s.r. spectrum of Mn(III,IV) complex formed at low concentration of Co(IV) ions. At (a) 294 K. (b) 124 K.

When in the place of manganese perchlorate, manganese acetate and manganesesulphatae are used in the presence of ceric ammoniumnitrate, the same kind of MnO_4^- band is observed in optical spectrum in the visible region. This makes it clear that driving force for the formation of MnO_4^- ions is the potential supplied by the large excess of NO_3^- ions (9.12×10^{-2} M). In such a high concentration of NO_3^- ions, very small amount (3.14×10^{-4} M) of CH_3COO^-, SO_4^{2-} are not much effective in affecting the overall reaction process.

Formation of MnO_4^- is dependent on cerium(IV) concentration. When concentration of Ce(IV) is nearly 100 times (9.12×10^{-2} M) greater than the Mn^{2+} (3.14×10^{-4} M) in the presence of 1N HNO_3 at about 0.3 pH nearly 95%. Mn^{2+} converted to MnO_4^- (Fig.3.5) where as cerium(IV) (9.12×10^{-4} M) concentration is nearly made equal to Mn^{2+} (3.12×10^{-4} M) a turbidity is formed (Fig.3.6). Manganese acetate with three times excess of cericperchlorate at pH ~ 1 in the presence of ligand gave a solid, the powder e.s.r spectrum of which showed a single line at g = 2.0. This may be because of Mn(III,IV) dimeric complex.[11] (Fig. 3.7).

3.4 CONCLUSIONS:

1. The parent and substituted Mn(III,IV) manganese complexes are found to be catalytically active towards the water oxidation in the presence of strong oxidant like cerium(IV).

2. The rate of oxygen evolution depends on the concentration of cerium(IV) ions in the medium.

3. MnO_4^- ion formation is possible only at certain potentials, which can be maintained only by certain anions like NO_3^- and ClO_4^- where as the presence of SO_4^{-2} prevents the MnO_4^- formation.

4. In addition the low pH of the medium prevents the hydrolysis of Ce^{4+} ions to Ce^{3+}.

5. Only those solutions in which MnO_4^- is formed are evolving the oxygen. Which conforms that MnO_4^- formation during the water oxidation is essential, but their presence further complicates the mechanism of water oxidation.

3.5. Abbreviations:

Phen   : 1,10-Phenanthroline

bipy   : 2,2'-bipyridine

Pic   : β-Picoline

DMF   : Dimethylformamide

Py   : Pyridine

103

3.6   REFERENCES:

1. Ram Raj, R.; Kira, A.; Kaneko, M. *Angew Chem. Int., Ed. Engl.*, 1986, **25**, 825.

2. Sarma, Y.R.; Sai Prakash, P.K. *Ind. J. Chem.*, 1980, **19A**, 1175.

3. Sai Prakash, P.K.; Sethuraman, B. *J. Ind. Chem. Soc.*, 1973, **50**, 211.

4. Aspay, M.J.; Rosensky, D.R.; Shaw, G.B. *Chemis. Ind.*, 1963, 911.

5. Allen, E.; Ogard; Tanke, H. *J. Phys. Chem.*, 1958, **63**, 357.

6. 'Vogel's Text Book of practical Organic Chemistry', Furniss, B.S.; Hannaford, A.J.; Ragers, V.; Smith, P.W.G.; Tatchell, A.R. Ed. ELBS, 1978.

7. Copper, S.R.; Calvin, M. *J. Am. Chem. Soc.*, 1977, **99**, 6623.

8. Swarnabala, G. Section I, Chapter II, Ph.D. Thesis, School of Chemistry, University of Hyderabad, Hyderabad.

9. Bhoomiah, K. M.Phil. Dissertation, 1990, School of Chemistry, University of Hyderabad, Hyderabad.

10. 'Vogels Text Book of Quantitative Inorganic Analysis', Bassett, J.; Denney, R.C.; Jeffery, G.H.; Hendham, J. Ed. ELBS, 1978, p.50.

11. Reddy, K.R.; Lakshmi, N.V.; Rajasekharan, M.V. unpublished results.

CHAPTER - IV

ELECTRON SPIN RESONANCE AND MÖSSBAUER STUDY OF HIGH-SPIN
-LOW-SPIN TRANSITIONS IN RED AND VIOLET FORMS OF
$[Fe(Phen)_2(NCS)_2]$

4.1 INTRODUCTION:

The phenomenon of thermally driven spin crossover or spin transition in various complexes of the transition metal ions with d^4 to d^7 configuration has received considerable attention in the last few years. A detailed survey of this problem has been given in review articles by Martin and White[1], Goodwin,[2] Gutlich,[3] Bacci[4] and Toftlund.[5]

Spin crossover or spin equilibrium is observed in such systems having cubic symmetry (octahedral symmetry) where $|\Delta-P^-|$ may be comparable to KBT. In the cubic ligand field there is possibility for two ground states, (1) high spin state $t_2^4 e^2$ and, low spin slate (t_2^6)

For $^5T_2$ ground state $\Delta < 5/2B+4C$

$^1A_1$ ground state $\Delta > 5/2B+4C$

where B and C are Racah parameters. The spin state of the complex changes from one spin multiplicity to another when the ligand field changes slightly from the critical value ($\Delta C = \dot{\bar{P}}$). At this crossover point the ligand field strength is equal to the

sum of the charges in coulombic repulsion (P_c) and quantum mechanical exchange energy (P_e). Orgel[6] determined the values of P_c and P_e for free metal ions of first row transition metal ions in Oh symmetry. But Konig et. al[7] derived the values for complexes from electronic spectra and found that the values are about one third of the values of orgel. This shows that upon complexation the Racah parameters reduce considerably.Which may be due to the ectron delocalisation towards ligand,leading to the reduction in the inter-electronic repulsion.

The mechanism of spin crossover is discussed by different authors in different ways. In terms of thermodynamic concepts the relative stability of the two different spin states constituting the equilibrium

LS ------- HS

is determined by the free energy changes

$$\Delta G = G(HS) - G(LS) = \Delta H - T\Delta S$$

But at low temperature ΔH (enthalpy) dominates ΔS(entropy) change. The ΔH and ΔS are due to various contribution accompanying the spin transition. They can be represented as

$$\Delta H = \Delta H_{el} + \Delta H_{(intravib)} + \Delta H_{(latVib)} \qquad (1)$$

$$\Delta S = \Delta S_{el} + \Delta S_{(intravib)} + \Delta S_{(latVib)} \qquad (2)$$

ΔH_{el} is the enthalpy change associated with the spin transition which is nothing but the energy separation between the lowest energy level in the cubic field of LS and HS states of the compound. Usually $\Delta H_{el} > 0$ for LS and it is the largest contributions in eq. (1) compared to other terms. Similarly ΔS_{el} comprises of ΔS_{el}^{Spin} and ΔS_{el}^{orb}. Since the spin crossover systems have exactly cubic symmetry, ΔS_{el}^{orb} can be neglected. Hence, when

$$\Delta H > \Delta S^{el} \qquad \text{LS is favoured.}$$

$$\Delta H < \Delta S^{el} \qquad \text{HS is favoured.}$$

At transition temperature (T_c) ΔH and $T\Delta S$ are of equal magnitude and thus gain in entropy drives the system from LS to HS.

Sorai and Seki[8] suggest that spin crossover occurs through a cooperative coupling of the electronic state and the phonon system *i.e.*, the conversion of electronic state occurs simultaneously in a group of molecules the so-called cooperative region whereas Kambara[9] in his model based on the static treatment of the intramolecular distortion, described it as the coupling with the lattic strain accompanying the cooperative intramolecular distortion. The cooperative behaviour of the spin transition in the solid state requires the interaction mechanism between HS and LS complex molecules. Several mechanisms have been proposed (i) coupling to lattice vibrations induced by the

Debye temperature θ of the lattice. On the HS fraction,[10] (ii) Jahn-Teller type distortions of HS/LS ions,[11] and (iii) elastic interaction between the HS and LS complex molecules via the image pressure[12,13]. It is known that the spin change is accompanied by a pronounced change of the metal, ligand[14,15] bond lengths in the first coordination sphere. Recently it has been shown that the important features involved in the spin transition of $Fe(2-pic)_3Cl_2$ EtOH [13,16] and $Fe(2-pic)_3Cl_2$ MeoH[17] can be explained based on the elastic theory. But[18]Hendrickson and coworkers[18] based on their experiments put forward a different mechanism which states that spin transitions involve the formation of small homogeneous regions (domains) of minority spin molecules in the crystallites of majority spin molecules. Nucleation and growth of a minority spin domain occurs only when it attains a critical size, which strongly effects the experimental results.

The transition or crossover can be broadly classified in to two types (1) discontinuous (abrupt) transition, which occurs at a well defined transition temperature, T_c eg $Fe(Phen)_2(NCS)_2$ or (2) continuous (gradual) transition which takes place over an extended range of temperature.for example in $(Fe(2-pic)_3)Cl_2$ EtOH. The first example of spin crossover was found by Cambi and his coworkers[19] in the early thirties. By now many more complexe systems have been discovered, particularly in the complex chemistry of Fe(II), Fe(III), and Co(II).

In the Fe-phen systems[47] $Fe(Phen)_2)NCS)_2$ and $Fe(Phen)_2$

$(NCSe)_2$ show very abrupt transitions in a short range of temperature. This change is associated with a phase transition. The substitution on Phen- changes the spin crossover behaviour. $(4,7 \text{ dimthyl}-1,10\text{-Phen})^2\text{Fe}$ showed a sharp transition, but most of the substituted Phen- like 4-methyl, 4-chloro, 4-cyano -1,10-Phen show spin transition over a broad range.[2] In bis 2-substituted phenanthroline incorporation of a substituent like carboximido,carbothioimido brings about spin-state changes. In these complexes O-bonded are high spin while S-bonded are low spin at room temperature Retention of a fraction of high spin species is a general phenomenon associated with $^5T_2$ ----- $^1A_1$ transition in Fe(II). But tris(2-methoxy-Phen) Fe(II)$(ClO_4)_2$ $^5T_2$ ------ $^1A_1$ transition occurs almost completely unlike in $[\text{Fe}(\text{Me-Phen})_3]^{2+}$, which may be due to the difference in electronic and steric factors of methyl and methoxy groups.[3] Thus Reiff and Long[18] suggested that the substitutents in the position adjacent to donor atom affect much more than in other positions and along with the spin orbit coupling and covalency, the steric effects also adds to the ligand field effects in the spin transition.[3]

Complexes with substituted bipy derivatives showed $^5T_2$ --- $^1A_1$ crossover over a wide range of temperature. Usually when one or two bipy replaced by py shows abrupt spin crossover.[3] Madeja et al[21] found that in Fe(pip)$_2$(NCS)$_2$ shows $^5T_2$ ---- $^1A_1$ (Oh) spin transition whereas Fe(pmi)$_2$(NCS)$_2$ show no spin crossover. This may be due to temperature dependent steric hindrance effect in case of large isopropyl substituent compared to the much smaller

methyl group in pmi complex. Goodgame and Machado[22] studied spin transition of two forms of $Fe(Pyimi)_3$ prepared by two different methods and found that spin states are sensitive to method of preparation.

Kelly *et al*[23] studied the five co-ordinated complexes of the type $M(pnp)X_2$, $M(pnp)XY$, (M = Fe(II), Co(II), Ni(II)),(X = Cl^-,Br^-, I^-, y = NCS^-). $M(pnp)X_2$ (X=Cl^-, $Br^- I^-$) remained high spin in the temperature range 293-93 K, where as $Fe(pnp)I_2$ and $Fe(pnp)NCSI$ showed temperature dependent $^5E(D_{3h})$---$^3A(D_{3h})$ transition. They also observed temperature dependent $^2E_2$---^4A transition in $Co(PnP)Br_2$.[23] ^1A--- ^3E transition in $Ni(Pnp)Cl_2$.[23] Tripod systems like FeN_2P_2I and $FeNP_2I_2$ show S=2...S=1 crossover.[24] $Fe(HB(Me-Pz)_3)_2$ exhibit temperature dependent $^5T_2$ ---$^1A_1$ (Oh) smooth transition, while $Fe(HB(Pz)_3)_2$[26] exhibit no spin transition. In the case of $[Fe(bt)_2(NCS)_2$ (T_c ~ 180 K) and $Febt(NCSe)_2$ (T_c ~ 200 K), a very sharp temperature dependent $^5T_2$ ---- $^1A_1$ (Oh) transition is observed.[27] This is a striking example where we see difference in T_c between NCS^- and $NCSe^-$ which is usually not observed. This may be due to the slight reduction of basicity of N-atom going from NCS^- to $NCSe^-$. $FE(bt)_2(NCS)_2$ also stands an example for the abrupt transition followed by[28-30] hysteresis. Among the phosphine complexes, $[Fe(dippen)]^{2-}$ is the first and only example for spin crossover.[31] $[Fe(6MePy)(Py)_2tren](PF_6)$[32] is a pseudo-octahedral FE(II) complex found to exhibit $^1A_1$----T_2^2 equilibrium. $[Fe(Isoxazole)_6]X_2$ is the only complex of the (Fe L_6) type exhibiting a sharp spin crossover at 212 K^2. Eibschutz[33-35]

investigated substitutionally iron doped layer-chalcogenide material $1T-Fe_xTa_{1-x}S_2$ with iron concentation, $X < 1/3$ by magnetic susceptibility and Mössbauer technique and found to exhibit $^1A_1 --- ^5T_2$ (Oh) gradual transition over 200 - 500K temperature range and found that with increasing X concentration. transition temperature range also moves to higher temperature and named this as metalo-organic Fe(II) spin-crossover.[36]   In $[Fe(P_4)X]BPh_4$ where P_4 is a tetradentate ligand,and $(X=Br^-, I^-)$ Bacci[37] found singlet ---- triplet transition.

Solid state effects also leads to spin crossover lattice effects and solvent effects can be considered, under this category.Some times upon aging for a long period, due to some slow lattice modifications spin transition is observed. $Fe(Phen)_2(NCS)_2$[38] show this type of $^5T_2 --- ^1A_1$ transition. It is found that the ground state properties of the $[Fe(2-Pic)_3]Cl_2 \cdot$ Solvent, are very much dependent on the crystalisation solvents[3] Mono hydrated molecule show very large hysteresis over a range of temperature (T_c = 204 K for cooling and T_c= 29 K for heating).[3] This may be due to the combined action of hydrogen bonding and changes in relevant phonon systems due to different geometrical packing. Usually $^1A_1$ will be the ground state when ethanol, methanol, and H_2O are used as solvents. They exhibited different crystal packing and magnetic behavior with these three different solvents.[39-42] Mikami et al. found an orientational disorder in ethanol solvate crystals. The variation of orientational ground state population with temperature variation is correlated with spin transition. Deuteration of the solvent of crystalization

affects the spin transition.[43]   Goodwin and co-workers studied

the effect of water of hydration on the spin state in

$[Fe(Pyben)_3](BF_4)_2 nH_2O$ and found that the more the lattice water

present the more facilitated will be the hydrogen bond formation

which in turn will be the cause for increasing acidity of the -NH

group and along with it the increased strengthening of the metal

ligand σ bond, as a result ligand field strength increases there

by favouring low spin state.   In the systems $Fe_x M_{1-X}$ (Phen)$_2$

$(NCS)_2$ (M = MN, Co, Ni, Zn), metal dilution favoured the HS state

when Fe is the host lattice and M is the dopent.   But when M is

the host and Fe is the dopent then LS state is favoured.   The

behaviour of metal dilution in the Fe system proved the

cooperative domain formation as suggested by Sorai and Seki.[8]

The formation of a red compound of $Fe(Phen)_2(NCS)_2$ with LS

component at room temperature and HS at LT was prepared and a

detailed study of this inverse spin crossover system was carried

out by first author.

Various techniques have been used to study the spin

transition phenomenon, like, i.r, Optical spectroscopy, magnetic

susceptibility, Mössbauer and magnetic resonance studies.   Since

the period of nuclear oscillations are of the order of 10^{-13}S the

separate existence of the two spin states should be revealed in

the i.r spectra.   In the i.r spectra of $Fe(Phen)_2(NCS)_2$ they

found a shift of ~ 40 cm^{-1} in CN band frequency from RT to LNT.

The frequency shift is indication to the π back bonding effect of

Fe-N(Phen) which in turn results in the delocalization of the

electron from C-N bond of NCS$^-$ to make up the t_2 electron

deficiency at the Fe(II).

The spin transition behavior is widely studied by magnetic susceptibility measurements. The applicability of this method lies in the fact that the large difference exist between the magnetic moments of the high spin low spin states. LS is diamagnetic and HS is paramagnetic. By the application of Vanvleck equation to Boltzman distribution over sixteen levels leads to an expression.[48]

$$\mu_{eff} = \{nK + (\chi_{xx}^{h} + \chi_{yy}^{h} + \chi_{zz}^{h}) / \mu_{B}^{2}A\}^{1/2}$$

where χ is the susceptibility tensor of the high spin, μ_B is the Bohr magneton, A is the Avagadro number. But they could not explain the discontinuous temperature dependent magnetism in Fe(Phen)$_2$(NCS)$_2$ system involving phase transition.

The X-ray technique was also used to find out existence of two spin states in spin crossover systems. In a recent paper by Gallois et.al[46] reported that there is a difference between the structure of the two spin states but have yet to develop relation between the lattice changes and structural differences.

Mössbauer spectroscopy is an effective tool in the study of spin crossover phenomenon of Fe systems. The preffered application of the Mössbauer effect rests on the fact that in the spectra, high spin and low spin state ions are resolved separately due to the , difference in isomer shifts and

quadrupole splittings, and in addition this resolution is subject to the long relaxation time ($> 10^{-7}$ sec) between the high spin and low spin state. Konig and Madeja found[47,48] that Fe(Phen)$_2$(NCS)$_2$ and Fe(Phen)$_2$(NCSe)$_2$ at 293 K showed $\Delta E_Q \sim 2.6$ m ms^{-1} and $\delta_{iso} \sim 1.0$ m ms^{-1}. At 77 K $\Delta E_Q \sim 0.2 - 0.3$ and $\delta_{iso} \sim$ 0.35 m ms^{-1}. This is the typical value for HS and LS respectively.

Very few e.s.r. studies of spin crossover have been carried out so far. Rao et al[49] has followed the spin transition behaviour in the Fe(Phen)$_2$(NCS)$_2$ and Fe(Pic)$_3$Cl$_2$ EtOH with the help of e.s.r. by putting Mn as impurity in Fe lattice. Low spin Fe(II) is diamagnetic and high spin Fe(II) is usually e.s.r. silent as it has very high Zero field splitting. The short relaxation time of $^5T_2$ state of Fe(II) remove the dipolar broadening caused by the paramagnetic neighbors in the lattice. So it should be possible to follow the behavior of the paramagnetic impurity in the lattice during spin transition. In these studies they found that in the case of Fe(PiC)$_3$Cl$_2$EtoH and 1% Mn doped sample showed the presence of high spin state at RT and e.s.r. spectrum show a well resolvd hyperfine splittings. The change in e.s.r. line width at low temperature revaled that spin transition occur in the Fe(II) simlar to the bulk lattice and there is no change in E and D parameters. They found continuous temperature dependent spin transition. In the case of low spin state e.s.r. spectrum is not resolved. Oliver Kahn and coworkers[50] investigated spin crossover phenomenon in Fe(NCS)$_2$(btr)$_2$H$_2$O, using Cu as e.s.r. probe in the Fe(II)

lattice. He found that the system is diamagnetic (low spin) below T_c and paramagnetic (high spin) above T_c. In the paramagnetic phase e.s.r. signal is poorly resolved, a very weak signal at g = 4.7, 3.4 is observed. This may be due to the exhange broadening. At temperature below T_c (144.5 K = $T_c\wedge$, 23.5 K = $T_c\vee$) a well resolved spectrum due to the magnetically isolated Cu(II)is observed. McGarvay and coworkers[51] studied spin transition in $Fe(C_6H_8N_2S_2)(NCS)_2$[51] single crystal and in $Fe(ptz)_6(BF_4)_2$[52]using MN,Cu as e.s.r. probes. We were indepedently pursuing the e.s.r. work on Cu doped Fe(II) spin crossover systems when the above two publications appeared. Our results on the $Fe(Phen)_2(NCS)_2$ system is presented in this chapter.

4.2 ·' EXPERIMENTAL:

4.2.1. Chemicals:

The starting material for the preparation of ligands are either bought from Aldrich or Fluka. Other solvents and common chemicals are of reagent grade or better quality. All the organic solvents are purified by standard procedures described in Vogel[53]. Acetonitrile is stored over Type 4A molecular sieves.

4.2.2. Synthesis of red form of $Fe(Phen)_2(NCS)_2$:

A number of synthetic procedures for preparation $Fe(Phen)_2(NCS)_2$ have been reported in the literature.[45,54,55] As pointed out by Gutlich *et al.* the complexes and the temperature

115

dependence of the spin-crossover phenomenon of these complexes appear to depend not only on the quality of the solid obtained but also on the subsequent treatment of the sample prepared.

In the present study aqueous procedure of Schilt and Fritsch[54] was adopted with slight modification. 0.003 mole (1.18 gm) $FeSO_4(NH_4)_2SO_4$ $6H_2O$ (Aldrich 99.99% pure) is dissolved in 50 ml of distilled water. 0.006 mol (1.190 gm) of Phen. is dissolved in 100 ml of distilled water by acidifying it with 1 ml of 6M H_2SO_4. To the clear ligand solution Fe(II) solution is added drop-wise with constant stirring. To the red coloured solution obtained 10 ml of saturated potassium thiocynate solution is added drop-wise. The red precipitate obtained is immediately filtered with out any aging and this is dried in vacuum, stored in desiccator over silica gel.

4.2.3. Preparation of the Cu^{2+} doped red-form of $Fe(Phen)_2(NCS)_2$:

0.00012 moles of (30 mg) $CuSO_4$ $5H_2O$ and 0.003 moles (1.18 gm) of $FeSO_4(NH_4)_2SO_4$ $6H_2O$ are dissolved in 50 ml of distilled water. 0.006 mol (1.199 gm) of Phen. is dissolved in 100 ml of distilled water acidified with 1 ml of 6M sulphuric acid (concentrated). The Cu^{2+}/Fe^{2+} mixed solution to the ligand. The red coloured solution formed is precipitated by adding 10 ml of saturated potassium thiocynate. The residue obtained is filtered off without any aging. The solid obtained is dried in vacuum and stored over silica gel in desiccator.

4.2.4. Preparation Mn^{2+} doped red form of $Fe(Phen)_2(NCS)_2$

0.003 moles of $FeSO_4(NH_4)_2SO_4.6H_2O$ (1.18 gm) and 0.00012 mol of $MnSO_4H_2O$ (20.3 mg) are dissolved in 50 ml of distilled water. 0.006 mol (1.198 gm) Phen. is dissolved 100 ml of distilled water by acidifying it with 1 ml of 6M sulpuric acid. The mixed Mn^{2+}/Fe^{2+} solution is added to ligand solution drop-wise with constant stirring followed by the addition of 10 ml of saturated potassium thiocynate. The red precipitate obtained was filtered off immediately with out aging. This was later dried in vacuum and stored over silica gel in a desiccator.

4.2.5. Preparation of single crystals from pure red-form and Cu^{2+} doped red-form $Fe(Phen)_2(NCS)_2$:

Pure red-form powder and copper and manganese doped red-form powders are dissolved in acetonitrile solution. To the filtrate obtained distilled water is added in 6:1 ratio (6 parts acetonitrile 1 part water). This solution is allowed for slow evaporation in the acetonitrile atmosphere. After 7-10 days reddish brown crystals of hexagonal plates appear in the solution. The manganese doped red-form crystal when checked for the manganese, did not show its presence in e.s.r. Hence it looks during the process of crystal growth manganese is not getting doped into this form,whereas copper could get doped.

4.2.6. Preparation of violet forms of the $Fe(Phen)_2(NCS)_2$ complexes from red-forms:

The red form of $Fe(Phen)_2(NCS)_2$ prepared is dissolved in acetonitrile and stirred for half an hour. Then the solution filtered off and the residue is kept for slow drying. The residue looks deep violet in colour and gives a violet streak on the tile. This compound is stored over silica gel in desiccator.

The i.r spectra of all these samples are recorded (table 4.1) and compared with earlier values reported by Maddock.[45]

4.2.7. The C,H,N Analysis:

The C,H,N analysis of pure red-form of $Fe(Phen)_2(NCS)_2$ is fitted to the formula $[Fe(Phen)_3]_2[Fe(NCS)_4](NCS)_2 3H_2O$. The details are given below:

Theoretical   : C = 56.73%, H = 3.30%, N = 15.27%, Fe = 10.15%

Experimental   : C = 56.9%,   H = 2.94%, N = 15.16%, Fe = 10.28%

Reported by Maddock[45] and co-workers   : C = 56.75%, H = 3.30%, N = 15.5%, Fe = 10.15%

C,H,N analysis data of the red form crystals is fitted to the formula $[Fe(Phen)_3(NCS)_2.2H_2O$. The values are given below:

Theoretical   : C = 60.97%, H = 3.8%, N = 14.96%, Fe = 7.46%

Experimental   : C = 60.62%, H = 3.23%, N = 14.97%, Fe = 7.36%

4.2.8. Physical Measurements:

The i.r. spectra are recorded on Perkin Elmer 297 or 1310 spectrometer as KBr pellets. Mössbauer spectra are recorded employing a constant acceleration Elscint drive in conjunction with a multi channel analyser (promeda) and sodiumnitropruside is used as standard. Low temperature measurements are made by mounting the sample on the cold finger attached to the liquid nitrogen dewar. The temperature is measured using a thermo-couple.

A JEOL FE-3X e.s.r. spectrometer is used for recording X-band e.s.r. spectra in the solid state and DPPH is used for calibration. Low temperature measurements are made using a variable temperature accessory employing, controlled boil off of nitrogen from a dewar. C, H, N analysis is done on Perkin-Elmer 240 C analyser.

4.3.0. RESULTS AND DISCUSSION:

4.3.1. C,H,N analysis data of the red form powder and crystals of $Fe(Phen)_2(NCS)_2$:

The C,H,N data of the red form powder $Fe(Phen)_2(NCS)_2$ complex obtained are given in the experimental section (4.2.7). The data fits well to the formula $[Fe(Phen)_3]_2 [Fe(NCS)_4] (NCS)_2$ $3H_2O$. These values are similar to those reported by Maddock and coworkers[45] to the same formula of the compound. But the C,H,N

data for the red crystals obtained from the red powder on crystallisation from the acetonitrile and water medium is found to be different. The C,H,N data of the crystals agrees to the formula [Fe(Phen)$_3$(NCS)$_2$.2H$_2$O. Fe(Phen)$_3$(NCS)$_2$.2H$_2$O has been prepared first in 1966 from a totally different route.[58] To our knowledge ours is the first preparation of the complex in crystalline form and no crystal structure is available at present.

4.3.2. I.r. spectral data of various forms of Fe(Phen)$_2$(NCS)$_2$:

I.r. spectra are recorded at room temperature for different forms of Fe(Phen)$_2$(NCS)$_2$ doped and undoped complexes. The spectra are analysed mainly in two regions (1) 2150-1950 cm^{-1} and (2) 900-600 cm^{-1} region. Red and violet forms of the doped and undoped complexes of Fe(Phen)$_2$(NCS)$_2$ gave very intense some what broad band in the region 2000-2040 cm^{-1}. It shows the presence of two to three unresolved bands. All these bands are comparable to the earlier reports.[45] The i.r spectra also show bands similar to the previous reports[45], in region of the spectra which gives the characteristic features of the compound (900-600 cm^{-1}) (Fig.4.1). The red form shows no absorption at 640 cm^{-1} and a very weak shoulder at 865 cm^{-1}. But the cis-compound show medium-strong absorption at these frequencies. These two bands are sufficiently isolated and can be used to detect mixtures of the two compounds. The absence of band at 637 cm^{-1} is adopted almost as a criterion of purity of the red compound. At 840 cm^{-1} a very strong absorption is showed by both the forms. A sharp
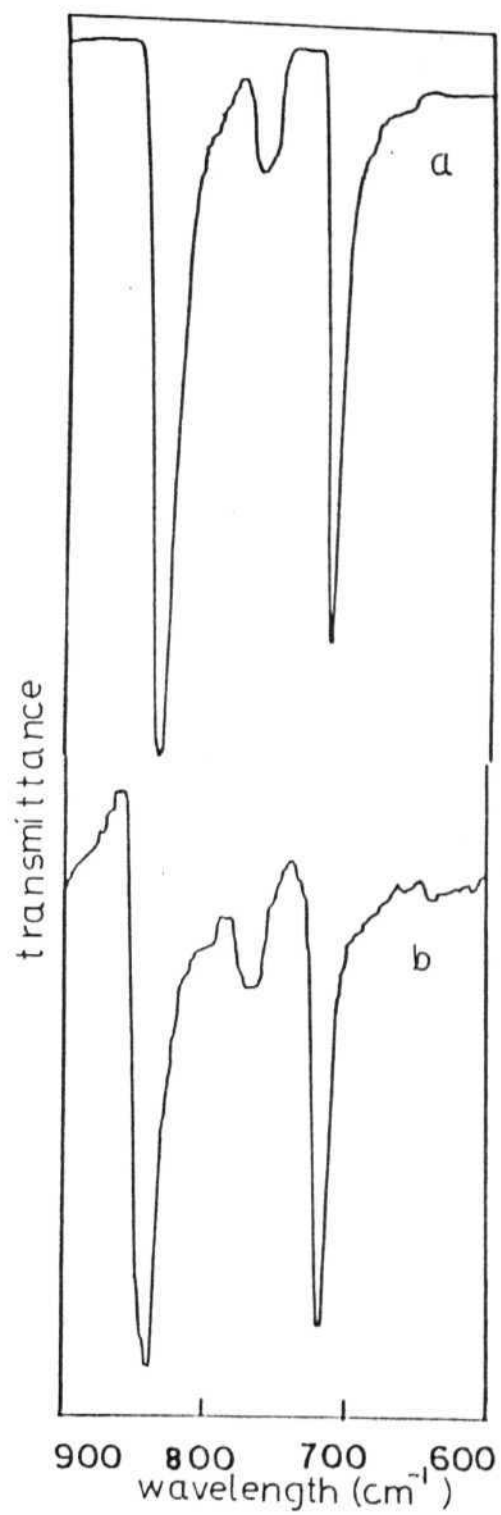
Fig. 4.1C I.r. spectra of $Fe(\text{Phen})_3(NCS)_2 \cdot 2H_2O$ crystal
(a) pure form and (b) Cu doped.
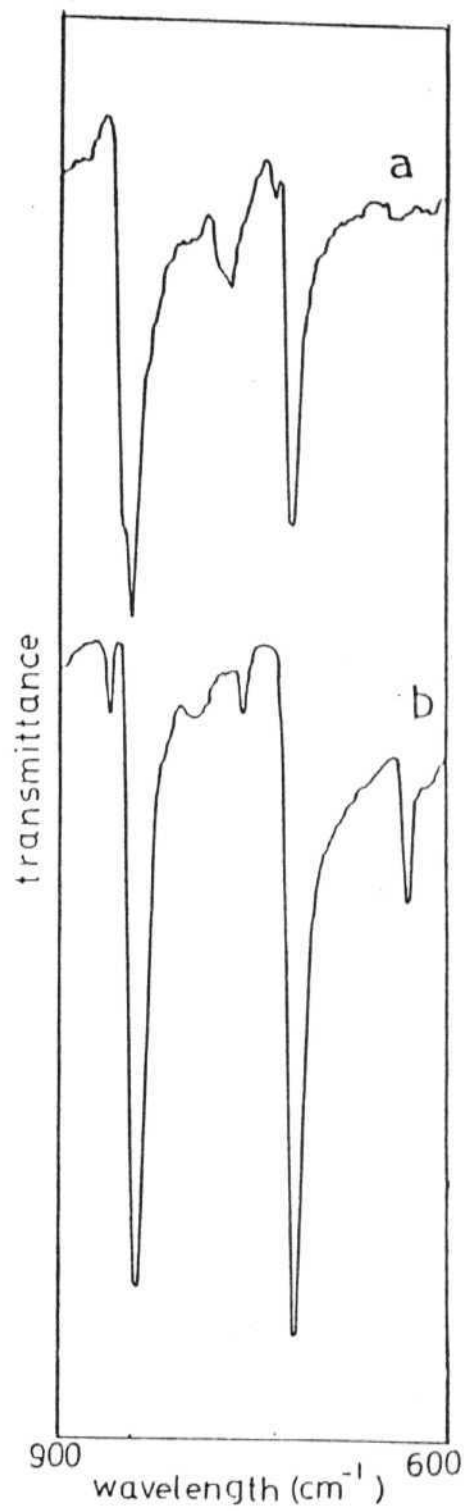
Fig. **4.1B** I.r. spectra of pure Fe(Phen)$_2$(NCS)$_2$ (a) red form and
(b) violet form.
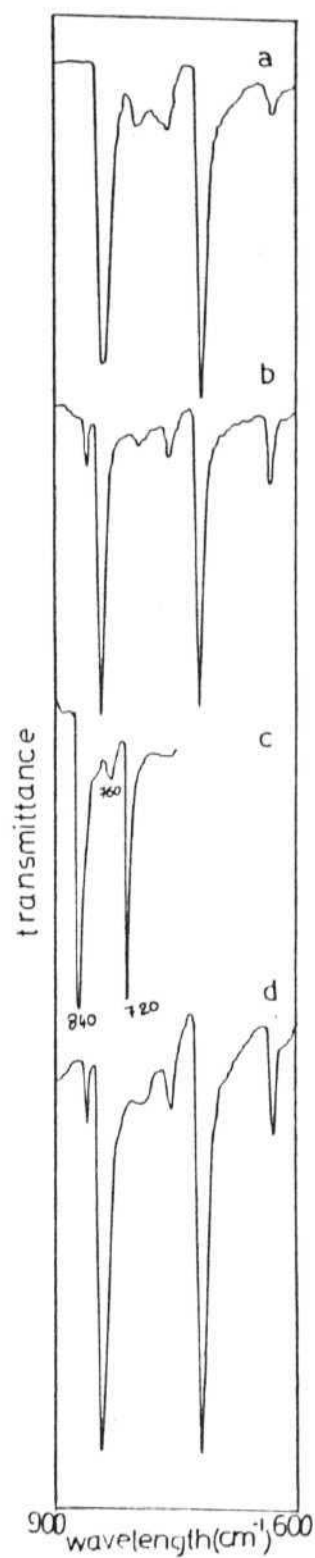
Fig.4.1A I.r. spectra of different powder forms of Fe(Phen)$_2$(NCS)$_2$ (a) Mn doped red form (b) Mn doped violet form (c) Cu doped red form and (d) Cu doped violet form.

Table - 4.1 : I.r. Spectral data in cm^{-1} for different forms of doped and undoped $Fe(Phen)_2(NCS)_2$ complexes

Pure Red-form power	Pure Red-form crystal	Cu doped Red-form power	Mn doped Red-form powder	Cu doped Red-form crystal	Pure Violet form powder	Cu doped Violet form powder	Mn doped Violet form powder
3000-3400(w,br)	3300-3400(br,s)	3300-3400(w,br)	3300-3400(w,br)	3300-3400(br,w)	2050(br,s)	2050(s,br)	2050(s,sh)
2040 (s.sp)	2040(s,m,br)	2050(w,br)	2040(br,s)	2040(br,s)	1570(v,w)	1510(v,w))	2060(s,m,br)
1590 (v,w)	1500(w)	1620(v,w))	1550(v,v,w)	1500(v,v,w)	1500(v,m,sp)	1500(m,sp)	1620(v,v,w)
1565 (v,w)	1415(s,sp)	1590(v,w)	1500(w)	1420(s,sp)	1480(m)	1480(m,sp)	1560(v,w)
1500 (v,w)	1400(sh)	1500(v,w)	1480(v,w)	1400(sh)	1440(s,m,br)	1420(s,sp)	1500(m,sp)
1420 (s,sp)	1390(v,w)	1430(s,sh)	1420(s,sp)	1330(v,w)	1330(v,w)	1340(v.w)	1480(m,sp)
1400 (s,m)	1330(v,w)	1420(s,sp)	1410(sh)	1220(v,w)	1220(v,w)	1220(v,w)	1420(sp,s)
1220 (v,v,w)	1200(v)	1400(s,m)	1330(v,v,w)	1200(sh)	1200(v,w)	1220(v,w)	1420(sp,s)
1200 (v,w)	1180(v,v,w)	1220(v,w)	1220(v,w)	1130(v,w)	1200(sh)	1200(sh)	1410(sh)
1130 (v,w,br)	1130(w)	1200(v,v,w)	1140(w)	1080(v,w)	1130(v,w)	1140(v,w)	1330(v,v,w)
1090 (v,w,)	1080(v,w)	1140(v,v,w)	1080(v,w)	1050(v,w)	1100(m)	1100(v,w)	1220(v,v,w)
980 (v,v,w)	835(v,s,sp)	1090(v,w)	840(s,sp)	840(s,sp)	840(s,s,p)	860(m,sp)	1130(v,v,w)
850 (sh)	765(m,s)	1050(v,w)	760(m)	765(m,sp)	805(w,br)	840(s,sp)	1100(v,v,w)
860 (s,sp)	720(s,sp)	985(v,w)	720(s,sp)	720(s,sp)	760(v,w)	760(m,sp)	860(w,v,p)
770-780(br,m)		850(sh)			720(s,s,p)	720(s,sp)	840(sr,sp)
720(s,sp)		840(s,sp)			630(m,sp)	630(m,sp)	800(v,w)
		760(w,br)					760(v,w)
		720(s,sp)					720(v,w)
							630(sp,m)

a Sp = sharp S = strong Sh = should

W = weak Br = broad M = moderate V = very

and medium strong band at 807 cm^{-1} in low spin cis-Fe(Phen)$_2$(NCS)$_2$ at 88 K observed is due to ν(C-S) stretching. In all the compounds this band is seen as very weak broad band in that region. The copper and manganese doped red and violet forms of the Fe(Phen)$_2$(NCS)$_2$ complex has showed no differences with pure complexes in the i.r. spectra at room temperature. The i.r. spectra of the crystals obtained from red form powder samples upon crystallisation are matching with the red form powder spectra. The data also matches with the most of the strong bands in [Fe(Phen)$_3$](NCS)$_2$.2H$_2$O spectra reported by Duncan et al[58]. Thus the i.r. data reveals that the presence of dopent in the lattice does not affect the i.r. spectra. In spite of the differences in C,H,N data the crystals and powder samples give similar i.r. spectra.

4.3.3. The Mössbauer spectral data of the different forms of the pure and doped complexes of Fe(Phen)$_2$(NCS)$_2$:

Mössbauer spectra of different forms (R.F. and V.F.) of powder Fe(Phen)$_2$(NCS)$_2$ (Fig.4.2, 4.4) and their copper doped samples (Fig.4.2) are recorded at 298 K and 77 K. The pure and copper doped crystal forms of Fe(Phen)$_2$(NCS)$_2$ are also subjected to Mössbauer studies at 298 and 77 K (Fig.4.3). All these spectra are showed in Figures 4.2, 4.3 and 4.4. The δ_{iso} values with respect to soft iron and ΔEq values for all these samples at room temperature are tabulated in table 4.2. Accurate parameters could not be obtained from the low temperature spectra due to poor quality of the spectrum. The fittings are therefore
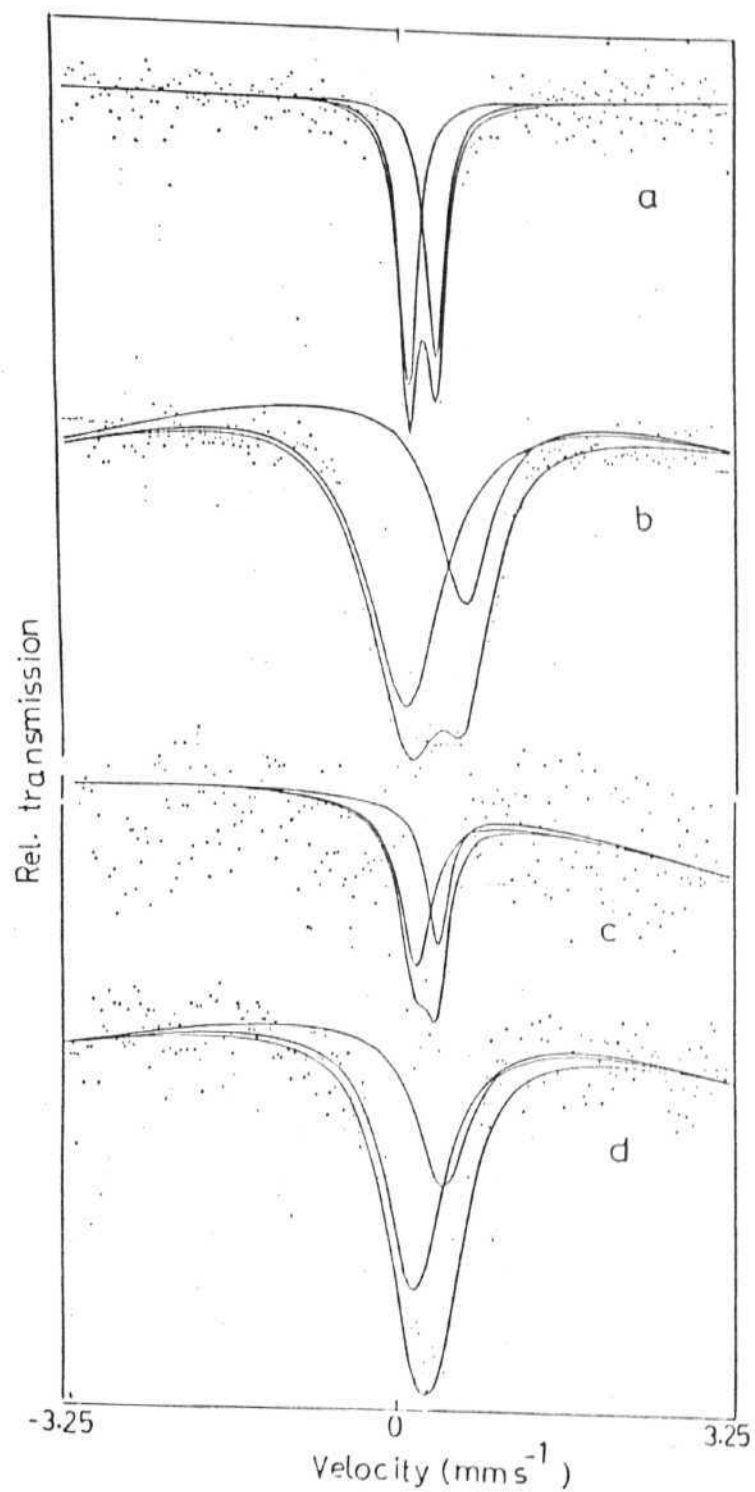
Fig. 4.2 Mössbauer spectra of powder Fe(Phen)$_2$(NCS)$_2$ pure red form at (a) 298 K (b) 77 K and copper doped red form at (c) 298 K (d) 77 K.
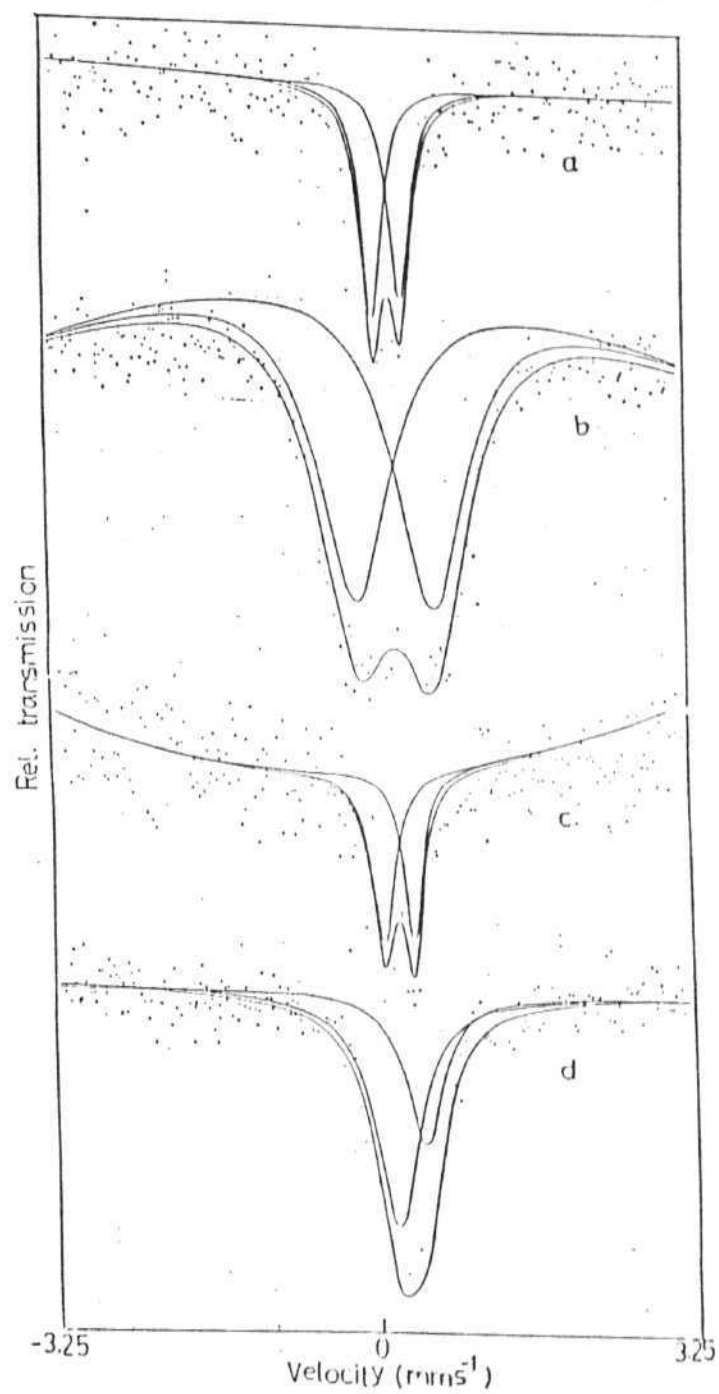
Fig. 4.3   Mössbauer spectra of crystalline Fe(Phen)$_3$(NCS)$_2$·2H$_2$O.
pure red form at (a) 298 K (b) 77 K and coper doped red
form at (c) 298 K (d) 77 K.

127
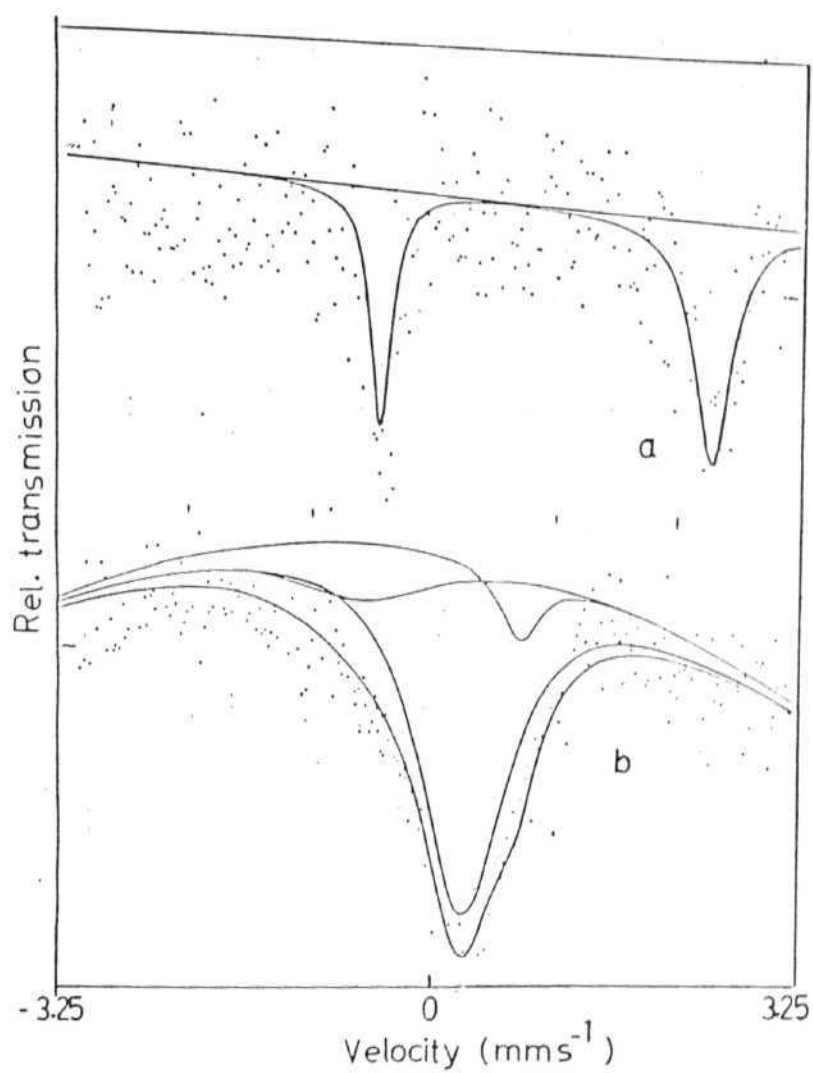
Fig. 4.4 Mössbauer spectra of cis Fe(Phen)$_2$(NCS)$_2$ at
a) 298 K and (b) 77 K.

128

Table 4.2 : Mössbauer Spectral Data

Complex	Temp. K	δ mms^{-1}	δEq mms^{-1}
Fe(Phen)$_2$(NCS)$_2$ pure U.F.	298	1.08	2.89
Fe(Phen)$_2$(NCS)$_2$ pure R.F.	298	0.336	0.247
Fe(Phen)$_2$(NCS)$_2$Cu doped R.F.	298	0.373	0.20
Fe(Phen)$_2$(NCS)$_2$ pure cryst.	298	0.336	0.30
Fe(Phen)$_2$(NCS)$_2$Cu doped cryst.	298	0.307	0.29

tentative and the parameters are given on the spectra. The red
form powder sample of Fe(Phen)$_2$(NCS)$_2$ shows an asymmetric doublet
at 298 K corresponding to low spin Fe(II) (Fig.4.2). The same
sample at 77 K shows the broadening of the signal (Fig.4.2).
These spectra show that at 77 K the asymmetric doublet lines are
moving apart, showing the broadening. This may be due to the
spin transition in the sample with change in temperature. The
δ_{iso} and ΔEq values of the red sample at room temperature are
comparable with the values reported by Maddock and co-workers for
the L.S. system.[45] However, we did not see any signals
corresponding to the H.S. component reported by them. Since they
did not present any spectra in their publication, actual spectra
comparison is not possible. The violet form powder
Fe(Phen)$_2$(NCS)$_2$ samples show low spin Fe(II) spectrum at 298 K
and a broad unresolved signal with a shoulder at 77 K. The δ_{iso}
and ΔEq values of this compound at room temperature are
comparable to cis-Fe(Phen)$_2$(NCS)$_2$ (δ_{iso} at 300 K 0.955, 60 K =
0.45, ΔEq at 210 K = 2.9, 60 K = 0.345)[45] sample at
room-temperature.

The pure and copper doped Fe(Phen)$_2$(NCS)$_2$ red crystals show
Mössbauer spectra similar to red form powder complex at both the
temperature. But the Mössbauer data reported by Duncan et al[58]
for [Fe(Phen)$_3$](NCS)$_2$.2H$_2$O at room temperature is found to be in
agreement (δ_{iso} = 0.34 m/sec, ΔEq = 0.12±0.1) with our values.
These Mössbauer results indicate that the presence of dopent in
the host lattice may not affect the spin transition behaviour in
the bulk of the sample. It also appears that the red crystals

and red form powder are of the same spin state at room temperature.

4.3.3. Influence of spin-crossover on the e.s.r. of paramagnetic impurity:

Spin-crossover which is a cooperative phenomenon can influence the e.s.r. of substitutional impurity sites. It associated with structural phase transition, it can bring about changes in zerofield splitting. Spin crossover may also affect the line width by modulation of dipolar broadening.

Important quantities, relevant for $^5T_2$ ---- $^1A_1$ crossover are (i) life times of the spin states $^5T_2$ and $^1A_1$, (ii) quintet-singlet energy separation (iii) life time of the individual Zeeman levels of the quintet (S = 2) state and (iv) zerofield splitting of the quintet state.

The lifetime of low-spin state (S=0) or high spin state (S=2) is > 10^{-7}S, as inferred from the observation of separate doublets for both states in the Mossbauer spectra and is greater than the e.s.r. time scale ($\sim 10^{-9}$S). Therefore, paramagnetic impurity ions in the neighbourhood of HS and LS host molecules will have different e.s.r. characterstic. The host compound when present in the low-spin state, all the five and hyperfine splitting will be revealed by the dopant ion (present in low concentration) due to magnetic dilution. In the high-spin lattice, two types of host-guest interactions are possible (i)

magnetic dipolar coupling and (ii) spin exchange interaction. Dipolar interaction leads to broadening of resonant lines. The magnitude of dipolar or magnetic fields depend on the magnetic moment of the host molecules, the relaxation times of its individual Ms states and host-guest separation. The presence of magnetic exchange interaction results in a variety of spectra depending on the value of exchange integral J. When J is comparable in magnitude to Zeeman splitting, a narrowing of e.s.r. signal is observed due to an averaging of g-anisotropy (J > 0.3 cm^{-1} for X-band) and an averaging of hyperfine splitting (J > 0.008 cm^{-1} for Mn^{2+} and 0.01 cm^{-1} for Cu^{2+}).

One of the models proposed for the mechanism of spin-crossover involves the formation of high-spin and low-spin (non interacting) domains. This should give an e.s.r. consisting of superposition of the two spectra due to HS and LS lattices. Whereas a statistical distribution (*i.e.* a binary mixture) of HS and LS sites will lead to an average dipolar broadening of e.s.r. spectrum.

4.3.5. E.s.r. Study of the Manganese(II) impurity in Fe(Phen)$_2$ (NCS)$_2$ Complex:

The structural changes in the system are detected by the changes in the line-width of the resonances of the paramagnetic ion. E.s.r. spectra of the paramagnetic ion should be detectable in the paramagnetic phase as well as in diamagnetic phase, due to the short electronic relaxation times for $^5T_{2g}$ state of Fe(II),

which will remove most of the dipolar broadening caused by paramagnetic neighbours in the lattice.

The e.s.r. spectra recorded for the Mn^{2+} doped complexes shows a typical powder spectrum for an S = 5/2, I = 5/2 system with zerofield interaction less than Zeeman interaction (Figs.4.5 and 4.6). The spectra are fitted using the spin hamiltonian

$$H = g\beta H.S + [D(S_z^2 + 1/3S(S+1) + E(S_x^2 - S_y^2)$$

Approximating g-values to be isotropic as it is very close to free spin value for ions with an orbital ground state (^6S). The D & E values are calculated using the second order perturbation equations reported by Taylor.[56] The D values thus calculated[52] for the violet form at 298 K is 0.065 cm^{-1} and is almost same at 133 K, while E values vary slightly (0.012 cm^{-1} at 298 K and 0.0135 cm^{-1} at 133 K). These results are similar to that observed by Rao *et al.*[49] However, they observed a decrease of D & E values (0.071 to 0.065 cm^{-1} for D and 0.018 to 0.012 cm^{-1} for E), with increasing temperature. The D values calculated in the same method[57] are similar for red form (D = 0.041 and E = 0.005 cm^{-1}). Even in this case there is no temperature dependence in these D and E values. However in the variable temperature e.s.r. measurements carried out on these samples (both R.F. and V.F.) shows a continuous change in the e.s.r. lines *i.e.* the low-temperature spectrum continuously transforms in to room temperature spectrum with gradual increase in temperature (Figs. 4.5 & 4.6). These results shows that spin
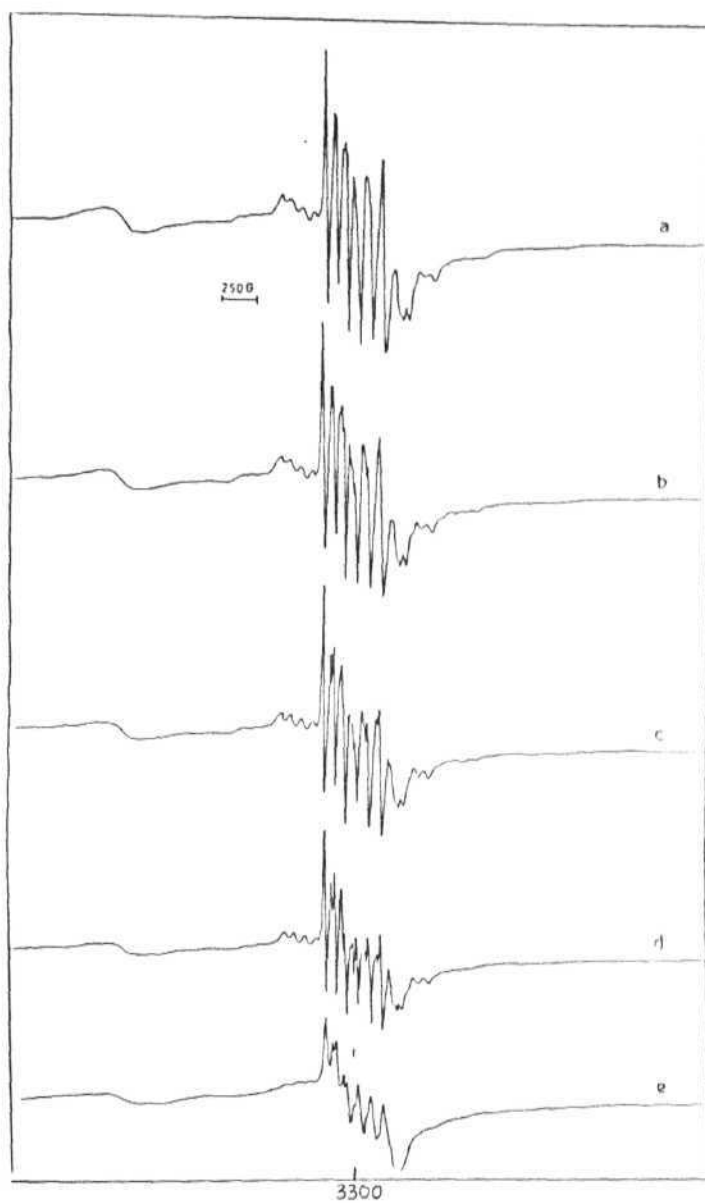
Fig. 4.5   E.s.r. spectra of Mn doped powder Fe(Phen)$_2$(NCS)$_2$ red form at (a) 125 K (b) 153 K (c) 193 K (d) 243 K and (e) 293 K.

134
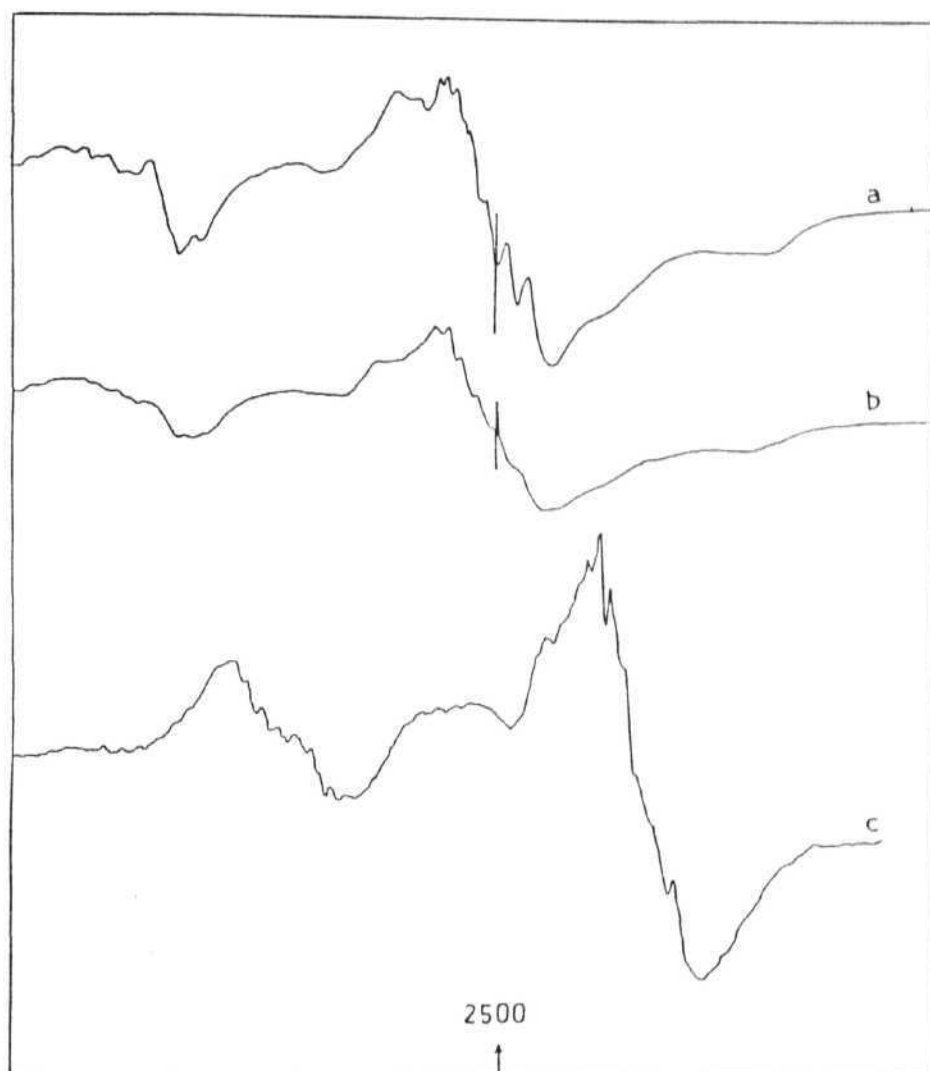
Fig.4.6   E.s.r. spectra of Mn doped cis Fe(Phen)$_2$(NCS)$_2$ at
          (a) 125 K (b) 213 K and (c) 298 K.

transitions observed is not an abrupt transition in these compounds. In both the red and violet forms the lines are better resolved and more intense at low temperatures. This indicates that there is a reduction in the dipolar broadening at low temperature.

These above discussed results differs from Rao $et.al$ observations in some aspects, like D resolved spectra from room temperature to low temperature (2) sharp lines at low temperature and no appreciable change in zerofield splitting except a slight increase in E values. So it can be said that in this case, if at all domains are present, they are to small (contains only few molecules), so that the spectra corresponds to a statistical distribution of dipolar broadening.

4.3.6. E.s.r. studies of Cu^{2+} impurity in $Fe(Phen)_2(NCS)_2$:

Cu^{2+} when present in the paramagnetic Fe(II) lattice, will have an exchange of spin between Cu^{2+} and neighbouring ions, giving rise to broadening of lines. g-anisotropy is seen to some extant only, when the exchange integral J is moderate. The spin hamiltonian which can be used for the isolated Cu^{2+} ion is

$$H = \beta H.g.s + h.s.A.I.$$

There will be no exchange of spin when Cu^{2+} is in a diamagnetic lattice and therefore the hyperfine ·splittings should be resolved. Cu^{2+} in a magnetically concentrated system with Cu^{2+}

neighbours will have exchange and completely an exchange averaged spectrum is usually seen. The e.s.r. spectra of copper doped red form powder and violet form powder recorded in a range of 298-123 K are shown in the Figs. 4.7 & 4.8 and the g values are given in the Table 4.3. The spectra are consistent with the values of exchange integral in the range

$$0.01 < J < 0.3 \text{ cm}^{-1}$$

As per the report of Maddock and co-workers they observed the presence of high spices Fe(II) state in the red form of the complex at low temperature.[45] The violet form exhibits opposite spin $i.e.$ low spin at low temperature when Cu^{2+} is doped in such a state the low-spin form do not give a resolved hyperfine. The hyperfine is not resolved in the red form, whereas to some extent in violet form of these compounds. The absence of hyperfine in the red form can be explained as due to high degree of exchange interaction between Cu^{2+} and high-spin Fe(II) lattice. The absence of well resolved hyperfine in the copper doped violet form can be attributed to the component of paramagnetic lattice existing throughout the temperature range. The Mössbauer spectra of the copper doped red compound (Figs.4.2 C & D) recorded at room temperature shows that the compound do not undergo total conversion and part of the residual paramgnetism is present throughout the temperature range.

4.3.7 E.s.r. studies of Cu^{2+} impurity in the crystals:

The single crystals obtained by the crystallisation of copper doped red-form powder from acetonitrile solution are checked for Cu^{2+} signals in e.s.r. Even though the crystals are big enough the signal obtained was very feeble. Hence a polycristalline sample obtained by powdering the sample is used to study e.s.r. Spectrum of this sample at 114 K gave a well resolved 4 line copper spectrum (Fig.4.9a). The g and A values are given in the Table 4.3. The variable temperature measurements showed the disappearance of hyperfine with increase in temperature. The total spectrum becomes broad and the intensity also decreases at room temperature (Fig.4.9e). These results clearly show that the Cu^{2+} exists in low spin Fe(II) environment at low temperature, which prevents dipolar exchange interactions thereby resulting in a resolved hyperfine, with increase of temperature the host lattice is gradually converting to high-spin. This results in the disappearance of hyperfine due to exchange and dipolar interactions of Cu^{2+} ions with paramagnetic lattice. Here also a continuous spin state transition is observed, which showed up in the gradual changes in the e.s.r. spectrum with change in the temperature from low temperature to room temperature. These results are inconsistent with the i.r. spectral data, which is comparable with the other red-form powder spectrum. However, the Mössbauer spectra of copper doped crystals (Fig. 4.9 C & D) showed the presence of residual paramagnetism. The C,H,N analysis as already mentioned
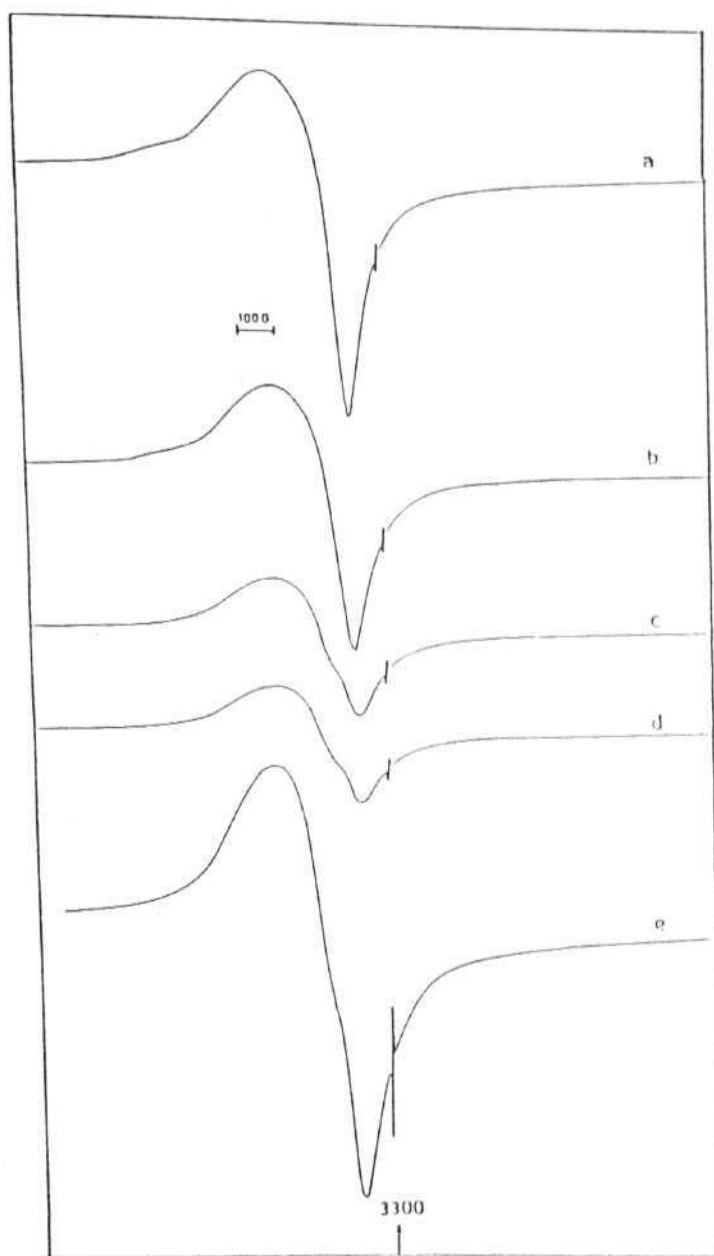
Fig.4.7 E.s.r. spectra of Cu doped powder Fe(phen)$_2$(NCS)$_2$ red form at (a) 123 K (b) 153 K (c) 253 K (d) 273 K and (e) 298 K.

139
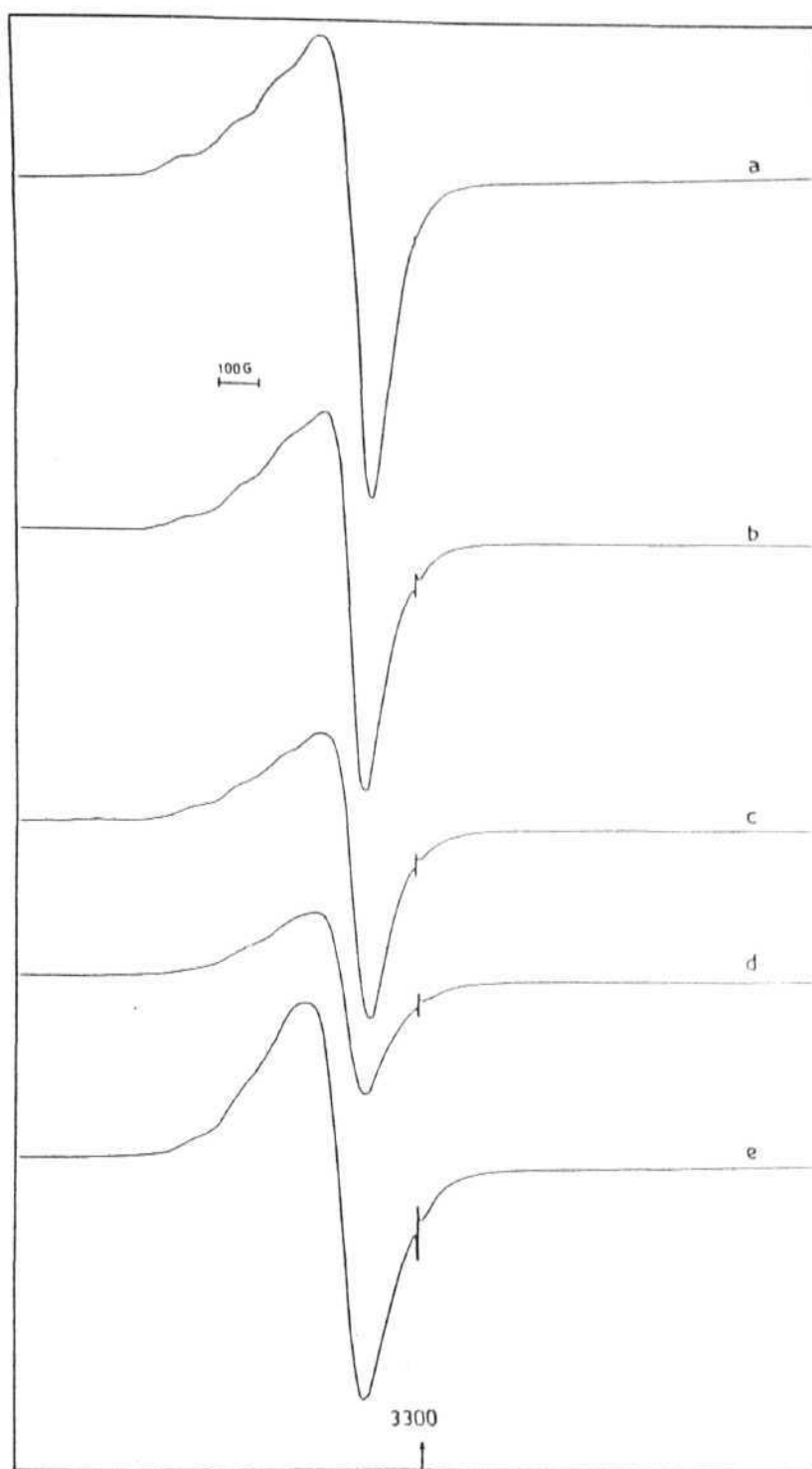
Fig. 4.8   E.s.r.   spectra   of   Cu   doped   powder $Fe(phen)_2(NCS)_2$
violet form at (a) 117 K (b) 153 K (c) 193 K (d) 293 K
and (e) 298 K.
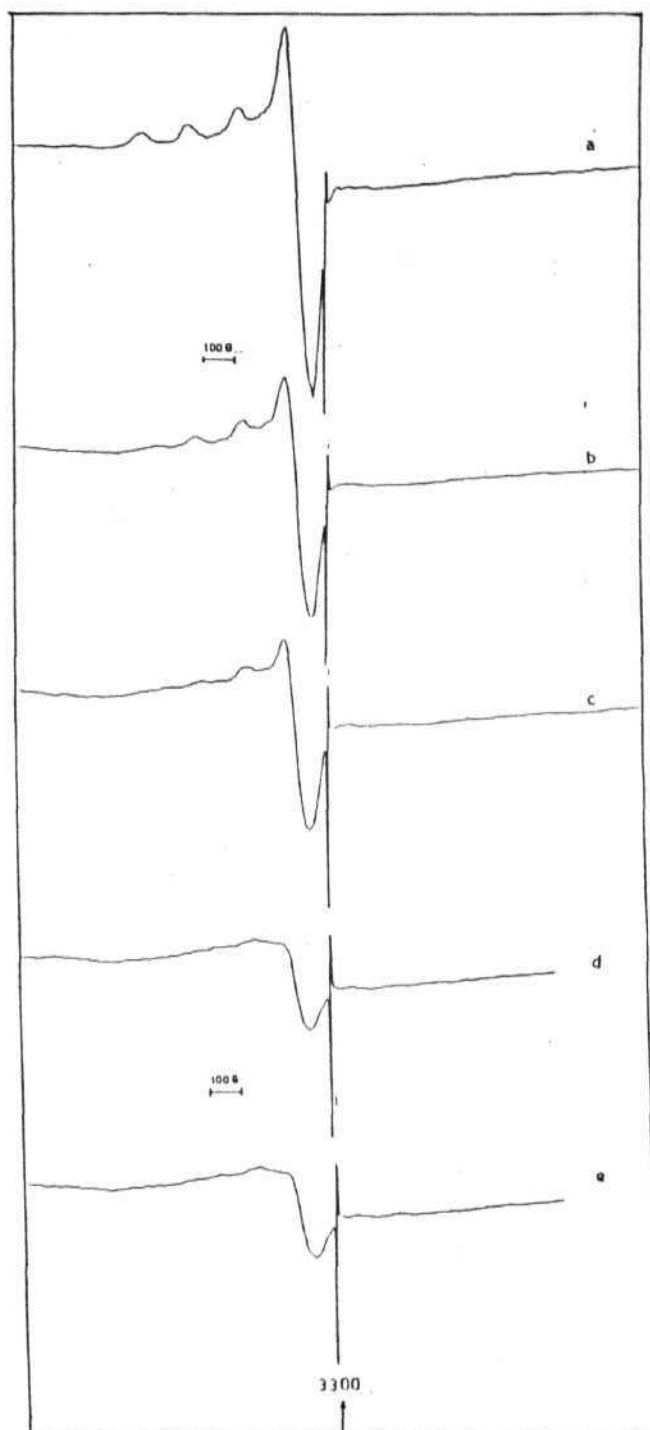
Fig. 4.9   E.s.r. spectra of Cu doped powder Fe(phen)$_3$(NCS)$_2$·2H$_2$O
at (a) 114 K (b) 153 K (c) 193 K (d) 273 K and (e)
293 K.

Table 4.3 : E.s.r. parameters of different forms of copper doped Fe(Phen)$_2$(NCS)$_2$

Complex	Temp K	$g_{\parallel}$	$g_{\perp}$	$A_{\parallel}$	$A_{\perp}$
			g	$10^{-4} \times A\ cm^{-1}$	
Copper doped	293		2.076		
Crystal	114	2.246	2.060	162.55	28.90
Copper doped	298	2.269	2.129	135.96	44.73
Violet form powder	117	2.261	2.103	140.76	31.1
Copper doped	298	2.212	2.079	---	---
red form powder	123	2.209	2.059	---	---

in section 4.3.1. clearly shows that the composition of red form crystal and powder is different. This discrepancy can be settled only by the crystal structure determination.

4.4   CONCLUSION:

In summary the e.s.r. results of copper doped forms of Fe-Phen-NCS system indicate the following:

1.   The violet form powder gives a hyperfine resolved e.s.r. spectrum below the spin transition temperature, which is to be expected when the environment of Cu^{2+} is almost completely made up of low spin (diamagnetic) Fe^{2+}. As the sample is warmed the lines broaden continuously implying a continuous spin state change in the neighbourhood of the Cu^{2+} ions. The mossbauer spectra generally indicates an abrupt transition in the system. This brings out a major drawback in the use of S = 1/2 spin probes for studying Fe(II) spin crossover, viz., the e.s.r. may sense the only the changes in the immediate neighbourhood of S = 1/2 impurity which is different from what is going on in the bulk of the sample. Exchange coupling between Cu^{2+} and Fe^{2+} centres might even inhibit the spin crossover.

2)   The red form powder gives a broad exchange average line at all temperature even though the width increases with temperature. No hyperfine structure is resolved even at room temperature where mössbauer spectra indicates a predominantly low spin compound. This   means   that   the   formulation   of   the   product   as

$[Fe(phen)_3][Fe(NCS)_4](NCS)_2 \cdot 3H_2O$ by Maddock and co-workers is essentially correct. Since the paramagnetic ion, $Fe(NCS)_4^{2-}$ expected to show exchange dipolar averaged signal. However, it is not clear from the spectrum whether the Cu^{2+} occupies a substitutional cationic or anionic site in the sample.

3) The e.s.r. of Cu^{2+} doped red crystal $[Fe(Phen)_3](NCS)_2\ 2H_2O$ is more puzzling. At low temperature a well resolved Cu^{2+} spectrum having g and A values typical of tetragonal site is observed, which rapidly broadens with temperature and the spectrum almost disappears at room temperature. $[Fe(Phen)_3]^{2+}$ which can be obtained with many anions is always found to be in low spin state with no spin crossover. Room temperature Mössbauer spectra also indicate no trace of high spin component. Possible reasons for the temperature dependence of the e.s.r. spectra are the thermal population of a low lying quintet state in the host ion and/or a roomtemperature dependent distortion leading to an intermediate spin state at higher temperature. The role of Jahn-Teller interaction of Cu^{2+} in the D_{3d} $Fe(Phen)_3^{2+}$ site should also be taken into account in interpreting the e.s.r. spectrum (single crystal spectra will be more informative for this purpose). In the absence of detailed structural studies and magnetic data these conclusions are tentative.

4·5 ABBREVIATIONS

Phen : 1,10-Phenanthroline

pic : α-picoline

2-pic : 2-picolylamine

pip : 2-Pyridinaldehyde-N-iso- Propylimine

pni : 2-Pyridinaldehyde-N-methylemine

pyimi : 2-(2'-Pyridyl)imidazoline

pnp 2,6-bis-(2-diphenylphosphinoethyl)

py Pyridine

$[HB(Pz)_3]$: Hydrotris(1-Pyrazolyl)borate

bt : 2,2'-bi-2-thiazoline

btz 2,2'-bi-4,5-dihydrohiazine

dippen : cis-1,2-bis-(diphenylphosphino)ethyline

(bt) : 4,4'-bi-1,2,4 triazole

4.6 REFERENCES:

1. Martin, R.L.; White, A.H. 'Transition Metal Chemistry', Ed. Carlin, R.L.; Dekker, M. New York, 1968, Vol.4, 133.

2. Goodwin, H.A. *Coord. Chem. Rev.* 1976, **18**, 293.

3. Gutlich, P. *Struct. Bonding.*, *1981*, **44**, 83. and the references therein.

4. Bacci, M. *Coord. Chem. Rev.*, 1988, **86**, 245.

5. Toftlund, H. *Coord. Chem. Rev.*, 1989, **94**, 67.

6. Orgel, L.E. *J. Chem. Phy.*, 1955, **23**, 1819.

7. Konig, E.; Kremer, S. *Theorit. Chem. Acta* 1971, **23**, 12.

8. Sori, M.; Seki, S. *J. Phys. Chem. Solids.* 1974, **35**, 555.

9. Kambara, T. *J. Chem. Phys.*, 1981, **74**, 4557.

10. Zimmerman, R.; Konig, E. *J. Phys. Chem. Solids.* 1977, **38**, 779.

11. Kambara, T. *J. Phys. Soc. Jpn.* 1981, **49**, 1806.

12. Ohnishi, S.; Sugano, S. *J. Phys.* 1981, **C14**, 39.

13. Spiering, H.; Merbner, E.; Kopper, H.; Miller, E.W.; Gutlich, P. *Chem. Phys.* 1982, **68**, 65.

14. Katz, B.A.; Strouse, C.E. *J. Am. Chem. Soc.* 1979, **101**, 6214.

15. Ceccioni, F.; Di Vaira, M.; Midoolini, S.; Orlandi.; Sacconi, L. *Inorg. Chem.* 1981, **20**, 3423.

16. Sanner, I.; Meibner, E.; Koppen, H.; Spiering, H.; Gutlich, P. *Chem. Phys.* 1984, **86**, 277.

17. Alder, P.; Weehl, L.; Merbner, E.; Kohler, C.; Spiering, H.; Gutlich, P. *J. Phys.Chem. Solids.* 1987, **48**, 517.

18. Haddad, M.S.; Lynch, M.W.;k Federer, W.D.; Hendrickson, D.N. *Inorg. Chem.* 1981, 20, 123.

19. Cambi, L.; Szego, L. *Ber. Dtsch. Chem. Ges.* 1931, **64**, 259.

20. Reiff, W.M.; Long, G.J. *Inorg. Chem.* 1974, **13**, 2150

21. Madeja, K. *Z. Anorg. Allg. Chem.* 1978, **5**, 447.

22. Goodgame, D,M.L.; Machado, A.A.S.G. *Chem. Commun.* 1964, 1420.

23. Kelly, S.J.; Ford, G.H.; Nelson, S.M. *J. Chem. Soc.* 1971, A, 388.

24. Sacconi, L. Di Vaira, M. *Inorg. Chem.* 1978, **17**, 810.

25. Jesson, J.P.; Weiher, J.E.; Trofimenko, S. *Ibid.* 1968, **48**, 2058.

26. Beathi, J.K. *Ibid.* 1973, **95**, 2052.

27. Bradley, G.; McKee, V.; Nelson, S.M. *J. Chem. Soc. Dalton Trans.* 1978, 522.

28. Irler, W. *Solid. State. Commun.* 1974, **39**, 29.

29. Konig, E. *Inorg. Chem. Acta,* 1979, **35**, 169.

30. Slichter, C.P.; Drickamer, H.G. *J. Chem. Phys.,* 1972, **56**, 2142.

31. Levason, W. *J. Chem. Soc. Dalton. Trans.* 1975, 1778.

32. Hoselton, M.A.; Wilson, L.J.; Drago, R.S. *J. Am. Chem. Soc.* 1975, **97**, 1722.

33. Eibschutz, M.; Lines, M.E.; Disalvo, F.J. *Phys. Rev.* 1977, **B15**, 103.

34. Eibschutz, M.; Disalvo, F.J. *Phys. Rev. Lett.* 1976, **36**, 184.

35. Lines, M.E.; Eibschutz, M. *J. Phys.* 1976, **C9**, L355.

36. Frank, E.; Abeledo, C.R. *Inorg. Chem.* 1966, **5**, 1453.

37. Bacci, M. *Inorg. Chem.* 1973, **12**, 1801.

38. Casey, A.T.; Issac, F. *Aust. J. Chem.* 1967, **20**, 2765.

39. Mikami, M.; Konno, M.; Saite, Y. *Chem. Phys. Lett.* 1979, **63**, 566.

40.. Greenway, A.M. *Inorg. Chem.* 1979, **18,** 2692.

41. Greenway, A.M. Sinn, E. *J. Am. Chem. Soc.* 1978, **100,** 8080.

42. Figgis, B.N. Introduction to Ligand Fields Inter Science Publishers, New York, London, Sydney, 1966.

43. Gutlich, P.; Koppen, H. Steinhauzer, H.G. 1980, **74(3),** 475.

44. Goodwin, H.A.; Baker, A.T. *Aust. J. Chem.* 1977, 30, 771.

45. Savage, S.; Jia-Long, Z.; Maddock, A.G. *J. Chem. Soc. Dalton. Trns.* 1985, 991.

46. Gallois, B.; Real, J.A.; Hallw, C.; Zarempowitch, J. *Inorg. Chem.* 1990, **28,** 1152.

47. Konig, E.; Madeja, K. *Chem. Commun.* 1966, **61,**

48. Konig, E.; Madeja, K. *Inorg. Chem.* 1967, **6,** 48.

49. Rao, P.S.; Reuveni, A.; McGarvey, B.R.; Gangooli, P. *Inorg. Chem.* 1981, **20,** 209.

50. Vreugdenhil, W.; Haasnoot, J.G. Oliverkhan, *J. Am. Chem. Soc.* 1987, **19,** 5272.

51. Ozarowski, A.; McGarvey, B.R.; Sarkar, B.; Drake, J.E. *Inorg. Chem.* 1988, **27,** 628.

52. Ozarowski, A.; McGarvey, B.R. *Inorg. Chem.* 1989, **28,** 2262.

53. 'Vogel's Text book of Practical Organic Chemistry', Furniss, B.S.; Hannaford, A.J.; Rogers, V.; Smith, P.W.G.; Tatchell, A.R. Ed. ELBS. 1978.

54. Schilt, A.A.; Fritsch, K. *J. Inorg. Nucl. Chem.* 1966, **28,** 2677.

55. Gutlich, P. "Spin Transitionin Iron Complexes" In Mossbauer Spectroscopy Applied to Inorganic Chemistry, Modern Inorganic Chemistry Series; Long. G.J., Ed., Plenum: New York, 1984, Vol.1.

56. Taylor, P.C.; Bangher, J.F.; Kriz, H.M. *Chem. Rev.* 1975, **75,** 203.

57. Sailaja, D. M.Phil. Dissertation, 1987, School of Chemistry, University of Hyderabad, Hyderabad.

58. Duncan, J.F. Mok, K.F. *J. Chem. Soc.* 1966, 1493.

CHAPTER - V

CRYSTAL AND MOLECULAR STRUCTURE OF NITRATO(6,6'-DIMETHYL-2,2'-BIPYRIDINE)SILVER(I) DIMER

5.1 INTRODUCTION:

Silver(I) complexes of 2,2'-bipyridine and related ligands have been known for a long time.[1,2] But structurally they are not characterized except in one case.[3] The growth of good single crystal is found to be difficult in these cases, which might be one of the reasons for not pursuing the single crystal X-ray diffraction studies, while bis-chelate coordination is more common for these ligands, **mono** chelate complexes are known for 2-methylphenanthroline[4], 2,9-dimethylphenanthroline[5] and 6,6'-dimethylbipyridine.[6] Some of these ligands also stabilise the copper(I) oxidation state which has an interesting photochemistry involving charge-transfer excited states.[7]

Though in principle d^{10} configuration of silver(I) is expected to give a tetrahedral geometry, it is rarely realised in practice and a convincing explanation for this is not available in the literature. Since silver(I) and copper(I) are isoelectronic, the wealth of structural data available on the similar copper(I) systems can be probed with a view to find out the reason for the tendency of silver(I) to adopt a distorted tetrahedral structure. Structural studies on copper complexes of the type $[CuL_2]^+$, where L = 2,2' bipyridine, 1,10-phenanthroline and their substituted derivatives,[8-12] blue copper proteins like plastocyanins[13] and[14] azurins have revealed significant flattening of the $[CuN_4]$

coordination sphere. Similar distortions were found in $[Cu(btz)_2](BPh)_4$ and $[Cu_2(bt)_4](ClO_4)_2$[3]. The origin of the flattening distortion has been a subject of some controversy being variously attributed to different sources. Drew et al explained it as due to admixture of Jahn-Teller active charge transfer excited state into the ground state.[15] Crystal packing forces,[16] as well as stacking interaction[3] between heteroaromatic ligands are the other explanations. Thus while no single factor can satisfactorily explain the structural features in copper(I) complexes, Goodwin et al.[3] explained the distortion in $[Ag(tmbp)_2]$ BF_4 as being due to inter-molecular stacking interactions.

If nitrate group is present in the complex, the study of the binding nature of this NO_3^- in the molecule or packing in the crystal lattice will be interesting as it influences the distortion in the structure. Usually nitrate binding is classified[17] into unidentate, bidentate and bridging. The bidentate mode could be either symmetric (where both M - O bond lengths are same) or unsymmetric (where they are different). The best example exhibiting all the three types of binding is silver (3-cryptates)[18]. In the case of $C_{11}H_{15}AsAg(NO_3)_2$[19] (Fig5.1a) one NO_3^- is bridging two silver atoms by doubly bidentate chelation with four equal bonds and the another NO_3^- completes the chain like structure by forming two unsymmetrical bidentate linkages with two sets of Ag - O bonds, one set (2.85, 2.81 Å) being significantly longer than the other (2.43, 2.35 Å) set. In [Ag $(P(OMe)_3)_2NO_3]_2$[20] the NO_3^- groups are using only one oxygen for bridging (Fig5.1b), but there is a twist in the nitrate plane, there by placing one of the oxygens close to silver. This long

151

Figure 5.1 : a) Structure of $C_{11}H_{15}As(AgNO_3)_2$ showing the principal bond lengths (e.s.d's in parenthesis) (Ref.19).

b) Structure showing the bending of the nitrate groups towards a silver atom in $[Ag(P(OMe)_3)_2NO_3]_2$ (Ref.20).

152

Ag-O distance of 3.102 Å is still considered as bonding interaction in this structure.

The important aspect in the binuclear complexes is usually the metal-metal interactions. The recent developments in cluster chemistry opened a new era in the polymer chemistry of silver(I) complexes. In silver(I) N,N-diethyldithiocarbomates[21] the Ag-Ag atoms are arranged in the form of bent chains with a distance almost similar to the Ag-Ag distance (2.889 Å) in silver metal[22]. This unusual arrangement of the metal atoms causes the formation of a chain polymer and also a complicated co-ordination of the six ligands to the metal atom. In the 2-sulfanilamide pyrimidine silver(I),[23] the Ag-Ag distance is 2.916 Å, here the chains are cross linked by imido nitrogen atoms but consideration of a bonding interaction between Ag-Ag atoms, leads to a better explanation for the other bonds in the structure. In the case of $[Ag(imid)_2][NO_3]$[24], the hydrogen bonding between pyridine nitrogens of imidazole rings and nitrate oxygens is expected to stabilise the NO_3^- ion position, whereas in the analogous $[Ag(imid)_2][ClO_4]$[25] (Fig.5.7) compound an Ag-Ag distance of 3.051 Å is still considered as a bonding interaction. It is felt that only Ag-Ag bond could possibly hold the whole structure intact in the absence of any hydrogen bonding and other packing interactions. In the case of cluster compounds like $Ag'_6\{S_2C = C(CN)_2\}_6]^{6-}$ and $Ag'_8\{S_2C = C(CN)_2\}_6]^{4-}$ a distance ranging from 3.0 - 3.8 Å is noticed between silver atoms.[26,27]

In this chapter we report the crystal structure of $Ag(dmbp)NO_3$, which has a near planar geometry with nitrate ion

153

acting   as an unsymmetrically chelating ligand.   There are
stacking interactions between the aromatic rings, which along with
silver-silver interaction result in the formation of dimeric units
in the lattice.   In addition there are inter-dimer interaction
resulting in a slipped stack arrangement of dimers in the crystal
lattice.

5.2 EXPERIMENTAL SECTION

5.2.1 Preparation of Crystals:

The preparation of Ag(dmbp)NO$_3$ has been reported earlier.[6] Colourless fibre-type crystals are obtained by dissolving the sample in 0.1 N nitric acid and concentrating the solution in a desiccator over sulphuric acid.

5.2.2 X-ray Data Collection:

Single crystal data were collected at room temperature for a thin crystal, measuring approximately 0.2 x 0.2 x 0.05 mm, by using an Enraf-Nonius CAD-4 diffractometer and graphite monochromated MoK$_\alpha$ radiation. Unit cell parameters were obtained by least square refinement of 25 centered reflections. Intensity data were collected for the range $2 < 0 < 23°$, by an $\omega - 2\theta$ scan technique. An empirical absorption correction was applied. Out of 3166 reflections measured, 1055 reflections with $F_o > 3\sigma (F_o)$ were used for structure refinement. Crystal data are summarised in Table 51.

5.2.3 Structure Solution and Refinement:

The structure was solved by Patterson and Fourier methods. A difference Fourier calculation after anisotropic refinement of the silver atom revealed all the non-hydrogen atoms. The ring hydrogen atoms were allowed to ride on the respective carbon atoms

155

```
-----------------------------------------------------------------
Table 5.1 :    crystal data for Ag(dmbp)NO₃
-----------------------------------------------------------------
```

Mol. Formula   = $AgC_{12}H_{12}N_3O_3$

Mol.Weight   = 354.1

Cryst. Syst.   = monoclinic

Space group   = C2/C

a   = 7.674 (4) Å

b   = 20.022 (9) Å

c   = 16.775 (6) Å

β = 96.00 (4) °

v   = 2563 (2) Å³

D (Calcd.)   = 1.835 g cm⁻³

D (expt)   = 1.80 g cm⁻³

z   = 8

Radiation   = MoK_α (λ = 0.7107 A)

μ (MoK_α) = 14.33

F (000)   = 1408

No.of data with $F_o > 3\sigma$ (F_o) = 1055

No. of variables   = 175

R   = 0.121

R_w = 0.104

```
-----------------------------------------------------------------
```

with a common isotropic thermal parameter which was refined. The methyl groups were refined as rigid groups with fixed isotropic thermal parameters for the hydrogen atoms. The function minimised is $\sum \omega (|F_o| - |F_c|)^2$, where the weight $\omega = 1/\sigma(F)$. Refinement converged to $R = 0.122$ and $R_\omega = 0.104$. The shift to error ratio in the final refinement cycle was less than 0.1 for all parameters. In the final difference map a maximum peak value of 3 eA^{-3} associated with the silver atom position was observed and else where the error density was below 0.7 eA^{-3}. The high R-factor is due to the poor quality of the crystal resulting in an over all low scattering power. The final atomic coordinates and equivalent isotropic temperature factors for the non-hydrogen atoms are in Table 5.2, anisotropic thermal parameters for non hydrogen atoms are in Table 5.3, atomic positions and isotropic thermal parameters for hydrogen atoms are in Table 5.4, bond distances and bond angles are given in Table 5.5, equations of some important least square planes and perpendicular distances of the fitted atoms are given Table 5.6. Table 5.7 gives the list of observed and calculated structure factors.

The computer programs used include SHELX[28] and ORTEP[29] Atomic scattering factors are taken from International tables for X-ray crystallography[30] Correction for the anomalous dispersion for Ag (f' = -1.085, f'' = 1.101) were those reported by Cromer and Libermen.[31]

Table 2

Positional parameters, equivalent Isotropic temperature Factors,[a] and their estimated standard deviations for non hydrogen atoms.

Atom	$10^3 x$	$10^3 y$	$10^3 z$	B, A^2
Ag	313.8(3)	272.6(1)	205.2(1)	6.88(7)
O(1)	418(3)	194.3(8)	119.1(9)	11.4(8)
O(2)	276(3)	142(1)	195(1)	14(1)
O(3)	404(3)	89.9(7)	108.6(9)	10.7(8)
N(1)	199(2)	324.8(8)	312.6(8)	5.5(5)
N(2)	315(2)	384.5(9)	181(1)	6.1(6)
N(3)	365(3)	140(1)	141(1)	8.1(8)
C(1)	123(4)	285(1)	377(1)	7.3(9)
C(2)	89(4)	319(1)	434(1)	9(1)
C(3)	97(4)	392(1)	434(2)	11(1)
C(4)	146(4)	428(1)	374(1)	10(1)
C(5)	203(3)	387(1)	310(1)	6.9(8)
C(6)	260(3)	425(1)	237(1)	6.6(8)
C(7)	244(4)	492(1)	229(1)	11(1)
C(8)	295(4)	520(1)	160(2)	12(1)
C(9)	362(4)	482(1)	104(2)	11(1)
C(10)	353(4)	414(1)	110(2)	9(1)
C(11)	411(3)	365(1)	52(1)	7.4(8)
C(12)	140(4)	216(1)	364(1)	9(1)

[a]Equivalent isotropic temperature factor are defined as $B = 8\Pi^2/3$ $(U_{11}a^2a^{*2} + U_{22}b^2b^{*2} + U_{33}c^2c^{*2} + U_{13}a^*c^* ac \cos\beta)$.

Table -53

Anisotropic Thermal Parameters $(\times 10^2)$ for non hydrogen atoms.

Atom	U_{11}	U_{22}	U_{33}	U_{23}	U_{13}	U_{12}
Ag	10.0(2)	8.4(1)	7.7(1)	-0.9(1)	0.8(1)	0.2 (1)
O(1)	23(3)	10(1)	11(1)	-2(1)	8(1)	-2(1)
O(2)	27(3)	11(1)	16(2)	2 (1)	14(2)	1(1)
O(3)	23(2)	6.2(8)	12(1)	-0.8(9)	7(1)	3(1)
N(1)	8(1)	7(1)	5.4(9)	-1.3(8)	0(1)	3(1)
N(2)	8(1)	10(1)	5(1)	1.5(9)	4(1)	2(1)
N(3)	13(2)	8(1)	9(2)	3(1)	2(1)	-1(2)
C(1)	13(2)	9(1)	5(1)	3(1)	2(1)	5(2)
C(2)	14(3)	12(2)	7(2)	0(1)	3(2)	-2(2)
C(3)	16(3)	14(2)	10(2)	-2(2)	6(2)	3(2)
C(4)	20(4)	10(2)	9(2)	4(1)	8(2)	3(2)
C(5)	12(2)	9(2)	6(1)	0(1)	3(1)	4(2)
C(6)	9(2)	10(2)	6(1)	2(1)	2(1)	2(1)
C(7)	22(4)	8(2)	13(2)	3(1)	7(2)	3(2)
C(8)	18(3)	14(2)	13(2)	6(2)	9(2)	6(2)
C(9)	18(4)	11(2)	13(2)	2(2)	8(2)	3(2)
C(10)	11(2)	11(2)	12(2)	-1(2)	2(2)	-2(2)
C(11)	9(2)	11(1)	8(1)	1(1)	1(1)	4(2)
C(12)	12(2)	10(2)	13(2)	7(1)	2(2)	0(2)

159

Table –5.4

Atomic Positions ($\times 10^3$) and Isotropic Thermal Parameter ($\times 10^3$) for hydrogen atoms.[a]

Atom	x	y	z	U
H(1)	49(4)	294(1)	486(1)	10(3)
H(2)	60(4)	419(1)	486(2)	10(3)
H(3)	146(4)	482(1)	373(1)	10(3)
H(4)	193(3)	522(1)	274(1)	10(3)
H(5)	284(4)	573(1)	151(2)	10(3)
H(6)	420(4)	505(1)	55(2)	10(3)
H(7)	439	409	18	12
H(8)	279	348	35	12
H(9)	502	325	40	12
H(10)	102	219	424	14
H(11)	256	187	364	14
H(12)	35	195	324	14

[a] Connectivities: H(1) – C(2); H(2) – C(3); H(3) – C(4); H(4) – C(7); H(5) – C(8); H(6) – C(9); H(7), H(8) H(9) – C(11); H(10), H(11), H(12) – C(12).

Table -5.5

Bond Distances (Å) and Angles (deg).[a]

Bond Distance (Å)		Bond Angles (deg.)	
Ag – Ag'	3.087(4)	N(1) – Ag – N(2)	72.7(5)
Ag – N(1)	2.33(1)	N(2) – Ag – O(1)	123.2(6)
Ag – N(2)	2.28(2)	N(1) – Ag – O(2)	117(1)
Ag – O(1)	2.33(1)	O(1) – Ag – O(2)	48.2(6)
Ag – O(2)	2.64(2)	Ag – N(1) – C(1)	121(1)
O(1) – N(3)	1.22(2)	Ag – N(1) – C(5)	114(1)
O(2)– N(3)	1.19(2)	C(1) – N(1) – C(5)	124(2)
O(3) – N(3)	1.20(2)	Ag – N(2) – C(6)	118(1)
N(1) – C(1)	1.50(2)	Ag – N(2) – C(10)	125(2)
N(1) – C(5)	1.25(2)	C(6) – N(2) – C(10)	117(2)
N(2) – C(6)	1.33(3)	O(1) – N(3) – O(2)	116(2)
N(2) – C(10)	1.39(3)	O(1) – N(3) – O(3)	120(3)
C(1) – C(2)	1.23(2)	O(2) – N(3) – O(3)	124 (2)
C(1) – C(12)	1.40(3)	Ag – O(1) – N(3)	105(2)
C(2) – C(3)	1.47(3)	Ag – O(2) – N(3)	91(1)
C(3) – C(4)	1.31(3)	N(1) – C(1) – C(2)	113(2)
C(4) – C(5)	1.45(3)	N(1) – C(1) – C(2)	111(2)
C(5) – C(6)	1.54(3)	C(2) – C(1) – C(12)	134(2)
C(6) – C(7)	1.36(3)	C(1) – C(2) – C(3)	123(2)
C(7) – C(8)	1.37(3)	C(2) – C(3) – C(4)	124(3)
C(8) – C(9)	1.35(3)	C(3) – C(4) – C(5)	113(2)
C(9) – C(10)	1.37(3)	N(1) – C(5) – C(4)	121(2)
C(10)– C(11)	1.48(3)	N(1) – C(5) – C(6)	121(2)
		C(4) – C(5) – C(6)	117(2)

N(2) - C(6) - C(5)	113(2)
N(2) - C(6) - C(7)	124(2)
C(5) - C(6) - C(7)	122(2)
C(6) - C(7) - C(8)	117(3)
C(7) - C(8) - C(9)	122(3)
C(8) - C(9) - C(10)	119(3)
N(2) - C(10)- C(9)	120(2)
N(2) - C(10)- C(11)	113(2)
C(9) - C(10)- C(11)	126(3)

' refers to a symmetry related atom at 1-x, y, 1/2-z

Table - 6

Equations of important least square planes and perpendicular distance in (Å) of the fitted atoms from the planes

1)Ag N(1) N(2) O(1) O(2).

$1.9071x - 0.0933y + 2.1861Z = 1$

Ag	= 0.0735
N(1)	=-0.1089
N(2)	=-0.1338
O(1)	= 0.1315
O(2)	=-0.2083

(The dihedral angle between Ag N(1),N(2) and Ag O(1),O(2) planes = $15°$)

2)C(1)-C(5) N(1) C(12)

$2.2556x - 0.2220y + 2.0236Z = 1$

C(1)	=-0.0719
C(2)	=0.0246
C(3)	= 0.0254
C(4)	= -0.0215
C(5)	= 0.0015
N(1)	= 0.0261
C (12)	= 0.0135

3) C(6)-C(10) C(11) N(2)

$1.877x + 0.3919Y + 1.4799Z = 1$

C(6)	= 0.0149
C(7)	=-0.0401
C(8)	=-0.0169
C(9)	=0.0812
C(10)	=-0.0413
C(11)	=-0.0362

N(2)   = 0.0358

4) N(3) O(1), O(2), O(3)

    1.7906x - 0.5307y + 2.9867z = 1

    N (3)   =-0.0042

    O (1)   = 0.0012

    O(2)   = 0.0013

    O(3)   = 0.0013

5.3. · **RESULTS AND DISCUSSION**

5.3.1 **Coordination Sphere Around Silver Atom:**

The structure of the complex is composed of a dimeric unit of two symmetry related [Ag(dmbp)NO$_3$] molecules. Each unit cell comprises of eight [Ag(dmbp)NO$_3$] molecules with weak Ag-Ag interactions.

In each molecule silver atom is coordinated (Fig.5.2) by dmbp molecule through its two nitrogen atoms. The nitrate is binding in unsymmetrical bidentate fashion. All these atoms are very nearly in plane with silver atom. The two Ag-N bonds are equivalent (2.33 Å) and similar to that found in [Ag(tmbp)$_2$]BF$_4$[3] where as Ag – O bond lengths in nitrate chelation are highly unsymmetrical. One is 2.32 Å and the other one is 2.64 Å. This type of asymmetric chelation is seen, for example in Ag$_2$(dpm)$_2$(NO$_3$)$_2$.[32] The coordination is very nearly planar with a dihedral angle of 15° between AgN(1)N(2) and AgO(1)O(2) (Fig. 2) planes. The two pyridyl rings are nearly coplanar with a twist angle of 7 between the two mean planes. The N(1)-C(5)-C(6)-C(7) twist angle is 9° and for N(2)-C(6)-C(5)-C(4), it is 2°. The two silver atoms in the dimer are connected by weak bond of 3.087 A^o length. The trans bonds N(1)-Ag-O(1) and N(2)-Ag-O(2) are nearly linear with bond angles, < N(1) Ag O(1) = 165° and < N(2) Ag O(2) = 171°. The equations for some important planes are given in Table 5.6.

5.3.2 Stacking Interactions:

The distortion from the tetrahedral configuration towards planar structure is explained as a combined effect of stacking and Ag-Ag interactions. As mentioned earlier the unit cell consists of eight molecules and their stacked arrangement is shown in Fig.5. 3, which is analogous to that observed in Cu(phen)(ppr)$^+$ ion as shown in Fig.5.4. The shortest atom-atom contact for stacking within the dimer is between N(2) and N(2)$'$ (3.47Å), while for inter- dimer stacking it is between C(6) and C(4)$''$ (3.46Å).[34] In general the stacking forces between aromatic rings are explained on the grounds of both charge transfer effect associated with eclipsed or face to face contacts of the heteroaromatic rings[3,33] and intra-dimer electrostatic interactions between carbon atoms and hydrogens of the rings which have slight -ve and +ve charges respectively (Fig.5.5a). In the present structure the observed staggered configuration in the dimer is expected to facilitate the coulombic interactions of the two rings. The charge transfer interaction between the aromatic ring planes of the dimeric unit add to the intra-dimer stacking interaction. On the whole intra-dimer interaction will have significant contribution from both the mechanisms, where as inter-dimer stacking will be dominated by electrostatic interactions. Thus both the intra and inter dimer interactions of the heteroaromatic ring systems are responsible for stacking in the lattice. The hydrogens of the methyl groups which point towards the centre of the aromatic rings should also be important for the intra-dimer interaction (Fig5.5b). If the structure is visualised along Ag - Ag bond, the dimeric

166
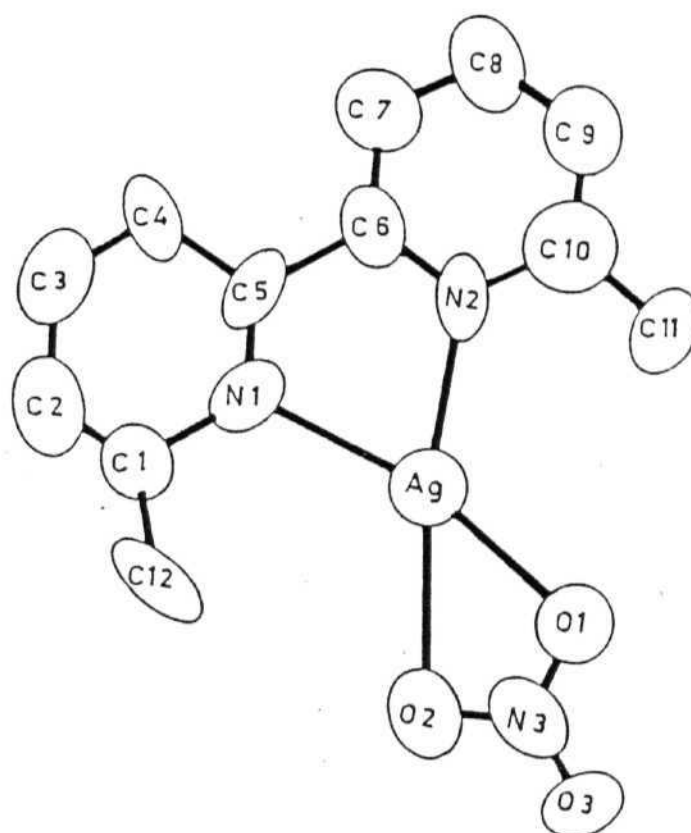
Figure 5.2 : The structure of single molecule of Ag(dmbp)NO$_3$ with numbering of the atoms and thermal ellipsoids at the 50% probability level.
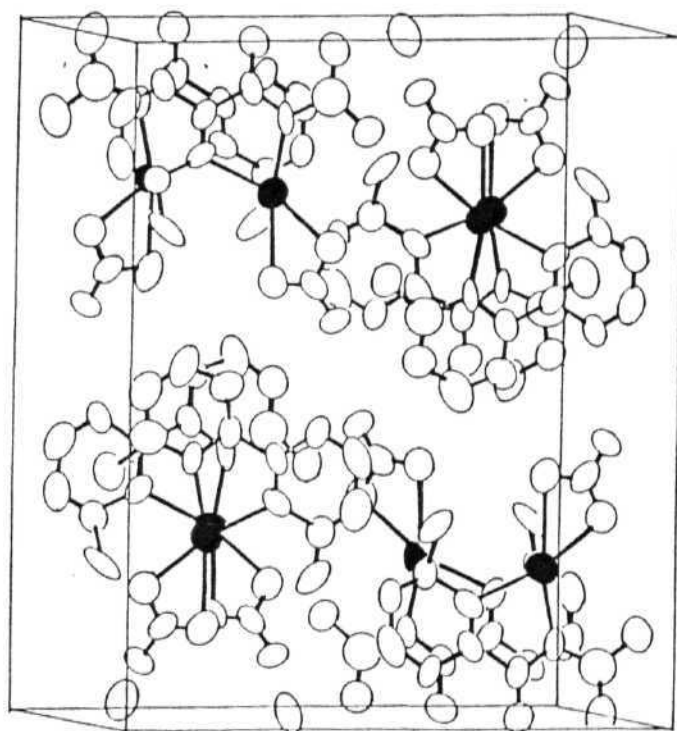
Figure 5.3 : Packing diagram of Ag(dmbp)NO$_3$. The unit cell is viewed along a direction close to the Ag-Ag' bond, c-axis horizontal and b-axis vertical (The silver atoms are shaded).

168
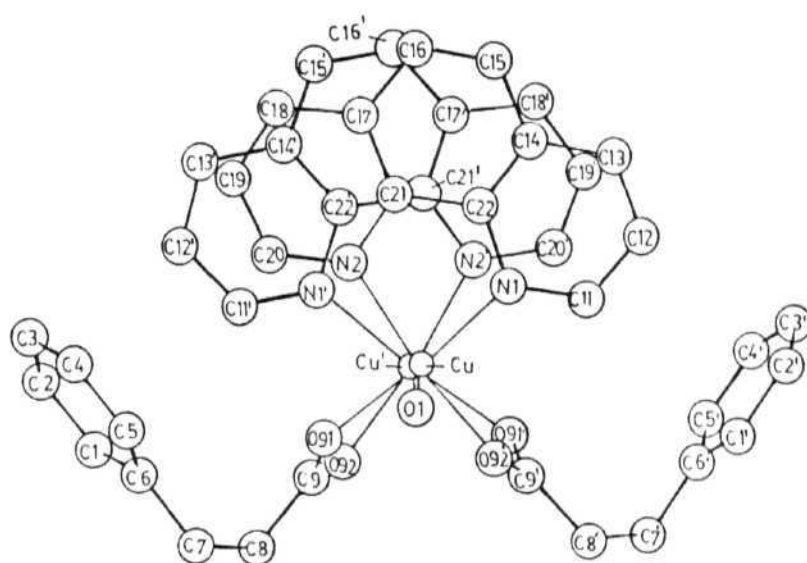
Figure 5.4 : View of the dimeric unit $[Cu_2(phen)_2(ppr)_2(H_2O)_2]^{2+}$ in the crystal of $Cu(phen)(ppr)NO_3 \cdot 2H_2O$ approximately perpendicular to the planes of the two phenanthroline ligands. (Ref.33).
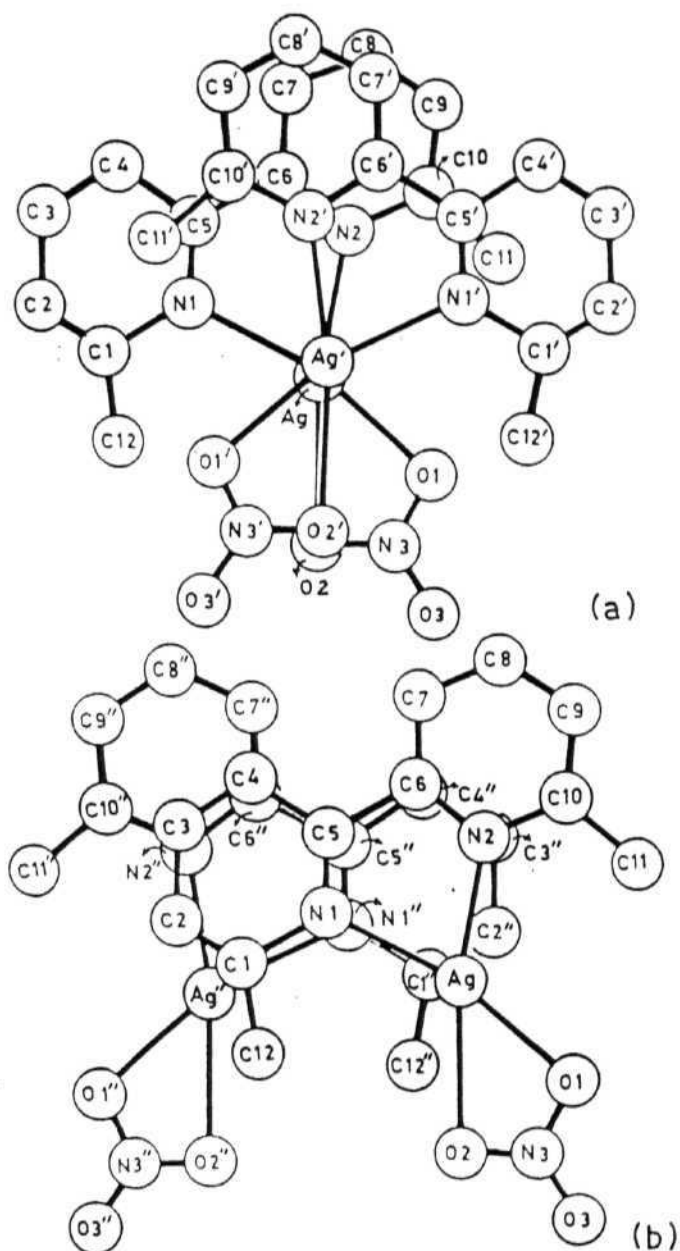
Figure 5.5 : Stacking interactions in the crystal.   a) The intra-dimer interaction with in the [Ag(dmbp)NO$_3$] dimeric unit. b) The inter-dimer interactions between the Ag(dmbp)NO$_3$] dimeric units.   Only one monomer belonging to each dimer is shown.

units are not stacked parallel to the ac plane instead a slipped stack nature is observed (Fig.5.6). The inter-dimer stacking interactions present are leading to this type of slipped stack arrangement of the dimer in the lattice.

5.3.3 Nitrate Chelation:

As mentioned earlier in the present structure the nitrate is chelated to the metal ion, in unsymmetrical bidentate fashion. Addison *et al*[17] explained that this type of unsymmetrical bidentate chelation is commonly observed due to two reasons (i) unsymmetrical distribution of electrons at the metal centre (ii) the presence of a ligand with a strong trans-effect situated in a position trans to only one of the two coordinated oxygens of each bidentate nitrate group. In the present example neither of these conditions are seem to be the reasons. The only reasonable explanation seems to be that the closely placed bulky methyl groups and oxygens of nitrate will have greater steric repulsions, if the nitrate chelation is symmetrical. To minimise these repulsions and to give a more stable planar structure, the unsymmetrical chelation will be helpful. The methyl groups of the molecule participating in the inter-dimer stacking (Fig.5.5b) are in part responsible for the lengthening of one of the two Ag-O bonds by steric repulsion between O(2)'' and C(12).[34]

5.3.4 Ag - Ag Interactions:

The intra-dimer Ag-Ag bond length is slightly more than that observed in the silver metal (2.889 $\overset{\circ}{A}$)[22]. Similar Ag-Ag contacts
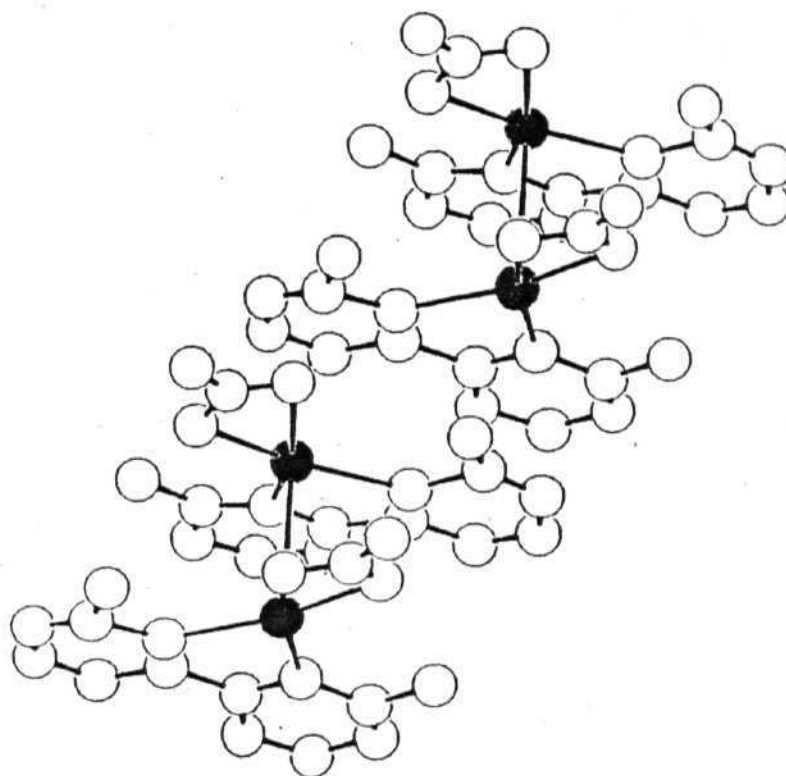
Figure 5.6 : View of the slipped stack arrangement of [Ag(dmbp)NO$_3$] dimeric unit. (The silver atoms are shaded.)
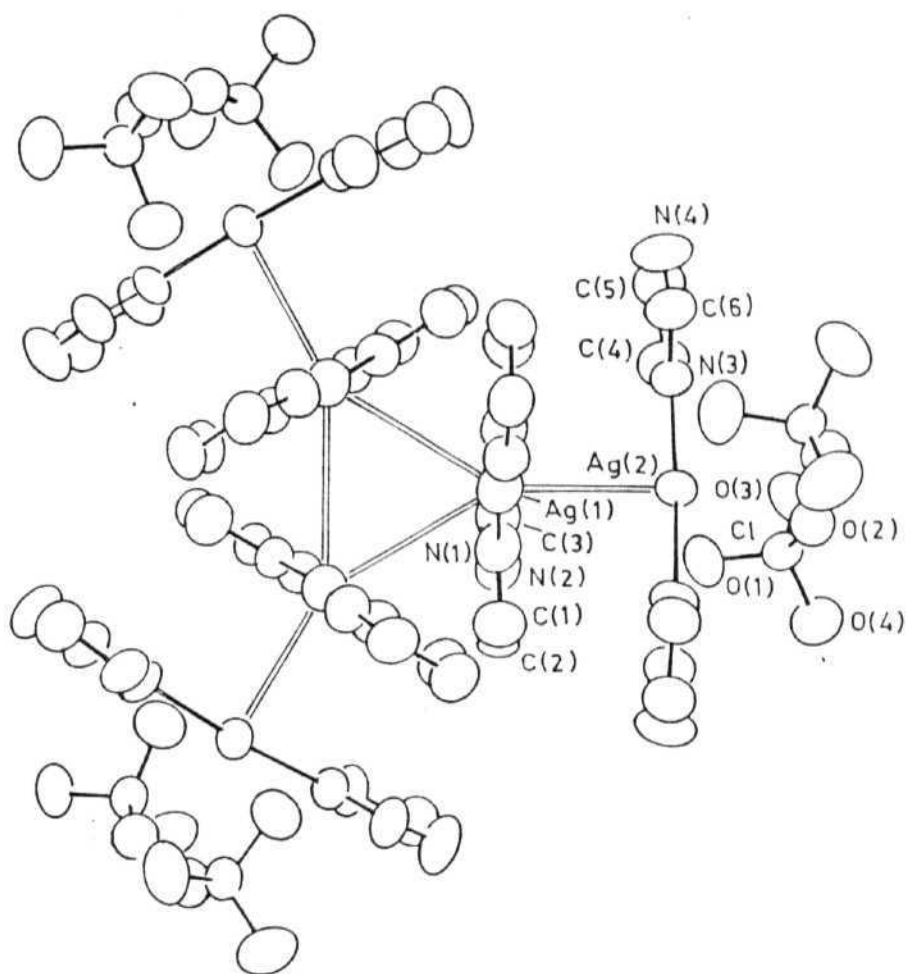
Figure 5.7 : The hexameric unit observed in the structure of [Ag(imid)$_2$][ClO$_4$]. (Ref.25).

173

are also observed in several other Ag(I) complexes.[32,23-25,27,35-42] Unlike in all other cases the present compound has a dimeric structure having direct Ag-Ag interactions without involving any bridging group. A weak bonding interactions between the two d^{10} ions is possible via the participation of 5s and 5p orbital, hence Ag-Ag interaction should be contributing to the stability of the structure. A comparable situation exists in the hexameric cluster formed by $Ag(imid)_2ClO_4$.(Fig.5.7)[25] In this crystal Ag-Ag distances of 3.051Å and 3.49Å are discussed in terms of definite bonding interactions in the absence of any other interactions like hydrogen bonding as seen in the case of $[Ag(imid)_2[NO_3]$.[24]

5.4 CONCLUSION:

Even though in principle a tetrahedral geometry is expected for a d^{10} metal ion purely based on steric considerations, in the present structure the Ag-Ag interactions and stacking forces produce a near planar Coordination around Ag(1).

Table5.7 : List of observed and calculated structure factors.

H	K	L	FO	FC	H	K	L	FO	FC	H	K	L	FO	FC	H	K	L	FO	FC	H	K	L	FO	FC
0	0	2	449	-406	0	6	5	19	22	0	12	6	30	-33	-1	1	11	55	56	1	3	12	5	6
0	0	4	117	-107	0	6	6	23	25	0	12	7	4	-8	-1	1	9	59	64	1	3	14	4	8
0	0	6	32	31	0	6	9	72	-75	0	12	8	25	26	-1	1	7	169	-180	1	3	15	27	29
0	0	8	118	-117	0	6	10	84	-87	0	12	9	34	34	-1	1	6	29	-30	-1	5	15	23	35
0	0	10	152	153	0	6	11	84	89	0	12	11	49	-56	-1	1	5	261	248	-1	5	14	32	41
0	0	12	141	-129	0	6	12	55	59	0	12	12	3	8	-1	1	4	101	89	-1	5	13	26	-29
0	0	14	34	31	0	6	13	45	-49	0	12	13	33	35	-1	1	3	253	-286	-1	5	12	25	-23
0	0	16	24	23	0	6	14	17	-23	0	14	0	66	65	-1	1	2	17	-19	-1	5	11	32	34
0	0	18	22	-12	0	6	15	25	20	0	14	1	104	95	-1	1	1	191	212	-1	5	10	2	2
0	2	0	321	-299	0	8	0	122	113	0	14	2	49	-39	1	1	0	38	-38	-1	5	8	44	48
0	2	1	166	186	0	8	1	266	-236	0	14	3	69	-64	1	1	1	50	50	-1	5	7	148	-153
0	2	2	210	215	0	8	2	107	-106	0	14	4	5	1	1	1	2	4	-4	-1	5	6	110	-105
0	2	3	35	-36	0	8	3	174	171	0	14	5	19	12	1	1	3	148	133	-1	5	5	218	196
0	2	4	77	-76	0	8	4	70	69	0	14	6	8	2	1	1	4	17	15	-1	5	4	161	148
0	2	5	137	127	0	8	5	3	-2	0	14	8	5	18	1	1	5	261	-227	-1	5	3	149	-154
0	2	6	80	-73	0	8	6	24	26	0	14	9	30	-36	1	1	6	56	56	-1	5	2	160	-175
0	2	7	105	96	0	8	7	76	-82	0	14	11	37	45	1	1	7	205	189	-1	5	1	48	50
0	2	8	141	134	0	8	8	62	-66	0	14	13	23	-34	1	1	8	42	-41	1	5	0	75	74
0	2	9	81	-82	0	8	9	77	83	0	16	0	62	-48	1	1	9	145	-131	1	5	1	31	32
0	2	10	132	-128	0	8	10	26	32	0	16	1	86	-75	1	1	10	8	11	1	5	2	56	55
0	2	11	23	24	0	8	11	68	-72	0	16	2	39	32	1	1	11	61	63	1	5	3	21	18
0	2	12	116	112	0	8	12	20	-32	0	16	3	37	38	1	1	12	9	-6	1	5	4	112	-116
0	2	13	22	-14	0	8	13	49	50	0	16	6	6	-8	1	1	15	20	-21	1	5	5	111	-113
0	2	14	62	-53	0	8	14	20	21	0	16	7	30	-34	-1	3	15	60	-66	1	5	6	104	106
0	2	15	21	-19	0	8	16	9	-9	0	16	8	15	15	-1	3	14	17	-16	1	5	7	186	169
0	4	0	104	104	0	8	17	5	-9	0	16	9	27	35	-1	3	13	54	60	1	5	8	91	-88
0	4	1	65	-66	0	10	0	86	66	0	16	10	21	-29	-1	3	12	15	15	1	5	9	136	-127
0	4	2	203	-212	0	10	1	157	147	0	16	11	22	-22	-1	3	11	22	-27	1	5	10	52	50
0	4	3	98	102	0	10	2	23	27	0	16	12	17	21	-1	3	10	2	2	1	5	11	26	21
0	4	4	98	98	0	10	3	98	-91	0	18	0	43	33	-1	3	7	95	104	1	5	13	8	12
0	4	5	54	-55	0	10	4	65	-62	0	18	1	49	46	-1	3	6	42	43	1	5	14	10	-10
0	4	6	20	-22	0	10	5	27	27	0	18	2	49	-41	-1	3	5	294	-255	1	5	15	11	-16
0	4	7	112	-104	0	10	7	47	48	0	18	3	20	-20	-1	3	4	124	-108	-1	7	14	47	-51
0	4	8	15	-11	0	10	8	18	21	0	18	4	29	26	-1	3	3	230	242	-1	7	13	26	26
0	4	9	111	105	0	10	9	84	-88	0	18	5	8	7	-1	3	2	48	-48	-1	7	12	30	28
0	4	10	95	93	0	10	10	3	4	0	18	6	12	10	-1	3	1	38	-39	-1	7	11	17	-26
0	4	11	52	-54	0	10	11	71	79	0	18	8	14	-27	1	3	0	70	72	-1	7	10	9	-11
0	4	12	76	-77	0	10	12	5	9	0	20	0	46	-40	1	3	1	44	-44	-1	7	8	29	-34
0	4	13	32	33	0	10	13	33	-42	0	20	1	9	3	1	3	2	127	122	-1	7	7	48	48
0	4	14	53	49	0	10	14	18	-15	0	20	2	36	30	1	3	3	4	-3	-1	7	6	138	133
0	4	16	26	-22	0	10	15	6	13	0	20	3	6	11	1	3	4	63	-58	-1	7	5	137	-126
0	4	17	5	-4	0	10	16	3	11	0	20	4	18	-11	1	3	5	200	180	-1	7	4	274	-260
0	4	18	2	-4	0	12	0	17	-4	0	20	5	6	-9	1	3	6	87	-88	-1	7	3	175	155
0	6	0	152	-149	0	12	1	108	-101	0	20	6	5	-7	1	3	7	226	-192	-1	7	2	187	184
0	6	1	194	186	0	12	2	4	5	-1	1	15	35	41	1	3	8	59	60	-1	7	1	134	-128
0	6	2	131	116	0	12	3	83	73	-1	1	14	28	-24	1	3	9	106	101	1	7	0	29	-30
0	6	3	131	-137	0	12	4	11	9	-1	1	13	52	-57	1	3	10	24	-26	1	7	1	9	-9
0	6	4	39	-39	0	12	5	17	-21	-1	1	12	12	16	1	3	11	26	-28	1	7	2	17	19

H	K	L	FO	FC	H	K	L	FO	FC	H	K	L	FO	FC	H	K	L	FO	FC	H	K	L	FO	FC
1	7	3	90	-93	1	11	2	45	-43	-1	17	10	2	-6	2	0	12	71	69	2	4	4	188	-163
1	7	4	128	139	1	11	4	67	79	-1	17	9	2	11	2	0	14	72	-64	2	4	5	81	80
1	7	5	101	101	1	11	6	95	-101	-1	17	8	31	27	-2	2	15	22	31	2	4	6	107	93
1	7	6	166	-176	1	11	7	9	-3	-1	17	6	18	-24	-2	2	13	32	-27	2	4	7	34	-33
1	7	7	92	-94	1	11	8	85	92	-1	17	5	41	-39	-2	2	12	63	-61	2	4	8	47	-45
1	7	8	111	115	1	11	10	30	-31	-1	17	4	30	28	-2	2	11	26	-20	2	4	9	39	-36
1	7	9	59	55	1	11	12	2	-2	-1	17	3	51	40	-2	2	10	152	132	2	4	10	2	-5
1	7	10	48	-45	-1	13	11	5	-7	-1	17	2	44	-34	-2	2	9	2	5	2	4	11	52	45
1	7	11	9	-10	-1	13	10	2	-2	-1	17	1	24	-13	-2	2	8	218	-172	2	4	12	58	51
1	7	13	4	-9	-1	13	9	31	33	1	17	0	20	20	-2	2	7	94	-88	2	4	13	36	-36
-1	9	14	40	44	-1	13	8	52	46	1	17	1	7	-8	-2	2	6	176	187	2	4	14	44	-45
-1	9	13	18	-21	-1	13	6	105	-93	1	17	4	13	-25	-2	2	5	97	101	-2	6	15	18	15
-1	9	12	39	-41	-1	13	5	76	-66	1	17	5	17	29	-2	2	4	89	-99	-2	6	13	23	20
-1	9	11	19	-17	-1	13	4	101	86	1	17	6	7	18	-2	2	3	54	54	-2	6	12	8	-19
-1	9	10	9	8	-1	13	3	57	51	1	17	7	24	-33	-2	2	1	31	-32	-2	6	11	57	-58
-1	9	8	39	41	-1	13	2	90	-81	-1	19	9	2	-2	2	2	0	108	105	-2	6	10	80	72
-1	9	7	10	-8	-1	13	1	24	-19	-1	19	8	2	-11	2	2	1	203	-202	-2	6	9	135	114
-1	9	6	126	-117	1	13	0	52	50	-1	19	5	54	39	2	2	2	260	-233	-2	6	8	115	-39
-1	9	5	103	90	1	13	1	2	2	-1	19	4	16	-16	2	2	3	101	89	-2	6	7	90	-78
-1	9	4	221	193	1	13	2	20	27	-1	19	3	44	-33	2	2	4	231	214	-2	6	6	17	26
-1	9	3	87	-81	1	13	3	6	-14	-1	19	2	22	8	2	2	5	47	-48	-2	6	5	36	36
-1	9	2	219	-192	1	13	4	47	-54	-1	19	1	3	3	2	2	6	96	-94	-2	6	4	22	-24
-1	9	1	71	66	1	13	5	30	37	1	19	1	3	5	2	2	7	65	62	-2	6	3	16	-21
1	9	0	97	86	1	13	6	69	74	1	19	2	2	-3	2	2	8	12	-10	-2	6	1	93	-101
1	9	1	11	-16	1	13	7	37	-44	1	19	3	2	-3	2	2	9	50	45	2	6	0	75	77
1	9	2	58	57	1	13	8	66	-77	1	19	5	26	-25	2	2	10	50	50	2	6	1	115	-135
1	9	3	39	41	1	13	9	20	-7	1	19	6	2	-11	2	2	11	43	-43	2	6	2	129	-131
1	9	4	127	-140	1	13	10	38	46	1	19	8	21	17	2	2	12	61	-62	2	6	3	142	142
1	9	5	47	-48	1	13	11	9	17	-1	21	5	23	-20	2	2	14	62	59	2	6	4	117	110
1	9	6	137	146	-1	15	8	35	-35	-1	21	3	32	23	-2	4	15	8	-9	2	6	5	103	-98
1	9	7	62	62	-1	15	7	40	-38	-1	21	2	2	1	-2	4	14	26	-24	2	6	6	60	-59
1	9	8	101	-108	-1	15	6	36	31	-1	21	1	25	-19	-2	4	13	11	-5	2	6	7	40	40
1	9	9	14	-8	-1	15	5	54	51	1	21	0	17	-3	-2	4	12	39	39	2	6	8	36	35
1	9	10	48	45	-1	15	4	60	-54	1	21	1	18	-1	-2	4	11	33	27	2	6	9	16	-12
1	9	13	7	-7	-1	15	3	47	-42	1	21	2	2	-3	-2	4	10	89	-80	2	6	11	33	-36
-1	11	12	42	43	-1	15	2	73	65	1	21	4	2	4	-2	4	9	59	-51	2	6	12	45	-40
-1	11	11	25	25	-1	15	1	49	45	-2	0	14	60	56	-2	4	8	124	97	2	6	13	45	44
-1	11	10	23	-23	1	15	0	27	-28	-2	0	12	30	21	-2	4	7	174	148	2	6	14	31	31
-1	11	9	5	-4	1	15	1	2	-2	-2	0	10	189	-156	-2	4	6	20	-26	-2	8	13	17	-12
-1	11	8	36	-33	1	15	3	35	32	-2	0	8	257	219	-2	4	5	129	-139	-2	8	12	21	22
-1	11	7	9	-8	1	15	4	38	44	-2	0	6	148	-166	-2	4	4	50	56	-2	8	11	60	56
-1	11	6	133	118	1	15	5	25	-33	-2	0	4	41	44	-2	4	3	21	-16	-2	8	10	32	-34
-1	11	5	18	-13	1	15	6	34	-40	-2	0	2	138	-143	-2	4	2	54	52	-2	8	9	107	-87
-1	11	4	127	-101	1	15	7	35	50	2	0	0	419	-359	-2	4	1	55	59	-2	8	8	50	47
-1	11	3	18	10	1	15	8	32	36	2	0	2	765	792	2	4	0	133	-127	-2	8	7	128	107
-1	11	2	126	112	1	15	9	21	-31	2	0	4	254	-233	2	4	1	61	70	-2	8	6	97	-95
1	11	0	97	-91	1	15	10	23	-35	2	0	6	41	43	2	4	2	97	98	-2	8	5	122	-127
1	11	1	5	3	-1	17	11	2	-13	2	0	10	51	-53	2	4	3	88	-83	-2	8	4	32	34

H	K	L	FO	FC	H	K	L	FO	FC	H	K	L	FO	FC	H	K	L	FO	FC	H	K	L	FO	FC
-2	8	3	30	30	2	12	1	37	65	-3	1	5	124	-122	-3	5	9	52	49	-3	9	13	42	41
-2	8	2	48	48	2	12	3	63	-91	-3	1	4	2	-4	-3	5	8	19	19	-3	9	12	68	51
-2	8	1	104	115	2	12	4	9	8	-3	1	3	167	177	-3	5	7	2	-5	-3	9	11	31	-29
2	8	0	74	-83	2	12	5	72	81	-3	1	2	63	63	-3	5	6	20	29	-3	9	10	67	-57
2	8	1	135	177	2	12	7	29	-33	-3	1	1	209	-203	-3	5	5	89	-88	-3	9	9	17	-17
2	8	2	73	84	2	12	8	26	-16	3	1	0	34	-28	-3	5	4	68	-70	-3	9	8	27	25
2	8	3	171	-177	2	12	10	18	9	3	1	1	160	-157	-3	5	3	124	138	-3	9	7	9	-2
2	8	4	64	-64	-2	14	10	35	-28	3	1	2	23	-20	-3	5	2	98	107	-3	9	6	13	9
2	8	5	115	121	-2	14	9	64	56	3	1	3	77	84	-3	5	1	118	-134	-3	9	5	7	-8
2	8	6	48	40	-2	14	8	18	2	3	1	5	19	26	3	5	0	106	-107	-3	9	4	69	-80
2	8	7	26	-31	-2	14	7	49	-43	3	1	7	103	-93	3	5	1	87	-81	-3	9	3	45	49
2	8	8	2	5	-2	14	5	18	19	3	1	8	10	19	3	5	2	50	50	-3	9	2	123	145
2	8	10	21	-19	-2	14	4	2	12	3	1	9	101	96	3	5	3	51	46	-3	9	1	54	-57
2	8	11	42	39	-2	14	3	9	-1	3	1	10	12	-21	3	5	4	9	-7	3	9	0	121	-140
2	8	12	18	15	-2	14	1	34	-41	3	1	11	71	-69	3	5	6	40	-36	3	9	1	45	-49
2	8	13	40	-41	2	14	1	38	-67	3	1	12	16	10	3	5	7	63	-56	3	9	2	62	73
-2	10	13	2	3	2	14	2	21	46	3	1	13	36	38	3	5	8	51	48	3	9	3	10	-9
-2	10	12	28	-26	2	14	3	40	75	-3	3	15	39	40	3	5	9	93	82	3	9	4	2	13
-2	10	11	42	-37	2	14	4	9	-24	-3	3	14	28	23	3	5	10	42	-43	3	9	6	55	-54
-2	10	10	17	21	2	14	5	51	-57	-3	3	13	93	-78	3	5	11	61	-61	3	9	7	23	-16
-2	10	9	112	92	2	14	6	2	6	-3	3	12	21	-24	3	5	12	29	29	3	9	8	71	70
-2	10	7	140	-114	2	14	7	18	17	-3	3	11	81	70	3	5	13	10	16	3	9	10	60	-60
-2	10	6	31	28	2	14	8	2	-8	-3	3	9	50	-50	-3	7	14	61	52	-3	11	12	59	-46
-2	10	5	77	67	2	14	9	12	3	-3	3	8	9	-6	-3	7	13	21	-20	-3	11	10	66	49
-2	10	4	18	-25	-2	16	8	40	-34	-3	3	7	35	35	-3	7	12	81	-66	-3	11	9	29	24
-2	10	2	38	-44	-2	16	7	60	50	-3	3	6	28	29	-3	7	11	41	35	-3	11	8	46	-45
-2	10	1	39	-41	-2	16	6	29	17	-3	3	5	66	67	-3	7	10	53	43	-3	11	6	19	-13
2	10	1	63	-100	-2	16	5	51	-43	-3	3	4	15	13	-3	7	9	29	-36	-3	11	4	79	92
2	10	2	30	38	-2	16	4	22	-13	-3	3	3	184	-190	-3	7	8	21	-13	-3	11	2	71	-84
2	10	3	103	123	-2	16	3	16	12	-3	3	2	72	-79	-3	7	6	17	-15	3	11	0	78	101
2	10	4	18	18	-2	16	2	2	7	-3	3	1	169	179	-3	7	5	25	24	3	11	2	61	-74
2	10	5	88	-94	-2	16	1	21	26	3	3	0	22	27	-3	7	4	72	84	3	11	6	33	32
2	10	6	34	-34	2	16	0	19	23	3	3	1	84	79	-3	7	3	87	-100	3	11	8	63	-58
2	10	7	39	36	2	16	1	12	53	3	3	2	7	-14	-3	7	2	143	-180	3	11	9	2	4
2	10	9	21	21	2	16	2	14	-38	3	3	3	74	-68	-3	7	1	106	115	3	11	10	45	47
2	10	11	44	-40	2	16	5	22	33	3	3	4	59	55	3	7	0	113	135	-3	13	10	35	-27
2	10	12	11	4	2	16	6	2	-6	3	3	6	9	-10	3	7	1	91	98	-3	13	7	29	30
-2	12	12	9	3	-2	18	4	29	19	3	3	7	86	77	3	7	2	66	-64	-3	13	6	30	25
-2	12	11	35	31	2	18	2	18	30	3	3	8	38	-38	3	7	3	17	-16	-3	13	4	62	-68
-2	12	9	73	-62	2	18	3	14	38	3	3	9	105	-88	3	7	4	23	22	-3	13	3	35	-51
-2	12	8	24	-7	-3	1	15	49	-45	3	3	10	33	33	3	7	5	43	-35	-3	13	2	55	69
-2	12	7	75	58	-3	1	14	14	16	3	3	11	59	59	3	7	6	58	56	-3	13	1	17	34
-2	12	6	44	33	-3	1	13	52	42	3	3	13	19	-23	3	7	7	43	41	3	13	0	48	-73
-2	12	5	45	-33	-3	1	12	36	-33	-3	5	14	47	-48	3	7	8	74	-72	3	13	1	10	18
-2	12	4	35	-36	-3	1	11	91	-78	-3	5	13	37	34	3	7	9	53	-49	3	13	2	36	42
-2	12	2	18	16	-3	1	9	85	89	-3	5	12	55	49	3	7	10	60	61	3	13	3	2	2
-2	12	1	35	37	-3	1	7	25	19	-3	5	11	45	-36	3	7	11	35	32	3	13	4	8	-1
2	12	0	2	-3	-3	1	6	14	-26	-3	5	10	38	-34	3	7	12	27	-32	3	13	6	29	-20

H	K	L	FO	FC	H	K	L	FO	FC	H	K	L	FO	FC	H	K	L	FO	FC	H	K	L	FO	FC
3	13	7	11	17	4	2	8	54	-54	-4	8	10	20	13	4	12	8	2	1	-5	5	11	17	24
3	13	8	41	40	4	2	9	19	18	-4	8	9	36	36	-4	14	7	28	42	-5	5	10	24	37
-3	15	8	16	-3	4	2	10	11	11	-4	8	7	59	-65	-4	14	5	24	-31	-5	5	9	30	-35
-3	15	6	11	-18	4	2	11	10	14	-4	8	6	31	42	-4	14	2	14	9	-5	5	8	29	-32
-3	15	5	20	-23	-4	4	13	21	-14	-4	8	5	66	79	-4	14	1	20	-11	-5	5	7	43	42
-3	15	4	2	12	-4	4	12	2	-8	-4	8	4	50	-61	4	14	0	9	-11	-5	5	6	24	21
-3	15	2	24	-44	-4	4	11	2	3	-4	8	3	80	-87	4	14	1	14	14	-5	5	5	16	-13
3	15	0	26	54	-4	4	10	16	8	-4	8	2	25	23	4	14	2	11	-11	-5	5	3	32	-28
3	15	2	12	-30	-4	4	8	51	-57	-4	8	1	36	38	4	14	3	30	-28	-5	5	2	26	-25
3	15	5	2	9	-4	4	7	37	-43	4	8	0	9	1	4	14	4	9	19	-5	5	1	63	64
-3	17	4	19	-18	-4	4	6	68	73	4	8	1	35	-30	4	14	5	32	38	5	5	0	47	45
-3	17	2	13	23	-4	4	5	102	110	4	8	2	34	-24	-4	16	2	2	-14	5	5	1	70	71
-3	17	1	14	35	-4	4	4	47	-52	4	8	3	82	76	4	16	0	16	9	5	5	2	42	-43
3	17	3	17	-15	-4	4	3	87	-87	4	8	4	39	36	4	16	1	16	-10	5	5	3	59	-47
-4	0	14	52	-39	-4	4	2	72	69	4	8	5	88	-83	-5	1	11	25	30	5	5	4	34	31
-4	0	12	70	67	4	4	1	16	-12	4	8	6	30	-28	-5	1	9	55	-57	5	5	5	30	30
-4	0	8	108	-102	4	4	2	40	-38	4	8	7	57	58	-5	1	7	67	61	5	5	7	9	-2
-4	0	6	144	164	4	4	3	54	44	4	8	8	24	19	-5	1	6	8	6	5	5	8	2	-6
-4	0	4	129	-136	4	4	4	61	54	4	8	9	24	-26	-5	1	5	17	-20	5	5	9	23	-16
-4	0	2	66	63	4	4	5	59	-54	4	8	10	2	-3	-5	1	4	10	-12	-5	7	10	42	-46
4	0	0	61	-58	4	4	6	88	-80	-4	10	10	24	-27	-5	1	3	46	-30	-5	7	9	27	31
4	0	2	166	-143	4	4	7	36	39	-4	10	8	13	20	-5	1	1	77	73	-5	7	8	38	34
4	0	4	229	235	4	4	8	55	50	-4	10	7	52	63	5	1	0	26	21	-5	7	7	28	-29
4	0	6	109	-105	4	4	10	26	-29	-4	10	6	8	3	5	1	1	102	91	-5	7	6	18	-13
4	0	8	53	55	4	4	11	2	-7	-4	10	5	76	-91	5	1	3	67	-77	-5	7	5	11	23
4	0	10	21	-10	4	4	12	8	3	-4	10	3	59	64	5	1	4	2	2	-5	7	4	10	1
4	0	12	20	-15	-4	6	13	24	20	-4	10	2	12	-14	5	1	5	54	47	-5	7	3	8	9
-4	2	14	44	37	-4	6	9	42	-44	-4	10	1	16	-23	5	1	6	2	-2	-5	7	2	33	26
-4	2	13	42	41	-4	6	8	46	52	4	10	0	7	-11	5	1	7	16	-11	-5	7	1	40	-45
-4	2	11	26	-27	-4	6	7	67	78	4	10	1	19	4	5	1	8	11	4	5	7	0	61	-73
-4	2	10	38	-40	-4	6	6	54	-61	4	10	3	46	-43	5	1	9	20	-22	5	7	1	51	-52
-4	2	9	19	-10	-4	6	5	35	-44	4	10	5	63	62	-5	3	11	47	-56	5	7	2	60	63
-4	2	8	84	87	-4	6	4	34	37	4	10	6	19	9	-5	3	9	46	50	5	7	3	49	47
-4	2	7	8	5	-4	6	3	46	46	4	10	7	56	-52	-5	3	7	56	-52	5	7	4	52	-42
-4	2	6	123	-132	-4	6	2	43	-41	4	10	8	23	-13	-5	3	6	21	-14	5	7	5	2	-12
-4	2	5	60	-62	-4	6	1	35	-39	4	10	9	22	24	-5	3	5	38	35	5	7	6	10	15
-4	2	4	140	137	4	6	0	20	13	-4	12	9	10	15	-5	3	3	34	28	5	7	8	10	14
-4	2	3	65	61	4	6	1	24	25	-4	12	7	37	-42	-5	3	1	75	-80	5	7	9	16	12
-4	2	2	88	-81	4	6	2	41	37	-4	12	5	52	57	5	3	0	39	-32	-5	9	10	36	39
-4	2	1	15	-8	4	6	3	62	-53	-4	12	4	14	22	5	3	1	88	-79	-5	9	9	23	-22
4	2	0	28	27	4	6	4	74	-63	-4	12	3	33	-40	5	3	2	29	28	-5	9	8	43	-48
4	2	1	28	24	4	6	5	76	70	-4	12	2	19	-22	5	3	3	53	50	-5	9	6	30	31
4	2	2	56	45	4	6	6	64	59	-4	12	1	16	8	5	3	4	25	-21	-5	9	4	11	-12
4	2	3	96	-95	4	6	7	50	-53	4	12	1	21	-12	5	3	5	46	-42	-5	9	2	32	-34
4	2	4	124	-114	4	6	8	38	-38	4	12	2	15	-4	5	3	7	10	11	-5	9	1	31	13
4	2	5	45	40	4	6	9	27	27	4	12	3	28	29	5	3	8	12	-3	5	9	0	61	65
4	2	6	104	104	4	6	10	21	23	4	12	5	44	-47	5	3	9	22	19	5	9	1	30	23
4	2	7	22	-25	-4	8	11	8	0	4	12	7	47	47	-5	5	12	20	-34	5	9	2	61	-65

178

H	K	L	FO	FC	H	K	L	FO	FC	H	K	L	FO	FC	H	K	L	FO	FC	H	K	L	FO	FC
5	9	3	23	-27	5	13	2	38	-41	6	2	2	24	23	-6	6	8	2	1	6	8	4	10	-2
5	9	4	42	40	5	13	3	19	10	6	2	4	23	12	-6	6	6	18	21	6	8	5	11	20
5	9	5	2	2	-5	19	1	59	11	6	2	5	31	-29	-6	6	5	30	31	-6	10	5	20	27
5	9	6	2	-4	-6	0	10	51	47	6	2	6	46	-35	-6	6	4	27	-24	-6	10	3	42	-45
-5	11	8	39	35	-6	0	6	44	-37	-6	4	8	2	-3	-6	6	3	21	-21	-6	10	1	38	35
-5	11	6	37	-39	-6	0	4	70	68	-6	4	6	30	-28	-6	6	2	25	23	6	10	1	11	19
-5	11	5	11	-7	-6	0	2	74	-68	-6	4	5	30	-26	-6	6	1	34	30	6	10	2	12	-1
-5	11	2	41	44	6	0	0	54	44	-6	4	4	37	37	6	6	0	29	-25	-7	1	6	2	-4
5	11	0	45	-49	6	0	2	25	-26	-6	4	3	53	51	6	6	1	26	23	-7	1	5	34	28
5	11	1	2	-6	6	0	4	37	-39	-6	4	2	43	-34	6	6	4	17	7	-7	1	3	9	-20
5	11	2	52	55	6	0	6	64	57	-6	4	1	38	-35	6	6	6	19	-18	7	1	1	28	-18
5	11	3	11	4	-6	2	9	22	-18	6	4	0	47	38	-6	8	7	18	9	7	1	3	33	28
5	11	4	31	-34	-6	2	7	2	-1	6	4	1	23	-16	-6	8	5	26	-29	-7	3	5	34	-29
5	11	5	10	0	-6	2	6	35	32	6	4	3	10	2	-6	8	3	30	35	-7	3	4	20	-12
5	11	6	2	7	-6	2	4	66	-59	6	4	4	2	-1	-6	8	2	26	-26	-7	3	3	21	17
-5	13	5	11	16	-6	2	3	40	-33	6	4	5	33	14	-6	8	1	37	-39	-7	3	2	11	8
-5	13	2	29	-27	-6	2	2	71	63	6	4	6	27	18	6	8	0	21	11	7	3	0	2	1
-5	13	1	33	-22	-6	2	1	31	22	6	4	7	25	-17	6	8	1	23	-23	7	3	1	26	21
5	13	0	31	36	6	2	0	56	-45	-6	6	9	2	-1	6	8	2	12	-8	-7	5	3	25	-9

5.5 ABBREVIATIONS

dmbp   : 6,6'-dimethyl-2,2'-bipyridine

bt   : 2,2'-bi-2-thiazoline

btz   : 2,2'-bi-4,5-dihydrothiazine

imid   : imidazole

tmbp   : 4,4',6,6'-tetramethylbipyridine

dpm   : diphenylphosphinomethane

phen   : 1,10-phenanthroline

ppr   : 3-phenylpropionate

5.6 REFERENCES:

1. Popov, A.I.; Marshall, J.C.; Stute, F.B.; Person, W.B. *J. Am. Chem. Soc.* 1961, **83**, 3586.

2. Hall, J.R.; Litzow, M.R.; Plowman, R.A. *Aust. J. Chem.* 1966, **19**, 197.

3. Goodwin, K.V.; McMillin, D.R.; Robinson, W.R. *Inorg. Chem.* 1986, **25**, 2033 and the references therein.

4. Aniscough, E.W.; Plowman, R.A. *Aust. J. Chem.* 1970, **23**, 699.

5. Hall, J.R.; Plowman, R.A.; Preston, H.S. *ibid.* 1965, **18**, 1345.

6. Swarnabala, G.; Rajasekharan, M.V. *Inorg. Chem.* 1989, **28**, 662.

7. McMillin, D.R.; Kirchoff, J.R.; Goodwin, K.V. *Coord. Chem. Rev.* 1984, **63**, 83.

8. Burke, P.J.; McMillin, D.R.; Robinson, W.R. *Inorg. Chem.* 1980, **19**, 1211.

9. Burke, P.J.; Hendrik, K.; McMillin, D.R. *Inorg. Chem.* 1982, **21**, 1881.

10. Dessy, G.; Fares, V. *Cryst. Struct. Commun.* 1979, **8**, 507.

11. Hamalainen, R.; Ahlgren, M.; Tupeinen, U.; Raikes, T. *Cryst. Struct. Commun.* 1979, **8**, 75.

12. Hamalainen, R.; Tupeinen, U.; Ahlgren, M.; Raikes, T. *Finn. Chem. Lett.* 1978, **199**, 274.

13. Colman, P.M.; Freeman, H.C.; Guss, J.M.; Nurata, M.; Norris, V.A.; Ramshaw, J.A.M.; Venkatappa, P.M. *Nature* 1978, **272**, 319.

14. Adman, E.; Stenkamp, R.E.; Sieker, L.C.; Jenson, L.H. *J. Mol. Biol.* 1978, **125**, 35.

15. Drew, M.G.B.; Pearson, T.R.; Murphy, B.P.; Nelson, S.M. *Poly-hedron* 1983, **2**, 269.

16. Dobson, J.F.; Green, B.F.; Healy, P.C.; Knennard, C.H.L.; Pakawatchai, C.; White, A.H. *Aust. J. Chem.* 1984, **37**, 649.

17. Addision, C.C.; Logan, N.; Wallwork, S.C.; Garner, C.D. *Quart Rev. Chem. Soc.* 1971, **25**, 289.

18. Weist, R.; Weiss, R. *J. Chem. Soc. Chem. Commun.* 1973, 678.

19. Cooper, M.K.; Nyholm, R.S. *J. Chem. Soc. Chem. Commun.* 1974, 343.

20. Meiners, J.H.; Clardy, J.C.; Verkade, J.G. *Inorg. Chem.* 1975, **14**, 632.

21. Yamaguchi, H.; Kido,A.; Uechi, T.; Yasukouchi, K. *Bull. Chem. Soc. Jpn.* 1976, **49**, 1271.

22. International Tables for X-ray Crystallography; Kynoch Press : Birmingham, England, 1962; Vol.III, p.278.

23. Baenziger, N.C.; Struss, A.W. *Inorg. Chem.,* 1976, **15**, 1807.

24. Antti, C.J.; Lundberg, B.K.S. *Acta Chem. Scand.* 1971, **25**, 1758.

25. Eastland, G.W.; Mazid, M.A.; Russel, D.R.; Symons, M.C.R. *J. Chem. Soc. Dalton Trans.* 1980, 1682.

26. Dietrich, H.; Storck, W.; Manecke, G. *J. Chem. Soc. Chem. Commun.* 1982, 1036.

27. Birker, P.J. M.W.L.; Verschoor, G.C. *J. Chem. Soc. Chem. Commun.* 1981, 322.

28. Sheldrick, G.M. SHELX-76, Programm for Crystal Structure Determination, University of Cambridge, England, 1976.

29. Johnson, C.K. ORTEP, Report ORNL 3794, Oak Ridge National Laboratory : Oakridge, USA, 1965.

30. International Tables for X-ray Crystallography, Kynoch Press : Birmingham, England, 1974, Vol.IV.

31. Cromer, D.T.; Liberman, D. *J. Chem. Phys.* 1970, **53**, 1891.

32. Ho,D.M.; Bau, R. *Inorg. Chem.* 1983, **22**, 4073.

33. Dubler, E.; Haering, V.K.; Scheller, K.H.; Baltzer, P.; Sigel, H. *Inorg. Chem.* 1984, **23**, 3785.

34. ' and '' refer to equivalent positions at 1-x, y, 1/2 -z and -x, y, 1/2 -z respectively.

35. Hazell, A.C. *Acta Crystallogr. Sect. B* 1974, **B20**, 2724.

36. Ansell, G.B.; Finnegan, W.G. *J. Chem. Soc. Chem. Commun.* 1969, 1300.

37. Ansell, G.B. *J. Chem. Soc. B* 1971, 443.

38. Hunt, G.W.; Lee, T.C.; Amma, E.L. *Inorg. Nucl. Chem. Lett.* 1974, **10**, 909.

39. Acland, C.B.; Freeman, H.C. *J. Chem. Soc. Chem. Commun.* 1971, 1016.

40. Schmidbaur, H.; Aly, A.A.M.; Schubert, U. *Angew. Chem., Int. ed. engl.* 1978, **17**, 846.

41. Dietrich, H.; Storck, W.; Manecke, G. *J. Chem. Soc. Chem. Commun.* 1982, 1036.

42. Rao, M.J.K.; Viswamitra, M.A. *Acta Crystallogr. Sect.B* 1972, **B28**, 1484.